JHN Journal

Volume 13 | Issue 1 Article 7

Winter 2018

Full Issue: Volume 13, Issue 1 - Winter 2018

VOL 13, ISSUE 1 | WINTER 2018

JHNJOURNAL

a publication of the **Vickie and Jack Farber Institute for Neuroscience – Jefferson Health**

Brain Tumor Care Special Issue

In collaboration with **Sidney Kimmel Cancer Center – Jefferson Health**

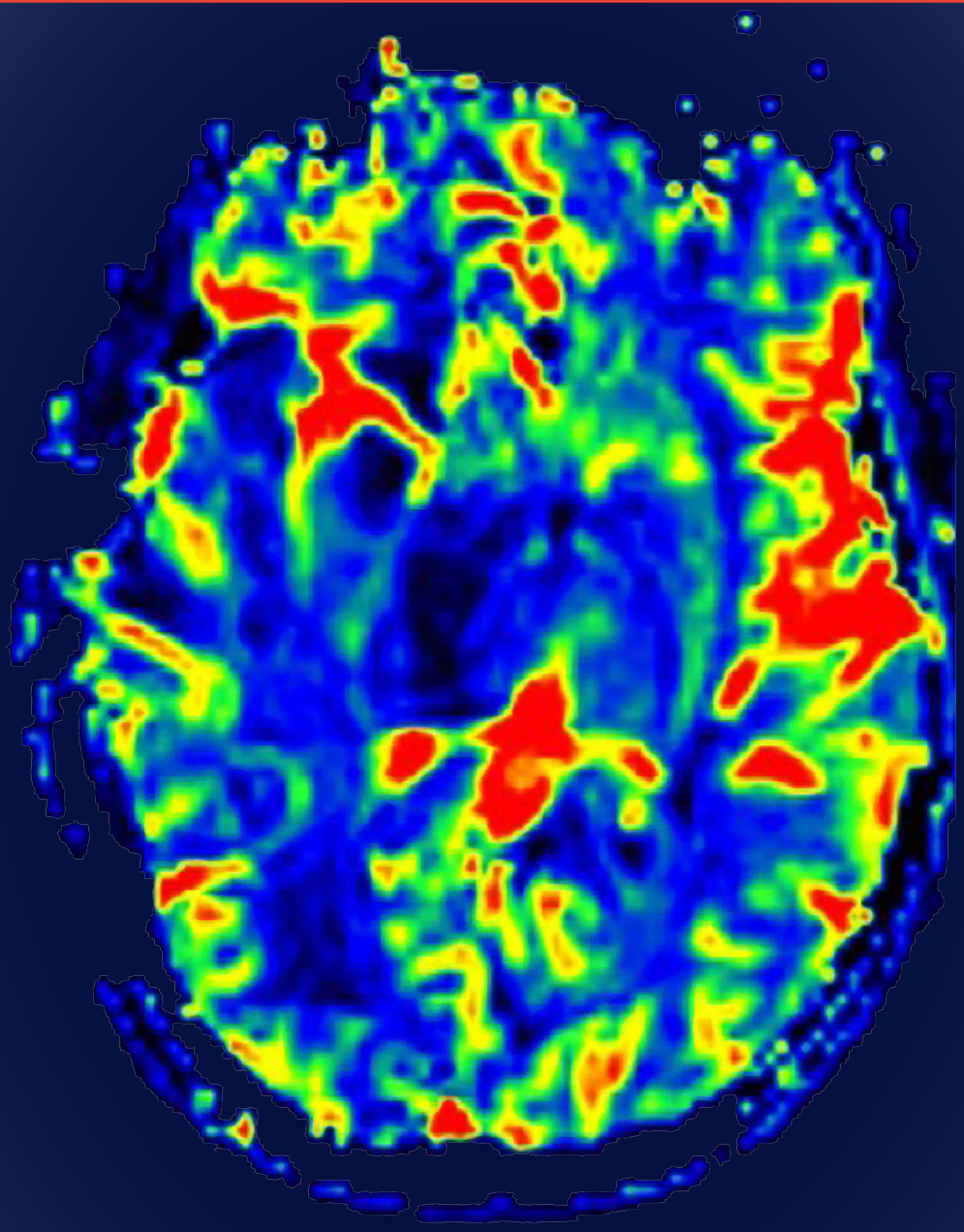

Vickie and Jack Farber Institute for Neuroscience Jefferson Health®

Photo: Dynamic susceptibility contrast MR perfusion image of the brain.

General Information

Correspondence, inquiries, or comments may be submitted to the Editor, JHN Journal, 909 Walnut Street, 3rd Floor, Philadelphia, PA 19107 or email at jhnjournal@gmail.com

 ISSN 1558-8726

Jefferson.edu/Neurosurgery

Vickie and Jack Farber
Institute for Neuroscience
Jefferson Health

Christopher J. Farrell, MD

Dear Reader,

Welcome to the neuro-oncology special issue of JHN Journal. The research you'll find in this issue highlights advancements we have made to further advance the science of this difficult field. I'm also pleased to report that our division, housed within the Vickie and Jack Farber Institute for Neuroscience – Jefferson Health, has continued to make great strides in our academic and clinical missions, as well.

Last year, we met with over 1,500 new patients and performed nearly 1,000 surgeries. In order to continue to care for these patients in the most seamless, multidisciplinary way, we added a third oncologist to our division. I'm proud to welcome Nina L. Martinez, MD, to our division. Dr. Martinez, an alumna of Jefferson's neurology residency, rejoins us after completing a neuro-oncology fellowship at Memorial Sloan Kettering Cancer Center and serving as an attending at Chicago's NorthShore University HealthSystem.

Our skull-base fellowship continues to offer trainees some of the country's most advanced training in the field. The graduates since our last neuro-oncology special issue, published two years ago, have achieved great success. Varun Khsettry, MD, joined the staff at Cleveland Clinic and Alan Siu, MD, is pursuing a second fellowship at Semmes Murphey Clinic, one of my alma maters. I'm confident our current fellow, Hermes Garcia, MD, will achieve similar success after his graduation this summer.

Finally, I wish to congratulate our division director and departmental vice chair, David Andrews, MD, the inaugural Anthony Alfred Chiurco, MD, Professor of Neurological Surgery. Dr. Chiurco, SKMC '67, is a practicing neurosurgeon in our area. A few years ago, our colleague became a patient of Dr. Andrews when an emergency room visit revealed he had a large brain tumor. His generous gift to our division will continue to fuel our growth.

None of this would be possible without our ongoing partnership with the NCI-designated Sidney Kimmel Cancer Center at Jefferson, particularly our colleagues in radiation oncology. As you'll find as you read this issue, we are partners in research, education and clinical care.

Best regards,

Christopher J. Farrell, MD

Assistant Professor of Neurological Surgery
Vickie and Jack Farber Institute for Neuroscience
Member, Sidney Kimmel Cancer Center

BRAIN TUMOR TREATMENT AT JEFFERSON

William W. Keen, a Jefferson physician, performed America's first successful brain tumor removal in 1888. This rich tradition of innovation and excellence continues today in our multidisciplinary brain tumor treatment program.

Our Physicians

The Vickie and Jack Farber Institute for Neuroscience, the home of our brain tumor program, consists of four fellowship-trained neurosurgeons, two neuro-oncologists and one medical oncologist working together in one center.

They're joined by our colleagues in the Sidney Kimmel Cancer Center (SKCC) at Jefferson, one of 69 National Cancer Institute (NCI)-designated clinical cancer centers for excellence in cancer care and research. We work particularly closely with our colleagues in radiation oncology, a department that treats nearly 1,000 cancer patients per year.

Our Resources

Our physicians have access to some of the most advanced technologies available for treating patients with brain tumors. This includes both the Visualase® and Neuroblate® MRI-guided laser ablation technologies, a GammaKnife™, a Varian True Beam STx Slim LINAC and advanced Brainlab® treatment planning software.

These resources are centered at Jefferson Hospital for Neuroscience (JHN), the Philadelphia area's only hospital dedicated to the treatment of neurological disorders. We're proud to say JHN has achieved Magnet® status, the highest distinction a healthcare organization can receive for excellence in nursing.

Physicians and basic science researchers from both the Farber Institute and SKCC are engaged in clinical and translational research to improve outcomes for people living with brain tumors. Some of these research projects include:

- **ANTISENSE 102, an ongoing immunotherapy clinical trial for glioblastoma developed here at Jefferson.**
- **CHECKMATE, a study that examines the efficacy of adding nivolumab to temozolomide and radiosurgery for patients with MGMT-methylated glioblastoma.**
- **Our area's only CAP-accredited brain tumor lab, operated in conjunction with our colleagues in the Department of Pathology.**

Educational Opportunities

Thomas Jefferson University, home to the Sidney Kimmel Medical College, is proud to offer both undergraduate and graduate medical education. We offer:

- **A third-year clerkship and a fourth-year sub-internship in neurological surgery. We are pleased to accept visiting students into the fourth year rotation. For Jefferson students, we also offer a fourth year research elective.**
- **An ACGME-accredited residency program training three residents a year.**
- **Multiple fellowships, including an SNS/CAST fellowship in neuro-oncologic surgery, with a special emphasis in skull base surgery.**

New Patient Appointments: **1-800-JEFF-NOW** | *Next day appointments usually available*

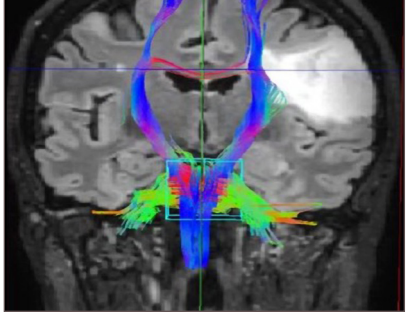

Table of Contents

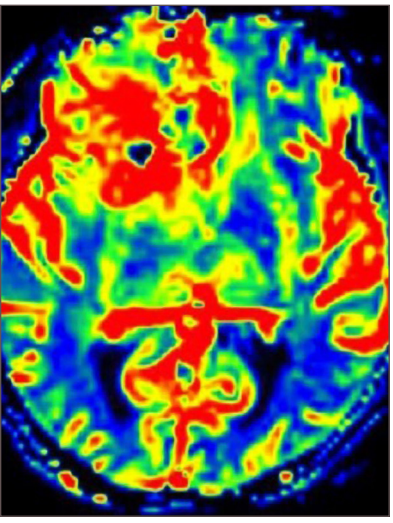

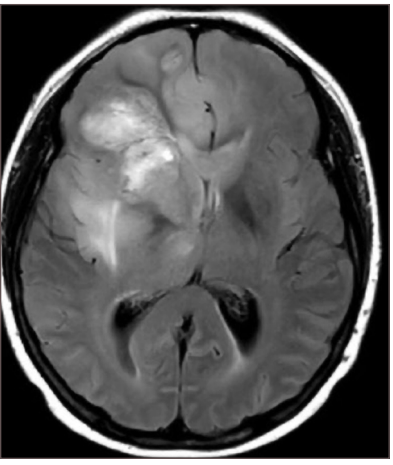

Salvage Fractionated Stereotactic Re-irradiation (FSRT) for Patients with Recurrent High Grade Gliomas Progressed after Bevacizumab Treatment

Wenyin Shi, MD, PhD[1]; Erik S. Blomain, BA[2]; Joshua Siglin, MD[3]; Joshua Palmer, MD[4]; Tu Dan, MD[5]; Yang Wang, MD[6]; Maria Werner-Wasik, MD[1]; Jon Glass, MD[7]; Lyndon Kim, MD[7]; Voichita Bar Ad, MD[1]; Deepak Bhamidipati, BS[8]; James J. Evans, MD[7]; Kevin Judy, MD[7]; Christopher Farrell, MD[7]; David W. Andrews, MD[7]

[1]Department of Radiation Oncology, Thomas Jefferson University, Sidney Kimmel Cancer Center at Jefferson, Philadelphia, PA
[2]Jefferson College of Population Health, Thomas Jefferson University, Philadelphia, PA
[3]Department of Radiation Oncology, University of Pittsburgh Medical Center, Altoona Cancer Center, Altoona, PA
[4]Department of Radiation Oncology, Ohio State University, Columbus, OH
[5]Department of Radiation Oncology, University of Texas Southwestern, Dallas, TX
[6]Cyberknife Center, Huashan Hospital Pudong, Fudan University, Shanghai, China
[7]Department of Neurological Surgery, Thomas Jefferson University, Philadelphia, PA
[8]Sidney Kimmel Medical College, Thomas Jefferson University, Philadelphia, PA

Running title

FSRT for recurrent high grade gliomas after avastin failure

Conflict of Interest Notification

No actual or potential conflicts of interest.

Acknowledgements

E.S.B. received an F30 Ruth Kirschstein MD-PhD Fellowship Award (CA180500).

ABSTRACT

Purpose/Objectives: Bevacizumab failure is a major clinical problem in the management of high grade gliomas (HGG), with a median overall survival of less than 4 months (m). This study evaluated the efficacy of fractionated stereotactic re-irradiation (FSRT) for patients with HGG after progression on Bevacizumab.

Materials/Methods: Retrospective review was conducted of patients treated with FSRT after progression on bevacizumab. A total of 36 patients were identified. FSRT was most commonly delivered in 3.5 Gy fractions to a total dose of 35 Gy. Survival from initial diagnosis, as well as from recurrence and re-irradiation, were utilized as study endpoints. Univariate and multivariate analysis was performed.

Results: Among the 36 patients, 31 patients had recurrent glioblastoma, and 5 patients had recurrent anaplastic astrocytoma. The median time from initial bevacizumab treatment to FSRT was 8.5 m (range 2.3 – 32.0 m). The median plan target volume for FSRT was 27.5 cc (range 1.95 – 165 cc). With a median follow up of 20.4 m, the overall survival of the patients since initial diagnosis was also 24.9 m. The median overall survival after initiation of bevacizumab was 13.4 months. The median overall survival from FSRT was 4.8 m. FSRT treatment was well tolerated with no Grade >3 toxicity.

Conclusions: Favorable outcomes were observed in patients with recurrent HGG who received salvage FSRT after bevacizumab failure. The treatment was well tolerated. Prospective study is warranted to further evaluate the efficacy of salvage FSRT for selected patients with recurrent HGG amenable to FSRT, who had failed bevacizumab treatment.

INTRODUCTION

Malignant gliomas are the most common brain tumors, with an estimated yearly incidence of 3 per 100,000 people in the United States.[1] Despite multiple modalities for definitive therapy (which include resection, radiation therapy (RT) and chemotherapy), these lesions have an unfortunately high rate of recurrence.[2] Therefore, even despite recent treatment advances in targeted therapies for glioblastoma (GBM) and high grade glioma (HGG) such as bevacizumab, the long-term outcomes for these patients remain poor.

In modern clinical practice, treatment failure of recurrent HGGs largely represents failure of bevacizumab therapy.[3] In addition to disease recurrence itself driving poor outcomes, there is evidence that these patients who fail bevacizumab also harbor disease that is resistant to other systemic therapies.[4] Therefore, treatment options for these recurrent patients remain limited and their prognosis is dismal with a recent review of sixteen studies reporting an overall survival (OS) of under 4 months after bevacizumab failure.[4-6]

Multiple modalities of radiotherapy have been investigated for this population, including stereotactic radiosurgery (SRS) and brachytherapy. These interventions have been shown to have modest utility, but with the potential for significant associated toxicity. In that context, fractionated stereotactic radiotherapy (FSRT) is a promising treatment modality for the treatment of these refractory HGGs. This modality possesses the precise targeting advantages of SRS but with the dose-sparing radiobiologic properties of fractionation to allow greater sparing of surrounding critical structures, thus limiting toxicity.[7,8] Taken together, FSRT therefore possesses the potential for decreased toxicity as compared to SRS while still providing excellent local control.[9] The present study sought

DOI: https://doi.org/10.29046/JHNJ.013.1

to evaluate the safety and efficacy of FSRT in patients who failed therapy with bevacizumab.

MATERIALS AND METHODS

Patients

The Thomas Jefferson University institutional review board approved this single-institution, retrospective study. Patients who received FSRT salvage after progression on bevacizumab were included. A total of 36 patients were identified from 2006 to 2013. Patients who received FSRT within 2 months of initiation of bevacizumab were excluded. Patients were followed with MRI scans and clinical assessment, which were obtained 6 to 8 weeks after FSRT and at approximately 2-month intervals thereafter.

Table 1. Patient Demographic and Treatment Information. Descriptive data on our study cohort is shown, encompassing demographic data, clinical information and treatment information.

Number of patients	36
Gender	
Male	17
Female	19
Median Age at FSRT salvage (range)	56 years (37-73)
Median KPS at FSRT salvage (range)	80 (50-100)
Histology at Recurrence	
GBM	30
Anaplastic glioma	4 (3-4)
Other	2 (1-2)
Median Volume of Recurrence (range)	27.5 cc (1.95-165)
Median Radiation Dose (range)	35 Gy (30-37.5)
Median time from Bev to FSRT (range)	(2.4-32.1)

Treatment Planning

Treatment decisions were based on consensus recommendations following discussion in our institution's multidisciplinary brain tumor board consisting of radiologists, neurosurgeons, neuro-oncologists, neuropathologists and radiation oncologists. Prior to 2004, treatment planning was conducted with the X-knife 3-D planning system (Radionics, Burlington, MA, USA), which delivered 6 MV photons with a dedicated stereotactic 600SR linear accelerator (Varian, Palo Alto, CA, USA). From 2004 to 2013, treatment planning was carried out with Brain Lab (Novalis) using mMLC leaves with a leave thickness of 3 mm and Exac Trac on board imaging. All patients undergoing irradiation were fitted with custom-made Brainlab (Munich, Germany) thermal plastic masks for immobilization. Treatment planning MRI and computed tomography (CT) images were obtained and fused. All patients had thin cut (1-1.5 mm) fat suppressed coronal post-contrast MRI. The gross tumor volume (GTV) was defined on MRI using the gadolinium enhanced T1 weighted series, as peripherally enhancing tissue. Surrounding edema was not purposely included in the treatment volume. The planning target volume was the GTV with minimum margin (0-2 mm per the treating physician). Critical normal structures, such as optic nerves, chiasm, and brainstem were also contoured. Treatment planning was carried out with Brain Lab Iplan (Munich, Germany). The radiation planning used dynamic conformal arcs, IMRT (intensity modulated radiation therapy) or hybrid-Arcs (Brainlab, Munich, Germany), a combination of dynamic arcs with IMRT beams. The patients were treated with FSRT to a median PTV dose of 35 Gy delivered in 3.5 Gy fractions.[10] The dose was reduced to 30 Gy in 3 Gy fractions for large targets, and high critical normal structure dose. The constraints for normal critical structures include: brainstem max dose <20 Gy; optic nerve max dose < 15 Gy, chiasm max dose < 15 Gy.

Statistical analysis

The primary end point of the study was overall survival from initial diagnosis, as well as survival from first recurrence and re-irradiation (described in greater detail under Statistical Analyses). Toxicity was also graded using Radiation Therapy Oncology Group (RTOG) criteria. Overall survival was defined as the time from initial diagnosis to the time of death. Date of recurrence was defined as the date of radiographic evidence of progression. Survival from recurrence and from reir-radiation were therefore defined as the time from this radiologic evidence or radiation therapy until death, respectively. Kaplan–Meier curves were generated for the overall survival endpoint. Cox proportional hazard modeling was used for multivariate analysis with factors analyzed in a step-wise fashion. All statistical analysis was performed using the STATA data analysis and statistical software version 13.1 (STATA Corporation).

RESULTS

Patient Population and Treatment Parameters

We identified 36 patients with either anaplastic astrocytoma (5 patients) or glioblastoma multiforme (GBM) (30 patients) who had clinical and radiographic evidence of tumor progression on bevacizumab and received FSRT between 2006 and 2013 (Table 1). One patient had gemistocytic astrocytoma. Patient characteristics are listed in Table 1. There were 17 males and 19 females. All patients received initial surgery and were treated with radiation and temozolomide. The median age at recurrence was 57.1 years (range 37-73). The median Karnofsky Performance Status at recurrence was 80%. Following disease progression on bevacizumab, the median target volume treated with FSRT was 27.5 cc (range 1.95 – 165 cc). The median dose was 35 Gy (range, 30 Gy – 37.5 Gy).

Survival

Patients underwent routine surveillance for a median follow up of 20.4 m after initial diagnosis, with an overall survival from initial diagnosis of 24.9 m. Upon evidence of initial disease recurrence, patients were promptly started on bevacizumab. The median overall survival after initiation of bevacizumab was 13.4 months. The median time from initial bevacizumab treatment to initiation of

Table 2. Survival Statistics. Survival data accrued from the study cohort is shown, expressed as OS from diagnosis, recurrence and from FSRT.

Median Overall Survival (Range)	
From Diagnosis	24.9 months (11.4-94.2)
From First Recurrence	12.0 months (4.2-49.1)
From FSRT	4.8 months (0.5-23.4)

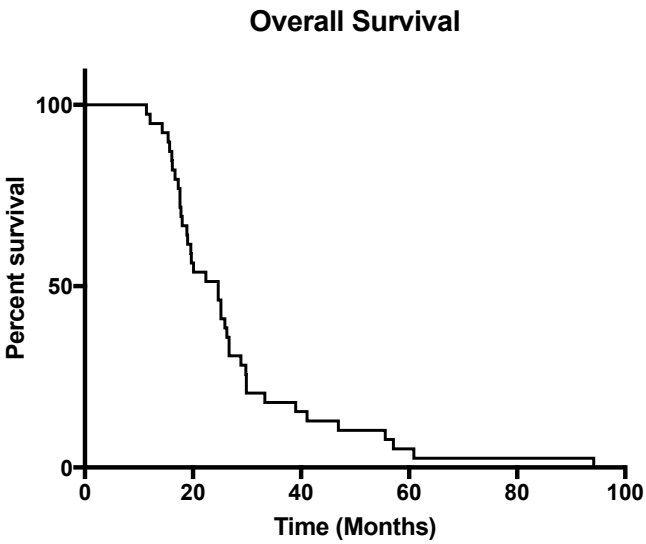

Figure 1. Kaplan-Meyer Overall Survival Curve.

Graph displays OS from the time diagnosis for patients who went on to fail bevacizumab therapy and require FSRT in our study cohort.

salvage FSRT was 8.5 m (range 2.4 – 32 m), and the median overall survival after FSRT was 4.8 m. Data are presented in table form (Table 2) as well as in the form of a Kaplan-Meyer survival curve (Figure 1).

Multivariate Analysis

Multivariate analysis was performed to investigate whether different variables in our study population influenced OS from recurrence or from FSRT therapy (Table 3). These included age at recurrence, KPS score, volume of recurrence, histology (AA vs GBM) or re-resection status. Importantly, out of all of these variables, only re-resection demonstrated a statistically significant association with overall survival from recurrence (HR 2.59; p=0.04). Additionally, there was a trend towards significance for re-resection status associated with OS from FSRT (HR 1.87 p=0.17).

Toxicity

No patients demonstrated clinically significant acute morbidity, with no grade III or higher toxicity observed. All patients were able to complete the prescribed radiation course without interruption. There were no observed hospitalizations or surgeries for early acute or delayed toxicity in the study population.

DISCUSSION

Despite recent advances such as bevacizumab that have extended overall survival in patients with high-grade gliomas, treatment failure and disease progression while on bevacizumab remain as an unfortunate reality in managing these patients. Therefore, overall prognosis remains quite poor. Despite this clinical need, there remains a paucity of literature regarding the management of patients who fail bevacizumab. In that context, the present study investigated FSRT as a potential treatment modality to address this problem.

Prior to FDA-approval of bevacizumab, FSRT had been previously studied in the setting of recurrent HGG, with generally favorable results. Multiple studies have shown FSRT to be efficacious, with OS in these studies ranging from 5-11 months. Moreover, these studies showed FSRT to be very well tolerated, with a low rate of grade 3 toxicities, radiation necrosis (RN) and reoperation.[10-12]

Of note, one study (Lederman et al.) observed significantly more toxicity and reoperation (11 of 88 patients) than the others. This toxicity outlier can perhaps be explained by the use of a different dosing regimen (24 Gy in 4 fractions in Lederman et al. versus 30-35 Gy in 6-10 fractions in the other studies).[13] In a head to head trial, Patel et al. compared stereotactic radiosurgery (SRS) with FSRT and showed comparable overall survival and radiographic tumor response between the two modalities, with a trend towards fewer events of radiation necrosis (RN) in the FSRT cohort.[14]

The data on FSRT treatment following bevacizumab failure is much more limited. In a retrospective study, Torcuator et al. looked at two cohorts of patients who failed bevacizumab: one that received either FSRT or SRS and one that received no FSRT/SRS. They demonstrated an increased overall survival in patients receiving FSRT/SRS (7.2 vs 3.3 months in untreated patients). Another study that is published only in abstract form by Nehaw et al. similarly looked at RT (including 6 patients who received FSRT) versus non-RT regimens following bevacizumab failure and showed statistically significant increased survival in the radiation group (8.8 vs. 5.4 months for untreated). Despite this small body of literature, neither of these studies investigated FSRT alone after bevacizumab

Table 3. Multivariate Analysis. Multivariate analysis is shown for the study cohort. Variables were tested for association with OS from Recurrence as well as OS From FSRT. Data are expressed as Hazard Ratios (HR) and p-value. P-value of <0.05 was considered significant.

OS from Recurrence Multivariate	
Age at Recurrence	HR=0.99; p=0.67
KPS <=80	HR=1.27; p=0.61
Volume of recurrence >50cc	HR=1.09; p=0.32
Re-resection yes vs no	HR=2.59; p=0.04
Histology AA vs GBM	HR=0.99; p=0.99
OS from FSRT Multivariate	
Age at Recurrence	HR=1.01; p=0.70
KPS <=80	HR=0.73; p=0.53
Volume of recurrence	>50cc HR=1.02; p=0.83
Re-resection yes vs no	HR=1.87; p=0.17
Histology AA vs GBM	HR=1.72; p=0.46

failure, nor did they report on safety or toxicity of these approaches.

In that context, the present study represents one of the first studies to specifically investigate the role of FSRT in the context of bevacizumab failure. Indeed, our work builds off of previous work by both our group and others showing comparable benefit and improved safety in FSRT regimens for HGGs as compared to SRS for treatment of HGG in other contexts.[10,11,13] Specifically, the present study demonstrates the feasibility, efficacy and tolerability of such an approach in patients who fail bevacizumab.

One limitation of our study is the lack of a control cohort for comparison in terms of outcomes to put our overall survival into context. Historically, patients who fail bevacizumab have been shown in a recent review of sixteen studies to have an overall survival of 3.8 months.[4-6]

Thus, our observed overall survival compares favorably to, and indeed exceeds that mark. Taken in the context of the aforementioned studies which show benefit of RT vs. no RT in bevacizumab failure, and also that FSRT and SRS provide similar OS in recurrent gliomas before bevacizumab treatment, our data are consistent with these previous studies and moreover suggest a role for FSRT in the management of patients who fail bevacizumab. Despite our findings, it is worth noting that one limitation of our study is the potential bias of our dataset in that it only includes patients who are amenable to therapy with FSRT. Therefore it is difficult to directly compare our survival data to the existing literature, given that the literature includes all patients, whether or not they are eligible for FSRT. Further head-to-head studies will be needed to evaluate FSRT versus other modalities to definitively establish a role and identify populations that would most benefit.

Notably, our multivariate analysis yielded only one variable that was associated with overall survival: re-resection status. Indeed, there is controversy in the literature regarding the prognostic value of re-resection in patients with recurrent HGG,[2] but our data suggest that re-resection is actually deleterious in terms of survival outcomes. However, given the retrospective nature of the current study, it is difficult to draw strong conclusions from these data, as re-resection status itself may be confounding by representing underlying patient characteristics that lead to poorer prognosis. Future studies will be needed to identify patient populations who will most benefit from an FSRT regimen.

Other limits to our study include a small patient cohort (36) as well as those shortcomings inherent to all retrospective studies including selection bias and potential treatment differences in a non-randomized study. Despite these potential drawbacks, this study represents, to our knowledge, the largest literature cohort of FSRT patients in the context of bevacizumab failure. Moreover, the dire prognosis of these patients and the paucity of data regarding their management underscores the relevance of the present study, and suggests the need for future prospective randomized trials to improve survival and positively impact the lives of patients with HGG.

CONCLUSIONS

Favorable outcomes were observed using FSRT to treat patients with recurrent HGG and the treatment was well tolerated. Prospective study is warranted to further evaluate the efficacy of salvage FSRT for patients with recurrent HGG after bevacizumab failure.

REFERENCES

1. Stupp R, Brada M, van den Bent MJ, Tonn JC, Pentheroudakis G, Group EGW. High-grade glioma: ESMO Clinical Practice Guidelines for diagnosis, treatment and follow-up. *Annals of oncology: official journal of the European Society for Medical Oncology* 2014; 25 Suppl 3:iii93-101.
2. Palmer JD, Siglin J, Yamoah K, Dan T, Champ CE, Bar-Ad V, et al. Re-resection for recurrent high-grade glioma in the setting of re-irradiation: more is not always better. *J Neurooncol* 2015; 124:215-21.
3. Iwamoto FM, Abrey LE, Beal K, Gutin PH, Rosenblum MK, Reuter VE, et al. Patterns of relapse and prognosis after bevacizumab failure in recurrent glioblastoma. *Neurology* 2009; 73:1200-6.
4. Kreisl TN, Kim L, Moore K, Duic P, Royce C, Stroud I, et al. Phase II trial of single-agent bevacizumab followed by bevacizumab plus irinotecan at tumor progression in recurrent glioblastoma. *J Clin Oncol* 2009; 27:740-5.
5. Norden AD, Young GS, Setayesh K, Muzikansky A, Klufas R, Ross GL, et al. Bevacizumab for recurrent malignant gliomas: efficacy, toxicity, and patterns of recurrence. *Neurology* 2008; 70:779-87.
6. Magnuson W, Ian Robins H, Mohindra P, Howard S. Large volume reirradiation as salvage therapy for glioblastoma after progression on bevacizumab. *Journal of neuro-oncology* 2014; 117:133-9.

7. Combs SE, Gutwein S, Thilmann C, Debus J, Schulz-Ertner D. Reirradiation of recurrent WHO grade III astrocytomas using fractionated stereotactic radiotherapy (FSRT). Strahlentherapie und Onkologi: Organ der Deutschen Rontgengesellschaft [et al] 2005; 181:768-73.
8. Combs SE, Gutwein S, Thilmann C, Huber P, Debus J, Schulz-Ertner D. Stereotactically guided fractionated re-irradiation in recurrent glioblastoma multiforme. *Journal of neuro-oncology* 2005; 74:167-71.
9. Shen X, Andrews DW, Sergott RC, Evans JJ, Curran WJ, Machtay M, et al. Fractionated stereotactic radiation therapy improves cranial neuropathies in patients with skull base meningiomas: a retrospective cohort study. *Radiation oncology* 2012; 7:225.
10. Fogh SE, Andrews DW, Glass J, Curran W, Glass C, Champ C, et al. Hypofractionated stereotactic radiation therapy: an effective therapy for recurrent high-grade gliomas. *J Clin Oncol* 2010; 28:3048-53.
11. Grosu AL, Weber WA, Franz M, Stark S, Piert M, Thamm R, et al. Reirradiation of recurrent high-grade gliomas using amino acid PET (SPECT)/CT/MRI image fusion to determine gross tumor volume for stereotactic fractionated radiotherapy. Int *J Radiat Oncol Biol Phys* 2005; 63:511-9.
12. Fokas E, Wacker U, Gross MW, Henzel M, Encheva E, Engenhart-Cabillic R. Hypofractionated stereotactic reirradiation of recurrent glioblastomas : a beneficial treatment option after high-dose radiotherapy? *Strahlenther Onkol* 2009; 185:235-40.
13. Lederman G, Wronski M, Arbit E, Odaimi M, Wertheim S, Lombardi E, et al. Treatment of recurrent glioblastoma multiforme using fractionated stereotactic radiosurgery and concurrent paclitaxel. Am J Clin Oncol 2000; 23:155-9.
14. Patel M, Siddiqui F, Jin JY, Mikkelsen T, Rosenblum M, Movsas B, et al. Salvage reirradiation for recurrent glioblastoma with radiosurgery: radiographic response and improved survival. *J Neurooncol* 2009; 92:185-91.

Corresponding Author

Wenyin Shi, MD, PhD
Department of Radiation Oncology
Sidney Kimmel Medical College
Thomas Jefferson University
Sidney Kimmel Cancer Center
at Jefferson

111 South 11th Street
Philadelphia, PA 19107

P: 215-955-6700
F: 215-503-0013
E: Wenyin.Shi@jefferson.edu

Phase 1 Trial of Vaccination with Autologous Tumor Cells and Antisense Directed Against the Insulin Growth Factor Type 1 Receptor (IGF-1R AS ODN) in Patients with Recurrent Glioblastoma

David W. Andrews, MD[1]; Kevin D. Judy, MD[1]; Larry A. Harshyne, PhD[1]; D. Craig Hooper, PhD[2]

[1]Department of Neurological Surgery, Thomas Jefferson University, Philadelphia, PA
[2]Department of Cancer Biology, Thomas Jefferson University, Philadelphia, PA

ABSTRACT

Background: Extending a previous Phase I study, we report the results of a second Phase I autologous tumor cell vaccination trial for patients with recurrent glioblastomas (IND 14379-101, NCT01550523).

Methods: Following surgery, subjects were treated by 24 hour implantation in the rectus sheath of ten biodiffusion chambers containing irradiated autologous tumor cells and IGF-1R AS ODN with the objective of stimulating tumor immunity. Patients were monitored for safety, clinical and radiographic as well as immune responses.

Results: There were no Grade 3 toxicities related to protocol treatment and overall median survival from initial diagnosis was 91.4 weeks. Two protocol survival cohorts with median survivals of 48.2 and 10 weeks were identified and predicted by our pre-treatment assessments of immune function, corroborated by post-vaccination pro-inflammatory cytokine profiles. Longer survival subjects had imaging findings including transient elevations in cerebral blood volume (rCBV) and sustained elevations of apparent diffusion coefficient (ADC) interpreted as transient hyperemia and cell loss.

Conclusions: The vaccine paradigm was well-tolerated with a favorable median survival. Our data support this as a novel treatment paradigm that promotes anti-tumor immunity.

KEYWORDS

Decompressive Hemicraniectomy, Intracerebral Hemorrhage, Malignant MCA Stroke, Traumatic Brain Injury, Aneurysmal Subarachnoid Hemorrhage, Intracranial Pressure, Herniation

INTRODUCTION

WHO Grade IV astrocytoma (glioblastoma) is a uniformly fatal primary intracranial malignancy with a median survival of 14 months.[1] We conducted an earlier pilot Phase I vaccine trial in patients with high grade astrocytomas[2] and designed a replacement Phase 1 trial with optimized reagents, expanded radiographic response criteria, and new exploratory objectives.

METHODS

Study Site and Patients

The study was conducted at Thomas Jefferson University and reached target accrual of 12 patients in 14 months. Criteria for enrollment included age > 18, a Karnofsky performance score of 60 or better, and no co-morbidities that would preclude elective surgical re-resection. Twelve patients were enrolled for treatment after failure from standard therapy.[1] A summary of enrolled patients, and all available pertinent data is included in Table 1.

Study Design and Objectives

As before, the combination product consisted of autologous tumor cells removed at surgery then treated overnight with the IGF-1R AS ODN (4mg/ml) prior to being added to semi-permeable chambers and irradiated.[2] Enhancements to the vaccine product included use of an 18-mer IGF-1R AS ODN with the sequence 5'-TCCTCCGGAGC-CAGACTT-3', two frameshifts upstream from the previous sequence; and, based on data showing that the AS ODN has immunomodulatory properties,[3,4] addition of 2 mg of exogenous antisense to the chambers (C-v). The protocol was also amended to include an eleventh control chamber containing PBS (C-p). Study objectives included assessment of safety and radiographic responses as well as exploratory objectives looking at immune function and response.

Radiological Assessments

Serial imaging assessments were performed on Philips 1.5T and 3T MRIs and GE 1.5 T MRIs. Routine anatomic MRI features were evaluated as well as physiologic measurements including dynamic susceptibility weighted (DSC) MR perfusion and 15-direction diffusion tensor imaging (DTI) were also utilized.

Immunological Assessments

Plasma leukopheresis was performed one week before surgery for baseline assessment of immune function. Blood

Table 1. Summary of Patients Enrolled.

Subject	Age	KPS	Interval between surgeries (weeks)	# chambers implanted	Original lymphocyte count (cells/mm2)	Lymphocyte count at enrollment (cells/mm2)	Previous treatments	IDH-1 mutation/ MGMT methylation
TJ01	39	70	177	10	N/A	400	S,RT + TMZ, Bev	-/
TJ02	57	80	90	9	N/A	1570	S,RT + TMZ	-/methylated
TJ03	75	70	32	7	700	300	S,RT + TMZ	-/
TJ06/R1	66	80	54	8	2000	1300	S,RT + TMZ	-/
TJ07	43	80	215	10	500	430	S, RT + TMZ, Bev; RTOG 0525	+/
TJ08	55	80	52	8	1000	500	S,RT + TMZ	-/
TJ09	57	80	61	7	1400	300	S, RT + TMZ, RTOG 0929	-/unmethylated
TJ10	47	60	376	7	N/A	1800	S, RT + TMZ, Bev	-/methylated
TJ11	39	70	32	11*	2400	200	S, RT + TMZ	-/
TJ12	60	80	74	7	1100	600	S, RT + TMZ, Panobinostat	-/
TJ13	64	80	182	11	N/A	2100	S, RT + TMZ	-/
TJ14/R	77	90	30	7/11	1800	1100	S, RT + TMZ	-/unmethylated

[1]Compassionate retreatment; *Protocol amendment to include control chamber filled with phosphate buffered saline; S: surgery; RT: radiation therapy; TMZ: temozolamide chemotherapy; Bev: bevacizumab chemotherapy; IDH-1: isocitrate dehydrogenase-1

was obtained post-operatively on days 7, 14, 28, 42, 56, and every 3 months after vaccination. Sera and cell fractions were separated by centrifugation and cells were treated with red blood cell lysis buffer and white blood cells either quantified by flow cytometry or stored in DMSO at -80°C. Serum samples were also stored at -80°C. Flow cytometry was performed as previously described[5] using an EasyCyte 8HT (Millipore) and fluorescently-conjugated mAb specific for human CD4, CD8,CD11b, CD14, CD16, CD20, CD45, CD56, CD80, CD83, and CD 86 (all from BD Biosciences), and CD163 (R&D Systems). Post- collection analysis was performed with FlowJo software (Tree Star Inc, Ashland, OR). Serum cytokine factors were quantified using Luminex bead arrays (human cytokine/chemokine panels I, II, and III from Millipore and HCMBMAG/ MILLIPLEX Mag Cancer multiplex assay (emdmillipore.com). This included 6 serum markers for glioma related to stem cell function including DKK-1, NSE, Osteonectin, Periostin, YKL-40, and TWEAK. T-cell stimulation was performed with phorbol 12-myristate,13 acetate (PMA) and ionomycin as previously described.6 PBMC from glioblastoma patients and normal donors were cultured for 24 hours at 37°C and 5% CO2 in AIMV media containing 10% fetal bovine serum (Gibco). Non-adherent lymphocytes were transferred to new plates in order to eliminate non-specific effects of contaminating monocytes. Lymphocyte cultures were stimulated with phorbol 12-myristate 13-acetate (PMA, 100 ng/ml) and ionomycin (0.1 mM, both from Sigma-Aldrich) for 18 hours. BD Golgiplug™ (1:1000, Brefeldin A, BD Bioscience) was added during the last 6 hours of culture to permit cytokine accumulation.

Tumor tissue sections were assessed by immunohistochemistry or immunofluorescence, adapting the method of Emoto7, for GFAP, IGF-1R, CD163, CD14, CD3, CD4, and CD8. Immunopositive cells were counted quantitatively with Aperio or qualitatively by an experienced neuropathologist (LEK) using an ordinal scale from 0 (no staining) to 6 (strong diffuse staining) with staining intensity rated as low, moderate and strong and staining patterns described as focal or diffuse.

Cytokine/chemokine levels in tumor cell supernatant were analyzed by Luminex kits as designated above. Membranes from paired vaccine and control chambers were embedded in paraffin for standard immunohistopathologic examination. Post-mortem autopsy was limited to examination of the brain and findings were compared to archival paraffin blocks of previously treated or untreated glioblastomas diagnosed at autopsy.

Statistical Analysis

The level of statistical significance between quantitative measures in different samples was determined by a two-tailed unpaired t-test or matched pairs t-test with $p < .05$. Survival analysis was performed by Kaplan-Meier analysis and significance established by log rank comparisons. All statistical analysis including mixture discriminant analysis was performed with JMP v. 11 software (SAS, North Carolina).

DOI: https://doi.org/10.29046/JHNJ.013.1

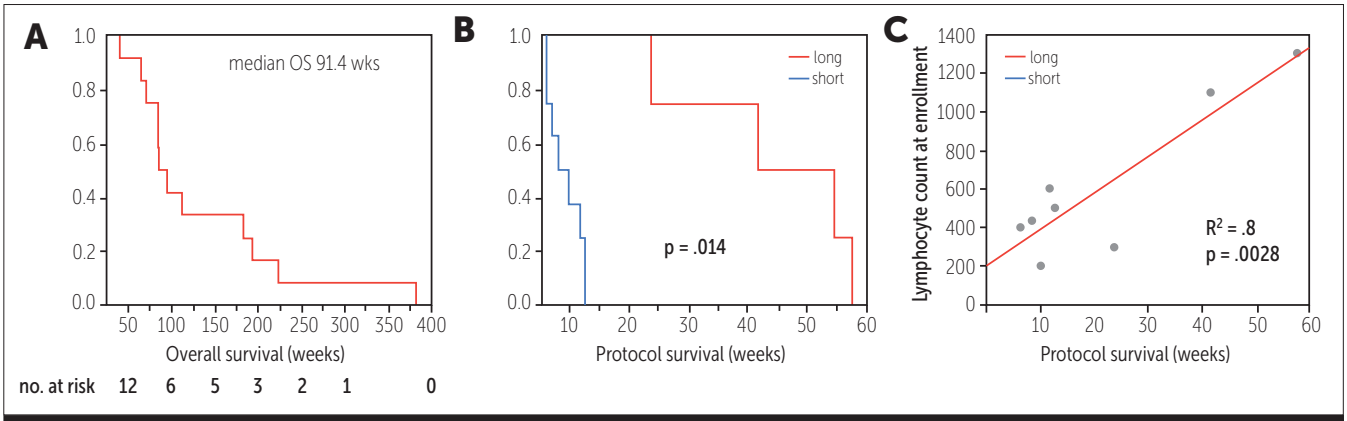

Figure 1. Survival Metrics.

A. Overall survival of patients in trial; **B.** protocol survival with two survival cohorts; Nine patients died of disease progression while one died of intracerebral hemorrhage and two of sepsis. Overall protocol survival was 48.2 weeks and 9.2 weeks, respectively for longer (N = 4) and short (N = 8) survival cohorts (log-rank = .014). **C.** Excluding one outlier and three non-disease-related deaths linear regression revealed high correlation between protocol survival and lymphocyte count at enrollment (R2 = .8, p = .0028).

RESULTS

Safety Assessment and Clinical Course

Only one SAE was related to the protocol (femoral vein thrombosis after leukopheresis). Nine patients succumbed to tumor progression while three patients died from other causes. Five autopsies were performed.

Median overall survival from initial diagnosis was 91.4 weeks which compared favorably to other recurrent glioma immunotherapy trials.[8-13] Two significantly different protocol survival cohorts of 48.2 and 10 weeks were identified as longer and short survival cohorts, respectively (Figure 1A&B). Excluding one outlier (TJ03), we documented a significant correlation between protocol survival and degree of lymphopenia at enrollment (Figure 1C). Comparison of CBC values at initial diagnosis and at protocol enrollment indicated that the mean lymphocyte count had dropped significantly (65%) after standard therapy (N=8, p = .012, paired t-test).

Radiographic Responses

Routine MRI features were assessed as previously described.[2] In the longer survivors we noted diminished size of enhancement and FLAIR envelope at the primary tumor site and slower progression. Examples of anatomic responses in both cohorts is included noted in Figure 2A&B. Physiologic MRI measurements augmented these anatomic observations for both cohorts is featured in Figure 2C&D. Sequential DSC MR perfusion was performed in 7 patients, including 3 longer-term survivors (TJ03, TJ06, and TJ09) who had a paradoxical increase in rCBV while improving clinically; however, this effect was transient and there was a more sustained decrease in rCBV. Sequential 15 directions DTI data included two long-term survivors (TJ03 and TJ06) who showed ADC values increasing in the affected hemisphere, reflecting loss of tumor cellularity associated with disease regression.

Immunologic Response Assessments after Vaccination by Survival Cohort

Levels of 24 of the 78 cytokines/chemokines assessed were significantly higher in serum from the longer survival cohort compared to the short cohort. A spike in serum CCL2 occurred after surgery but was absent at re-operation in two patients. CCL2 levels remained significantly higher throughout the post-operative period in the short survival cohort. These post-operative spikes were highly correlated with TNF-a spikes. (data not shown).

Actual CD4 and CD8 T cell counts as well as DC counts were significantly higher in the longer cohort compared to the short cohort. There was a significant correlation between CD4 and DC cells and between CD4 and CXCL12 only in the longer cohort. Coordinated changes between circulating levels of T cells, monocytes, and pro-inflammatory chemokines/cytokines after vaccination were seen in three of four longer cohort subjects.

As a distinguishing feature differentiating the cohorts, peripheral blood cells from the longer survival subjects manifested significantly higher Th-1 cytokine production including IFN-γ after stimulation with PMA and ionomycin from PBMC obtained on day 14.

Levels of circulating lymphocytes were significantly decreased (p<0.0001) in all GBM patients when compared to normal subject samples (Figure 1A, left panel) and the medians of both patient populations fell outside of the normal range (Figure 1A, gray lines). Patients in this same cohort exhibited significantly higher levels of monocytes (Figure 1A, right panel, p<0.05), but the medians of these cell populations fell within normal range.

The mere presence of a given cell subset is not enough to ensure proper immune function. The cell must also be able to respond to stimuli and produce

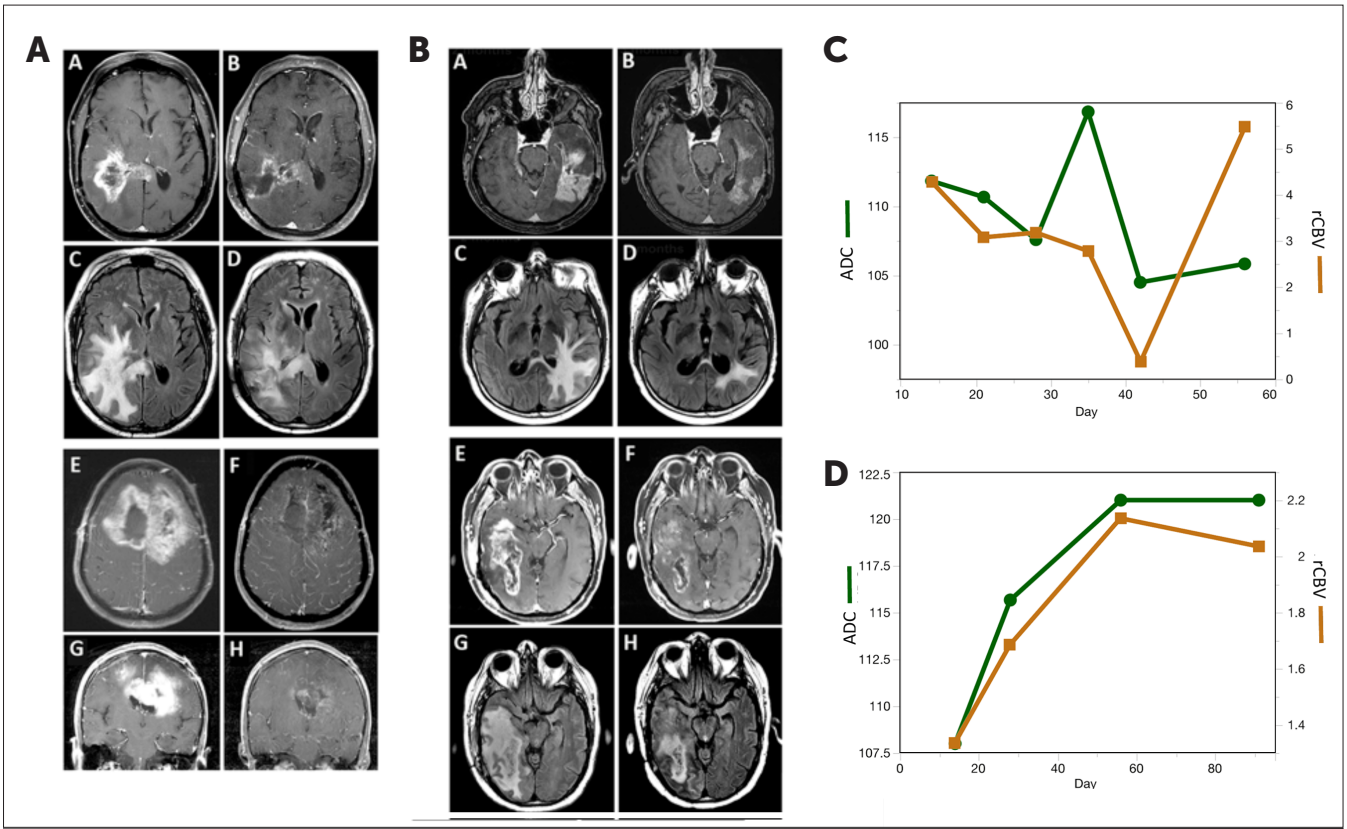

Figure 2. Radiographic responses with associated physiologic measurements and cytokine profiles.

A. Examples of short survival cohort. TJ11: A-D; TJ10: E-H. A,E: pre-operative T1-gadolinium-enhanced axial images; G: T1-gadolinium-enhanced coronal image; C: pre-operative axial FLAIR image. B,D,F,H: respective 3 month post-operative images. **B.** Examples of longer survival cohort. TJ06: A-D: TJ09: E-H. A,E: pre-operative T1-gadolinium-enhanced axial images; C,F: pre-operative axial FLAIR images. B,D,F,H: respective 3 month post-operative images. **C.** Relationship between relative cerebral blood volume in tumor v. apparent diffusion coefficient in short survival cohort. **D.** Relationship between relative cerebral blood volume in tumor v. apparent diffusion coefficient in longer survival cohort; there is a high correlation between the ADC and rCBV (R2 = .96, p = .0005).

appropriate immune modulators. T-helper type 1 immunity is considered to be the appropriate anti-tumor immune response. Cultures of non-adherent lymphocytes were stimulated nonspecifically with phorbol 12-myristate 13-acetate (PMA) and ionomycin overnight in order to stimulate the production of IFN-γ, the prototypical Th1 cytokine which was detected by intracellular cytokine flow cytometry. Viable, CD3+ T cell-specific gates were established (Figure 1B) and the median fluorescence intensity (MFI) of IFN-γ+ T cells was normalized to T cells that did not produce cytokine (IFN-γ+ T cells). PMA/ionomycin stimulation of normal T cells resulted in a 26-fold increase in the IFN-γ MFI (Figure 1B, right panel). T cells enriched from patients with primary and recurrent GBM produced significantly less IFN-γ when compared to normal controls ($p < 0.01$), but there was no difference between GBM patient cohorts (Figure 1B, right panel).

Moreover, while a difference in the quantity of IFN-γ produced by the T cells was observed, there was no difference in the frequency of IFN-γ+ T cells between these two cohorts (data not shown). In order to assess the relationship between lymphocyte numbers and immune functional capacity, we performed linear regression analyses. Lower levels of circulating lymphocytes are associated with a statistically significant ($R2 = 0.508$, $p = 0.0093$) decrease in IFN-γ production following PMA/ionomycin stimulation (Figure 1C, left panel). Furthermore, recursive partitioning analyses identified two different populations ($R2 = 0.547$) of recurrent GBM patients enrolled in our clinical trial (Figure 1C, right panel).

Reanalyzing these data focusing on single parameters based on the functional immune capacity confirmed the highly significant differences identified by recursive partitioning (Supplementary Figure 1). Patients with higher immune function possessed 3-fold higher levels of lymphocytes ($p < 0.0001$) and half as many monocytes ($p < 0.005$) when compared to the lower functioning group (Supplementary Figure 1). In addition to higher levels of lymphocytes, the T cells from patients with higher immune function produced twice as much IFN-γ following stimulation

https://jdc.jefferson.edu/jhnj/vol13/iss1/7
DOI: https://doi.org/10.29046/JHNJ.013.1

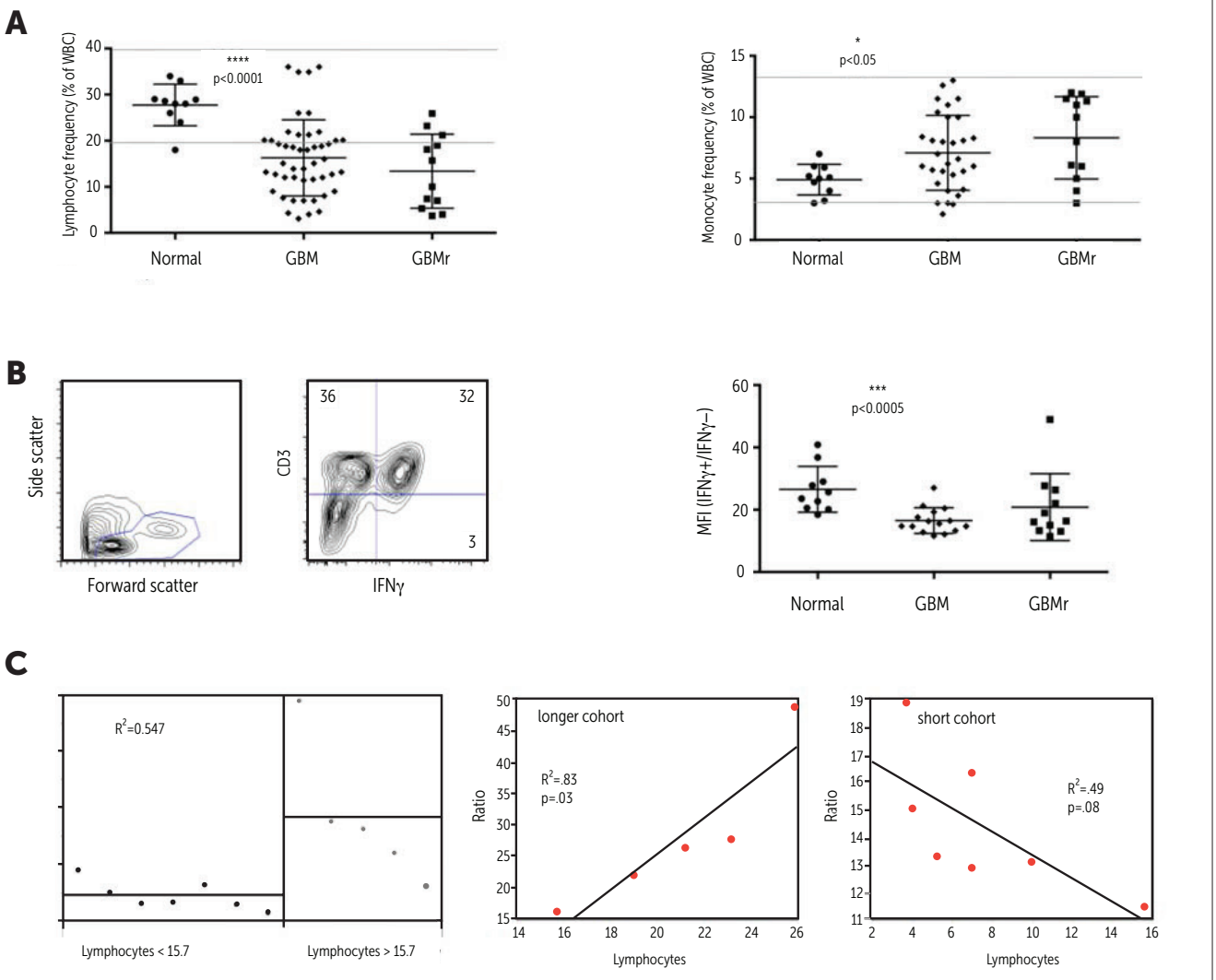

Figure 3. Functional immune capacity varies in glioblastoma patients.

A. Lymphocyte and monocyte frequencies are expressed as a percentage of white blood cells as determined by clinical blood counts performed by Thomas Jefferson University Hospital. Frequencies in trial patients are compared to primary glioblastoma patients and normal blood donors. Scatter dot plots indicate the mean frequency and standard deviation. Statistical significance of differences between tumor patients and normal blood donors were assessed by ANOVA followed by Dunnett's post-test (****p<0.0001 and *p<0.05). Gray lines represent the upper and lower range of normal values. GBM signifies newly diagnosed patients; GBMr signifies recurrent glioblastoma patients. **B.** Non-adherent peripheral blood mononuclear cells were stimulated with PMA/ionomycin and cytokine production was assessed by intracellular flow cytometry. Live cell gates were established in forward- and side-scatter plots (left panel). Quadrant gates were used to assess IFN-γ production in CD3+ T lymphocytes (middle panel). Numbers indicate the frequency of cells in a given quadrant. Median fluorescence intensity of IFN-γ +CD3+ cells was normalized to IFN-γ -CD3+ cells and is presented as a ratio in scatter dot plots (right panel). Statistical significance of the difference between tumor patients and normal blood donors was assessed by ANOVA followed by Dunnett's post-test (***p<0.0005). **C.** Left panel: Recursive partitioning analysis separated the trial patients into groups with higher and lower immune functional capacity (R2=0.547). Right panel pair: Linear regression analysis of IFNγ production versus peripheral blood lymphocyte frequency revealed a significant association of these variables only in the longer survival cohort with a positive correlation (R2=0.83).

with PMA/ionomycin (Supplementary Figure 1, p<0.01). Subsequent analyses will focus on patients with higher/lower functional immune capacity. Analysis of hospital-acquired blood cell counts fail to take in to consideration immune cell subsets. We performed flow cytometry phenotyping in order to further characterize the white blood cells. Frequencies of CD20+ B cells were significantly decreased in those patients with lower cohort (p<0.005) and fell outside of the normal average (Figure 2). CD4+ T cells in both cohorts were significantly lower than the normal average, while CD14+ monocytes were significantly increased compared to normal averages (Figure 2) in both partitioned cohorts. CD8+ T cells in both cohorts were similar to normal averages (Figure 2). There was no difference between the lower and higher cohorts with respect to CD4+ or CD8+ T cell, or CD14+ monocyte frequencies (Figure 2).

DISCUSSION

Like its predecessor, the revised autologous cell/chamber-based GBM vaccination trial did not raise any significant safety concerns. We recognized, however, that an immunotherapy trial for recurrent GBM faces incumbent challenges. Patients emerging from standard therapy for GBM often have severe leukopenia,[14] which was also documented in the current trial. It was therefore not surprising that we could not document T cell infiltrates in the TME after treatment. Surgery itself enhances host immune mechanisms favoring tumor growth through the attraction of M2 macrophages to the tumor environment postoperatively[15,16] suggested by the CCL2 serum spike provoked by craniotomy. Other than this post-operative serum spike, the highest levels of CCL2 expression were found in the tumor supernatants during vaccine preparation supporting well-documented observations that CCL2 is produced from cells in the TME.[17,18] The lack of a CCL2 peak after re-vaccination in two patients suggested loss of these cells after the first vaccination.

We identified two significantly different survival cohorts with different responses to this vaccine paradigm allowing us to explore the nature of potentially therapeutic immune mechanisms. Serum from the longer cohort subjects contained higher levels of tumor-specific antibody isotypes and cytokines/chemokines commonly associated with Th1 immunity including IgG1, IgG3, IL12, CXCL10, CXCL12, CCL7, CCL19, and CCL21 not seen in the short cohort.

The short survival cohort had longer overall survival perhaps in part due to MGMT methylation and better responses to temozolamide in three patients. However the treatment-induced lymphopenia and the lower CD4:CD8 ratio could perhaps also be ascribed to temozolamide. Also, elevated serum CCL2 levels found in the short cohort have been associated with the mesenchymal gene expression profile[19] and a poor prognosis[20] in glioma patients.

Cytokine production is a hallmark feature of immune function in lymphocytes. We used phorbol ester-mediated, non-specific stimulation of patient lymphocytes in order to stimulate maximal cytokine output as a surrogate indicator of immune function. IFN-γ is the classical Th1 cytokine and the logical choice for assessing immune fitness of T lymphocytes in our GBM patients. The amount of IFN-γ production by T cells following overnight stimulation was approximately half the amount produced by normal donor cells treated similarly. IFN-γ production and lymphocyte counts were strongly associated and predictively identified patients with different levels of immune fitness that fell into either the longer or short survival cohort. Lymphocytes from patients with higher functional immune capacity were more frequent and produced higher levels of IFN-γ that approached levels to those produced by normal lymphocytes stimulated under similar conditions. In contrast, T cells from trial patients in the lower immune function cohort were less in number (50%) and unable to respond to PMA stimulation.

The implanted chambers have inherent adjuvanticity. We have confirmed that the antisense sequence, its CpG motif, and the direct mixture with glioma cells in situ effectively initiate anti-tumor immunity[3] also noted by others.[21,22] The CpG motif specifically interacts with TLR94 causing plasmacytoid DC activation, measured by CD80 and CD86 expression.[5] The elevated CD4:CD8 ratio after vaccination in the longer survival cohort could reflect local TLR9 DC activation and CD4 T cell stimulation.

Evolution of resistance to treatments in gliomas has now been associated with activation of the IGF-1R signaling axis and IGF-1R inhibition through a small molecule inhibitor overcomes this resistance with improved outcomes.[23] We are currently exploring the impact of the IGF-1 bioregulatory system in recurrent gliomas and the impact of the IGF-1R AS ODN in this vaccination paradigm.

Differences in the radiographic observations between the longer and short survival patient cohorts provide further support for the concept that the vaccination paradigm may have an impact on the glioma TME. Higher rCBV values are typically associated with tumor progression,[24] and MR perfusion had only transient increases in the longer cohort, a finding not previously described. ADC measurements differentiated tumor progression (lower values) from what we interpreted as cell loss (higher values).[25]

In summary, we have established the safety profile of an improved combination glioma vaccine product and have documented alterations in immune parameters associated with clinical and radiographic improvements. Despite immune compromise, we documented favorable immune responses associated with tumor regression and longer survival after treatment. To be most effective, however, a replacement trial should include screens for immune compromise and means by which immune function could be restored prior to vaccination.

Study Oversight

The physician sponsor (DWA) was primarily responsible for the design and funding of the study. All authors participated in the conduct of the study, analysis of the data and the reporting of the results. After IRB approval, this study was overseen by an independent data safety and monitoring board appointed by the Sidney Kimmel Cancer Center at Thomas Jefferson University.

DWA and DCH have financial interests in the Imvax Corporation related to this work.

REFERENCES

1. Stupp R, Mason WP, van den Bent MJ, et al: Radiotherapy plus concomitant and adjuvant temozolomide for glioblastoma. *N Engl J Med* 352:987-96, 2005
2. Andrews DW, Resnicoff M, Flanders AE, et al: Results of a pilot study involving the use of an antisense oligodeoxynucleotide directed against the insulin-like growth factor type I receptor in malignant astrocytomas. *J Clin Oncol* 19:2189-200, 2001
3. Morin-Brureau M, Hooper KM, Prosniak M, et al: Enhancement of glioma-specific immunity in mice by "NOBEL", an insulin-like growth factor 1 receptor antisense oligodeoxynucleotide. *Cancer Immunol Immunother* 64:447-57, 2015
4. Agrawal S, Kandimalla ER: Role of Toll-like receptors in antisense and siRNA [corrected]. *Nat Biotechnol* 22:1533-7, 2004
5. Harshyne LA, Hooper KM, Andrews EG, et al: Glioblastoma exosomes and IGF-1R/AS-ODN are immunogenic stimuli in a translational research immunotherapy paradigm. *Cancer Immunol Immunother* 64:299-309, 2015
6. Verbrugge I, Hagekyriakou J, Sharp LL, et al: Radiotherapy increases the permissiveness of established mammary tumors to rejection by immunomodulatory antibodies. *Cancer Res* 72:3163-74, 2012
7. Emoto K, Yamashita S, Okada Y: Mechanisms of heat-induced antigen retrieval: does pH or ionic strength of the solution play a role for refolding antigens? *J Histochem Cytochem* 53:1311-21, 2005
8. Bloch O, Crane CA, Fuks Y, et al: Heat-shock protein peptide complex-96 vaccination for recurrent glioblastoma: a phase II, single-arm trial. *Neuro Oncol* 16:274-9, 2014
9. Kikuchi T, Akasaki Y, Abe T, et al: Vaccination of glioma patients with fusions of dendritic and glioma cells and recombinant human interleukin 12. *J Immunother* 27:452-9, 2004
10. Okada H, Lieberman FS, Edington HD, et al: Autologous glioma cell vaccine admixed with interleukin-4 gene transfected fibroblasts in the treatment of recurrent glioblastoma: preliminary observations in a patient with a favorable response to therapy. *J Neurooncol* 64:13-20, 2003
11. Prins RM, Soto H, Konkankit V, et al: Gene expression profile correlates with T-cell infiltration and relative survival in glioblastoma patients vaccinated with dendritic cell immunotherapy. *Clin Cancer Res* 17:1603-15, 2011
12. Rutkowski S, De Vleeschouwer S, Kaempgen E, et al: Surgery and adjuvant dendritic cell-based tumour vaccination for patients with relapsed malignant glioma, a feasibility study. *Br J Cancer* 91:1656-62, 2004
13. Schuessler A, Walker DG, Khanna R: Cellular immunotherapy directed against human cytomegalovirus as a novel approach for glioblastoma treatment. *Oncoimmunology* 3:e29381, 2014
14. Grossman SA, Ye X, Lesser G, et al: Immunosuppression in patients with high-grade gliomas treated with radiation and temozolomide. *Clin Cancer Res* 17:5473-80, 2011
15. Hamard L, Ratel D, Selek L, et al: The brain tissue response to surgical injury and its possible contribution to glioma recurrence. *J Neurooncol* 128:1-8, 2016
16. Predina J, Eruslanov E, Judy B, et al: Changes in the local tumor microenvironment in recurrent cancers may explain the failure of vaccines after surgery. *Proc Natl Acad Sci USA* 110:E415-24, 2013
17. Desbaillets I, Tada M, de Tribolet N, et al: Human astrocytomas and glioblastomas express monocyte chemoattractant protein-1 (MCP-1) in vivo and in vitro. *Int J Cancer* 58:240-7, 1994
18. Leung SY, Wong MP, Chung LP, et al: Monocyte chemoattractant protein-1 expression and macrophage infiltration in gliomas. *Acta Neuropathol* 93:518-27, 1997
19. Engler JR, Robinson AE, Smirnov I, et al: Increased microglia/macrophage gene expression in a subset of adult and pediatric astrocytomas. *PLoS One* 7:e43339, 2012
20. Arimappamagan A, Somasundaram K, Thennarasu K, et al: A fourteen gene GBM prognostic signature identifies association of immune response pathway and mesenchymal subtype with high risk group. *PLoS One* 8:e62042, 2013
21. Wu A, Oh S, Gharagozlou S, et al: In vivo vaccination with tumor cell lysate plus CpG oligodeoxynucleotides eradicates murine glioblastoma. *J Immunother* 30:789-97, 2007
22. Morishita M, Takahashi Y, Matsumoto A, et al: Exosome-based tumor antigens-adjuvant co-delivery utilizing genetically engineered tumor cell-derived exosomes with immunostimulatory CpG DNA. *Biomaterials* 111:55-65, 2016
23. Quail DF, Bowman RL, Akkari L, et al: The tumor microenvironment underlies acquired resistance to CSF-1R inhibition in gliomas. *Science* 352:aad3018, 2016
24. Gasparetto EL, Pawlak MA, Patel SH, et al: Posttreatment recurrence of malignant brain neoplasm: accuracy of relative cerebral blood volume fraction in discriminating low from high malignant histologic volume fraction. *Radiology* 250:887-96, 2009
25. Hein PA, Eskey CJ, Dunn JF, et al: Diffusion-weighted imaging in the follow-up of treated high-grade gliomas: tumor recurrence versus radiation injury. *AJNR Am J Neuroradiol* 25:201-9, 2004

Phase I Study of Ipilimumab Combined with Whole Brain Radiation Therapy or Radiosurgery for Melanoma Patients with Brain Metastases

Noelle L. Williams, MD[1]; Evan J. Wuthrick, MD[2]; Hyun Kim, MD[1]; Joshua D. Palmer, MD[2]; Shivank Garg, MD[1]; Harriet B. Eldredge-Hindy, MD[3]; Constantine Daskalakis, ScD[4], Kendra J. Feeney, MD[5]; Michael J. Mastrangelo, MD[5]; Lyndon J. Kim, MD[5]; Takami Sato, MD, PhD[5]; Kari L. Kendra, MD[6]; Thomas Olencki, DO[6]; David A. Liebner, MD[6]; Christopher J. Farrell, MD[7]; James J. Evans, MD[7], Kevin D. Judy, MD[7]; David W. Andrews, MD[7]; Adam P. Dicker, MD[1]; Maria Werner-Wasik, MD[1]; Wenyin Shi, MD[1]

[1]Department of Radiation Oncology, Thomas Jefferson University, Sidney Kimmel Cancer Center at Jefferson, Philadelphia, PA.
[2]Department of Radiation Oncology, Ohio State University, Columbus, OH.
[3]Department of Radiation Oncology, Baystate Medical Center, Springfield, MA.
[4]Department of Biostatistics, Thomas Jefferson University, Philadelphia, PA.
[5]Department of Medical Oncology, Thomas Jefferson University and Sidney Kimmel Cancer Center, Philadelphia, PA.
[6]Division of Medical Oncology, Ohio State University, Columbus, OH.
[7]Department of Neurosurgery, Thomas Jefferson University and Sidney Kimmel Cancer Center, Philadelphia, PA

Running Title
Ipilimumab with RT for Melanoma Brain Metastases

Funding sponsor
Bristol-Myers Squibb

Conflict of interest
none

Key Words
immunotherapy, ipilimumab, metastatic melanoma, brain metastases

ABSTRACT

Purpose: We performed a phase I study to determine the maximum tolerable dose (MTD) and safety of ipilimumab with stereotactic radiosurgery (SRS) or whole brain radiotherapy (WBRT) in patients with brain metastases (BM) from melanoma.

Methods: Based on intracranial (IC) disease burden, patients were treated with WBRT (Arm A) or SRS (Arm B). Ipilimumab starting dose was 3 mg/kg (every 3 weeks, starting on day 3 of WBRT or 2 days after SRS). Ipilimumab was escalated to 10 mg/kg using a two-stage, 3+3 design. The primary endpoint was to determine the MTD of ipilimumab combined with radiotherapy. Secondary endpoints were overall survival (OS), IC and extracranial (EC) control, progression free survival (PFS), and toxicity. This trial is registered with ClinicalTrials.gov, number NCT01703507.

Results: Characteristics of the 16 patients enrolled between 2011 and 2014 were: mean age, 60; median BM, 2 (1 to >10); number with EC disease, 13 (81%). Treatment included WBRT (n=5), SRS (n=11), ipilimumab 3mg/kg (n=7), 10 mg/kg (n=9). Median follow-up was 8 months (Arm A) and 10.5 months (Arm B). There were 21 grade 1-2 neurotoxic effects with no dose-limiting toxicities (DLTs). One patient experienced grade 3 neurotoxicity prior to ipilimumab administration. Ten additional grade 3 toxicities were reported with gastrointestinal (n=5, 31%) as the most common. There were no grade 4/5 toxicities. Median PFS and OS, respectively, in Arm A were 2.5 months and 8 months, and in Arm B were 2.1 months and not reached.

Conclusion: Concurrent ipilimumab 10 mg/kg with SRS is safe. The WBRT arm was closed early due to slow accrual, but demonstrated safety with ipilimumab 3 mg/kg. No patient experienced DLT. Larger studies with ipilimumab 10 mg/kg and SRS are warranted.

INTRODUCTION

Brain metastases (BM) occur in more than half of patients with advanced melanoma, and central nervous system disease burden often contributes to their death.[1,2] The historic median survival of patients with BM from melanoma is 4.7 months.[3] Traditional BM treatment options includes surgery, whole brain radiation therapy (WBRT), and stereotactic radiosurgery (SRS), and can prevent neurological decline and may also improve overall (OS).[4-7] There has been increasing interest in radiotherapy (RT) combined with immunotherapy (IT) with growing evidence supporting a potential synergistic effect. It remains unclear the role that this synergism has on toxicity.[8]

Activated T-cells and antibodies targeting tumor-associated antigens (TAAs) detected in blood from cancer patients supports an active role for an anti-tumor immune response.[9] T-cell infiltrates in melanoma have prognostic significance, and when identified within nodal metastases, predict benefit in patients treated with neoadjuvant interferon-α-2b.[10-13] Cytotoxic T-lymphocyte-associated antigen 4 (CTLA-4), is a negative regulator of T-cell-mediated anti-tumor immune responses and therefore represents a critical checkpoint, controlling both response duration and intensity.[14-16] Ipilimumab (MDX-010, Bristol-Myers Squibb) is a fully human monoclonal antibody

DOI: https://doi.org/10.29046/JHNJ.013.1

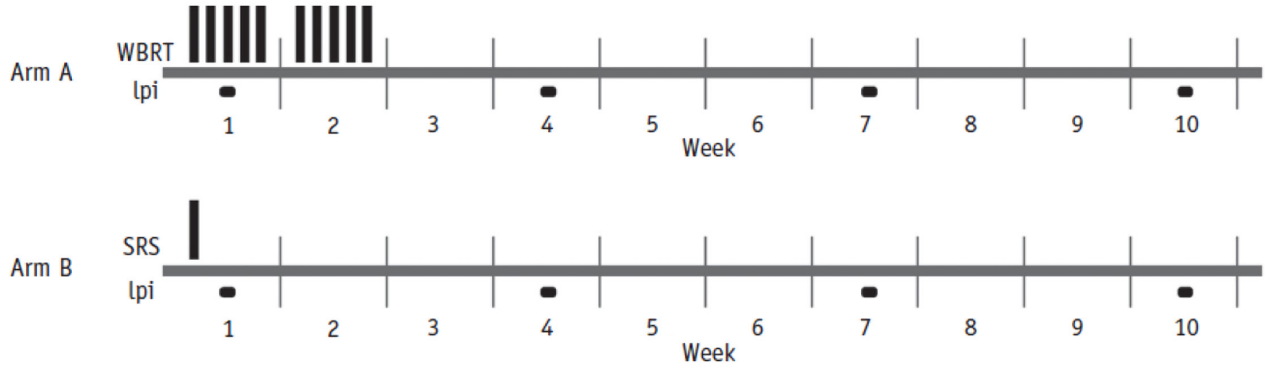

Figure 1. Treatment Schedule

directed against the CTLA-4 receptor and is FDA approved for patients with unresectable or metastatic melanoma.[17,18,19] One of the larger studies to investigate ipilimumab evaluated 127 patients and demonstrated an OS benefit (93 v. 42 weeks, P=0.0028) for patients who received concomitant IT and RT.[20]

Early in vitro studies showing a broad shoulder in the cell survival curves and a high repair rate in melanoma cells have inferred better tumor response with higher radiation doses.[21,22] Moreover, SRS delivery in close proximity to IT yields the possibility of increased immunomodulation which has been hypothesized to have an effect on distant control. This so-called "abscopal effect" is rare and intriguing, although specific mechanisms are currently incompletely understood.[23,24] In addition to the potential immunogenic advantages, concomitant treatment also limits delays in subsequent therapy.

To the best of our knowledge, we report the first prospective phase I study evaluating concurrent ipilimumab with SRS or WBRT for patients with melanoma BM, assessing the safety and tolerability of concomitant therapy as well as intracranial (IC) and extracranial (EC) control, progression-free survival (PFS), and OS.

MATERIALS AND METHODS

Study Design and Participants

This IRB-approved, open-label, phase I, clinical trial was performed between October 2012 and August 2014, at Thomas Jefferson University and Ohio State University. All patients were over 18 years old, Eastern Cooperative Oncology Group (ECOG) performance status 0 or 1, with normal hepatic and renal function and with histologic and radiographic confirmation of diagnosis. Blood count requirements were as follows: absolute neutrophil count ≥ 1000/μL, hemoglobin ≥ 9g/dL, platelets ≥ 75,000/μL. Patients were excluded if they had a history of chronic infection (HIV or Hepatitis), autoimmune condition, abnormal thyroid function, or leptomeningeal carcinomatosis.

Radiotherapy

Patients were enrolled onto one of two arms depending on their IC disease burden. Arm A (WBRT) included patients with 5 or more BM, any lesion >4 cm maximal diameter, or 1 completely resected BM with postoperative cavity >4 cm. Arm B (SRS) included patients with fewer than 5 BM (all ≤4 cm in diameter) or a single postoperative cavity <4 cm. Within each arm, RT dose was predetermined. WBRT dose was 30 Gy in 10 fractions. Ipilimumab was administered on day 3 of RT in Arm A. Arm B patients received SRS according to the maximum diameter of the BM or resection cavity according to dose prescriptions in RTOG 90-05.25 Ipilimumab was administered 2 days following SRS in Arm B (Figure 1).

Dose-Escalation Scheme

Ipilimumab was administered intravenously over 90 minutes once every 3 weeks for 4 total doses and was dose-escalated independently in each arm with no intra-patient escalation. The FDA approved dose of 3 mg/kg was the starting dose. Rationale for ipilimumab dose escalation to 10mg/kg was based on findings from the randomized, double-blind, phase 2 dose-ranging study of ipilimumab monotherapy demonstrating the best overall response rate in the 10 mg/kg group (11.1%, 95% CI 4.9-10.7) versus the 3 mg/kg group (4.2%, 95% CI 0.9-11.7), suggesting further investigation of this higher dose.[26] Following the initial 4 treatments, maintenance dosing was offered to patients without unacceptable toxicity (refractory grade > 3 immune-related adverse events [irAEs]) at the same dose level given every 12 weeks until disease progression, toxicity requiring discontinuation, or consent withdrawal.

Dose-Limiting Toxicity

Adverse events (AEs) were recorded with the Common Terminology Criteria for Adverse Events version 4.0 (CTCAE v.4). Dose-limiting toxicity (DLT) was defined as any grade 3 or higher treatment related toxicity occurring within 30 days of completing RT. Any neurological toxicity of grade 3, 4, or 5 was considered dose-limiting (except symptoms present prior to study enrollment or expected sequelae of surgery or SRS). All patients were followed for AEs for 4 weeks following the last dose of ipilimumab. Intratumoral hemorrhage

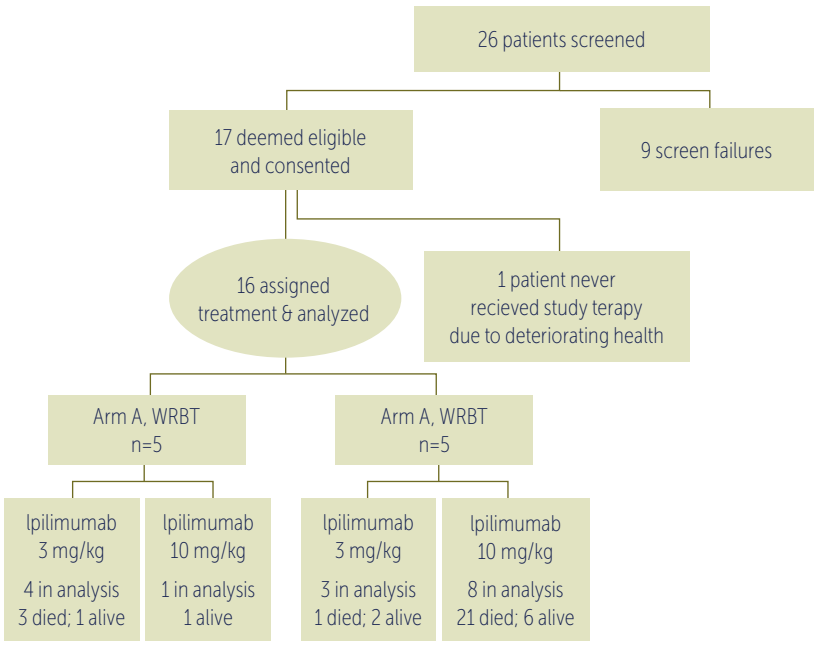

Figure 2. Consort Diagram

was defined as new or worsening signs of bleeding within the irradiated tumor or cavity volume.

Assessment of Efficacy

Contrast-enhanced MRI of the brain was performed at week 7 and then every 2 months for 1 year, then every 3 months. All MRIs were interpreted using Response Evaluation Criteria In Solid Tumors (RECIST, version 1.1)[27] and immune-related response criteria (irRC).[28] Overall response using irRC was classified as immune-related complete response (irCR), partial response (irPR), stable disease (irSD), or progressive disease (irPD) based on the predefined combination of parameters.[28] For evaluation of EC disease, CT of the chest, abdomen, and pelvis was performed at week 7 and 13 following enrollment, and every 3 months subsequently.

Statistical Methodology

A two-stage 3+3 accrual design[29] was used at each dose considered with goal accrual of up to 12 patients for each arm, with up to 9 patients accrued from either Thomas Jefferson University or Ohio State University. Initially 3 patients were enrolled at the 3 mg/kg level. If none of these patients experienced a DLT, enrollment continued to the 10 mg/kg level. If 1 of the 3 experienced toxicity at that level, 3 additional patients were accrued to the initial dose level. While waiting to complete the toxicity assessment for each triplet, additional patients could be accrued on the same dose, although their outcome was not considered for dose escalation purposes. No patient was treated at a higher dose until the 3 or 6 patients completed their toxicity evaluation period at the current dose.

Data were analyzed separately for the two arms. Kaplan-Meier estimates for OS and PFS were computed in Stata 14 (StataCorp, College Station, TX). PFS was analyzed from the date of SRS (or first day of WBRT) to the date of recurrence or progression. OS was analyzed from the date of first RT fraction to the date of death or last patient contact (censored observation). Analysis of EC control, new BM development, and safety/tolerability was done separately for each arm. All subjects enrolled in the study who received at least one dose of ipilimumab were analyzed.

Role of the Funding Source

This study was funded by Bristol-Myers Squibb (New York City, NY) which provided the study drug and worked with the senior authors in the design and analysis. All authors jointly approved this work for submission and confirm the accuracy of the data. No additional authors not listed contributed to this work. All authors affirm that this trial was performed in accordance with the protocol and all amendments.

RESULTS

Patient Characteristics

Of the 26 patients screened for the trial, 17 signed informed consent and were deemed eligible. One patient never received protocol therapy due to deteriorating health following consent. Sixteen patients received study therapy and were analyzed (Figure 2). Table 1 summarizes the patient and clinical characteristics, separately for the two arms. Overall, the mean age at time of BM diagnosis was 60 (SD, 5-13) and 75% of the patients were male. There were 8 patients each with ECOG performance status of 0 and 1. Nine patients (56%) had initial BM surgery. Thirteen patients (81%) had EC metastases at the time of BM diagnosis and 5 (38%) received RT for their EC disease.

In Arm A (WBRT, n=5), the median number of lesions was 6 (range, 1 to >10) and the dose was 30 Gy in 10 fractions for all patients. In Arm B (SRS, n=11, the median number of lesions was 2 (range, 1 to 3) and the median dose was 24 Gy (range, 15 to 24 Gy). In total, 20 lesions/cavities were treated with SRS with a median planning target volume of 3.25 cc per individual lesion (range, 0.1-22.7 cc). The median per patient treatment volume was 8.5 cc (range 0.5-29.2 cc). The median number of completed cycles of ipilimumab was as follows: 4 (range, 2 - 4+14 maintenance) for dose level 3 mg/kg (n=7), and 3 (range, 2 - 4

Table 1. Baseline Patient, Lesion, and Treatment Characteristics

Characteristic			Value
Patients (n=16)			
Mean age at IC diagnosis (range)			60 (37-75)
Sex, No. (%)	Male		13 (81%)
	Female		3 (19%)
ECOG performance status (n)	0		8
	1		7
	2		1
Number with extracranial metastases			13 (81%)
Number with pre-RT surgery			8 (50%)
Radiation technique	WBRT		5 (31%)
	Median # lesions (range)		6 (1->10)
	SRS		11 (19%)
	Median # lesions (range)		2 (1-3)
	Median dose, Gy (range)		24 (15-24)
Ipilimumab	Dose	3 mg/kg	9
	Median # cycles completed (range)		4 (2-4+14 maintenance)
	Dose	10 mg/kg	7
	Median # cycles completed (range)		3 (2-4)
Median length of follow-up after RT, months (range)			9.1 (2-37)

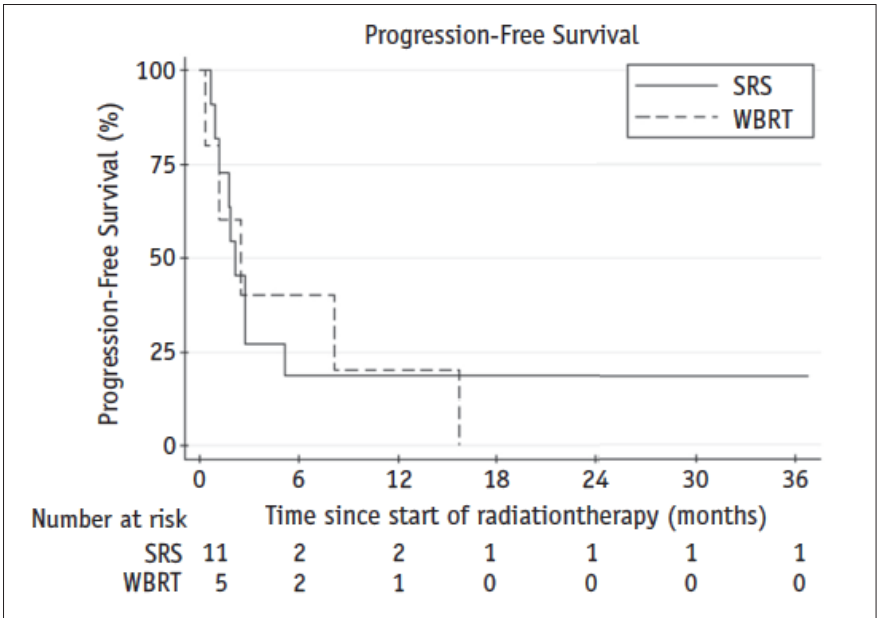

Figure 3. Progression-free survival for the SRS and WBRT patients

maintenance) for dose level 10 mg/kg (n=9). Two patients in both arms received pre-treatment dexamethasone (mean dose 6 mg/day and 3.5 mg/day in the SRS and WBRT arms, respectively).

Toxicity

Ipilimumab in combination with RT was well tolerated. There were 21 grade 1-2 neurotoxic effects including the following: headache (n=6, 37.5%), nausea/vomiting (n=3, 18.8%), subclinical intracranial hemorrhage (n=4, 25%), dizziness (n=1, 6.3%), vision changes (n=1, 6.3%), tinnitus/hearing loss (n=3, 18.8%), facial palsy (n=1, 6.3%), weakness/neuropathy (n=1, 6.3%), and seizure (n=1, 6.3%). There were no documented reports of pseudoprogression in our small sample of patients.

One patient experienced headache prompting emergency room evaluation, categorized as a grade 3 neurotoxic event. This toxicity occurred following SRS but prior to first IT administration and was therefore not considered a dose-limiting toxicity (DLT), but rather, an effect of surgery and SRS. The patient went on to receive 4 doses of ipilimumab plus one maintenance cycle prior to disease progression. There were no additional grade 3 neurotoxicities.

Table 2 summarizes the AEs in detail. In addition to the neurotoxicity above, there were 10 additional grade 3 toxicities, including gastrointestinal most commonly (n=5, 31%). There were no grade 4 or 5 toxicities. Of note, no patients experienced radionecrosis.

Progression-Free Survival and Overall Survival

Median follow-up time was 8.0 months in Arm A (range, 3.5 to 24.1) and 10.5 months in Arm B (range, 1.8 to 36.8) from first day of RT to last follow-up or death. At time of analysis, no patients were still on treatment. Fourteen patients in total progressed and/or died during the study's follow-up (5/5 = 100% in Arm A and 9/11 = 82% in Arm B). Thirteen patients had IC progression (including the 6 who subsequently died). Median time to IC progression was 2.53 months (WBRT, range 0.3-18) versus 2.45 months (SRS, range 1-37). Overall response intracranially as defined by the irRC (15

Table 2. Adverse effects in SRS (n=11) and WBRT (n=5) arms

	Grade 1 – 2		Grade 3		Grade 4	
	SRS	WBRT	SRS	WBRT	SRS	WBRT
Headache	4	2	1	0	0	0
Post-treatment subclinical intracranial hemorrhage	4	0	0	0	0	0
Nausea, vomiting, abdominal pain	2	1	0	0	0	0
Fatigue	1	1	0	1	0	0
Hearing loss, otitis, tinnitus	1	2	0	0	0	0
Skin reaction, pruritis	2	3	0	0	0	0
Diarrhea	3	2	4	1	0	0
Insomnia	0	1	0	0	0	0
Anorexia	1	2	0	0	0	0
Hot flashes	0	1	0	0	0	0
Constipation	0	1	0	0	0	0
Lymphopenia	1	0	0	1	0	0
Visual changes	0	1	0	0	0	0
Hypophysitis	0	0	0	1	0	0
Hypertension	0	1	0	0	0	0
Alopecia	0	2	0	0	0	0
Dizziness	0	1	0	0	0	0
Bone pain	0	1	0	0	0	0
Anemia	1	1	1	0	0	0
Thrombocyopenia	1	0	0	0	0	0
Depression	1	0	0	0	0	0
Lipase increase	1	0	0	0	0	0
Weakness, neuropathy	1	0	0	0	0	0
Seizure	1	0	0	0	0	0
Facial palsy	1	0	0	0	0	0
Pleuritic pain, effusion	1	0	0	0	0	0

Abbreviations: SRS=stereotactic radiosurgery; WBRT=whole brain radiation therapy.

evaluable patients) was a follows: irSD (n= 5, 33%), irPD (n=9, 60%), irPR (n=1, 7%). Following SRS, of the patients who experienced new BM or progression of existing BM (n=8), salvage treatment was as follows: 4 received salvage WBRT, 3 received further SRS, and one patient received no further IC treatment. All patients who failed following WBRT received SRS as salvage.

Median PFS time was 2.5 months in Arm A and 2.1 months in Arm B (Figure 3). Six patients died during follow-up (3/5 = 60% in Arm A and 3/11 = 27% in Arm B). Cause of death for these patients was as follows: urosepsis (n=1), cardiac arrest (n=1), hemorrhagic progression of BM (n=2), IC progression (n=1), EC progression (small bowel rupture secondary to tumor, n=1).

Median OS was 8 months in Arm A and not reached in Arm B (Figure 4).

Of the 13 patients with EC metastases at the time of BM diagnosis, 3 patients received targeted RT to the EC disease with treatment sites as follows: lung (n=2), thoracic/lumbar vertebrae and lower leg soft tissue metastasis (n=1). Of the 3 patients with no EC disease at the time of BM diagnosis, all 3 remained without EC disease at 2 month follow-up. Overall, 6 patients experienced EC progression at 2 months, 5 patients had stable disease, 3 patients continued with no EC disease, 1 patient had a partial response (after having her EC disease treated), and 1 patient did not receive systemic imaging at the 2 month time point.

Seven patients developed new BM (as differentiated from previously treated BM) on follow-up imaging (Arm A, n=1 and Arm B, n=6) with the median time from first RT fraction to new BM diagnosis of 1.9 months (range, 0.97 to 8.2). The median time from first RT fraction to development of new BM in the one patient having received WBRT was 8.2 months.

DISCUSSION

To the best of our knowledge, we report the first prospective phase I study evaluating concurrent ipilimumab with SRS or WBRT for patients with melanoma BM. The toxicity profile of escalating doses of ipilimumab demonstrated no grade 4/5 toxicity, radionecrosis, or DLTs. Ipilimumab 10 mg/kg with SRS is safe and we recommend this dose for further study with concurrent SRS. Additional phase I studies will be necessary to determine the safety of WBRT with ipilimumab 10 mg/kg, as we had to terminate this part of the trial due to slow accrual, however safety was demonstrated with concurrent WBRT and ipilimumab 3 mg/kg.

CA184-04230 was a phase II trial that evaluated ipilimumab in patients with melanoma BM. Patients were specifically excluded from the trial if they received any RT within 14 days of ipilimumab and only 8% of patients had received prior SRS. There were no unexpected toxicities and activity was demonstrated particularly when BM were small and asymptomatic.[30] However, this trial does not specifically evaluate the safety of concurrent RT and ipilimumab.

Hodi et al[18] reported a large study evaluating 676 patients randomized to receive ipilimumab 3 mg/kg in combination with an investigational peptide vaccine

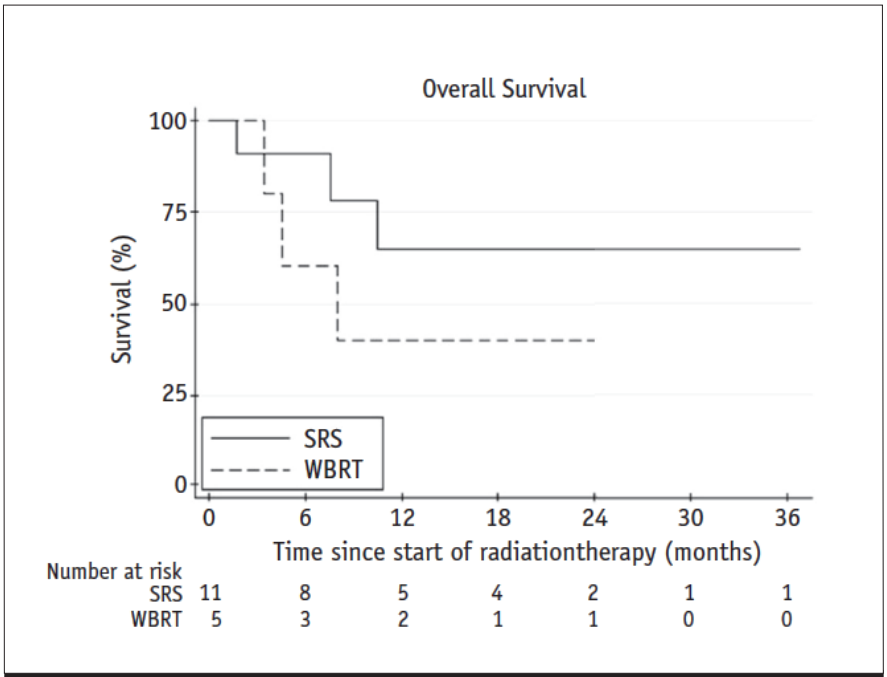

Figure 4. Overall survival for the SRS and WBRT patients

(gp100), ipilimumab alone, or gp100 alone. OS was 10.0 months in patients receiving ipilimumab plus gp100, compared to 10.1 months in the ipilimumab alone arm and 6.4 months in the gp100 alone arm (p<0.001). Eighty-two patients (12.1%) had CNS disease in this study.[18] This data is comparable to our study with the median OS not reached in the SRS arm and 8 months in the WBRT arm (median follow-up 10.5 and 8 months, respectively). Given that OS has not been reached in the SRS arm of our trial, we hypothesize that the timing of ipilimumab in close proximity to SRS may mechanistically promote duration and intensity of response in these patients, although this study is hypothesis-generating in that regard.

To this end, a recent report by Johnson et al.[31] demonstrated the impact of systemic agents on the clinical outcomes of patients with BM. Although this review included patients with many primary tumor types, and a variety of agents (BRAF inhibitors, ipilimumab in patients with melanoma primaries), the authors did show that patients receiving IT with SRS compared to SRS alone had a median survival of 18 versus 7 months and a 1-year OS of 65% versus 30% (p<0.0001).[31]

In terms post-RT lesion size, reports with combined therapy have been conflicting. Qian et al.[8] recently reported results regarding 313 melanoma BMs in 53 patients treated concurrently (defined as RT and IT delivery within 4 weeks of each other).8 IT was as follows: 54 patients (72%) received anti-CTLA-4 and 21 patients (28%) received anti-PD-1. No patients received combination IT. The median percent reduction in lesion volume was significantly greater for the concurrent group. The timing of IT and SRS did not appear to effect post-treatment lesion size.[8] In this report, only 39 lesions in 24 patients demonstrated regrowth to >120% baseline volume. Authors concluded that the early response is greater and more rapid with concurrent therapy. There was not specific mention of tumor hemorrhage in this study.[8] In contrast to this report, preliminary data reported by Shen et al. showed an increase in lesion size in 13 of 26 lesions treated concurrently (defined as IT starting "prior to or with SRS").[32] Lesion enlargement in the SRS alone cohort occurred with similar frequency. Seven of the 13 patients treated concurrently had documented hemorrhage partially accounting for the enlargement and 2 lesions had documented recurrence. Of note, the IT was not standardized in this retrospective review and included ipilimumab, nivolumab, and pembrolizumab.[32]

Kiess et al.[33] retrospectively reported response and toxicity on 46 patients with melanoma BM who received ipilimumab (3 mg/kg or 10 mg/kg) with SRS (median dose 21 Gy) between 2005 and 2011. Patients treated with SRS either before or during ipilimumab had improved OS compared to those having SRS afterward (1-year OS 56% vs 65% vs 40%, p=0.008). Moreover, only approximately 20% of patients experienced grade 3 or 4 toxicities. Interestingly, SRS before or during IT was more likely to be associated with a temporary increase in size or hemorrhage of the irradiated lesion, likely secondary to inflammation, and asymptomatic in the majority of cases.[33] Most likely due to the small numbers in our study and the frequency of neurosurgical intervention prior to SRS (6/11 patients, 55%), we did not observe the same temporary lesional edema following combination therapy. Similarly, no lesions were deemed to undergo pseudoprogression following SRS.

When evaluating the effects of IT, EC disease control is also of interest. First described in the 1950s, the abscopal effect refers to the seldom-reported phenomenon of tumor regression of a secondary site following RT to a separate primary site.[34] Seromic analysis and immunologic correlates of the abscopal effect in a patient with melanoma has demonstrated antigenic targets with increased antibody responses following RT.[35] The surprising response achieved by the patient in this report provided new insight in the mechanisms of combination therapy. Our study evaluated EC control as a secondary endpoint with a similar hypothesis that IT delivered in close proximity to SRS may impact distant control. In our study, we did not observe the abscopal effect extracranially or intracranially at non-target sites.

Limitations of our study include slow accrual to Arm A, leading to its early closure. This arm did show safety with ipilimumab 3 mg/kg, however. An additional caveat to

Table 3. Previously reported series of melanoma brain metastases treated with immunotherapy.

Primary author	Year	Analysis type	Primary	Patients who got SRS (n)	IT agent/timing	Patients receiving IT and SRS (%)	Median survival (months)	OS	Other
Knisely[41]	2012	Prospectively collected, retrospectively	melanoma	7	Ipilimumab (SRS first, n=16; IT first, n=11)	27 (35%)	21.3 (with IT) v. 4.9 (no IT)	2 year: 47.2% (with IT) v. 19.7% (no IT) p=0.044	Grade ≥3 toxicity NR
Johnson[3]	2015	retrospective	renal cell, melanoma, breast, colon, esophagus, lung	737	various agents (including BRAF inhibitors & ipilimumab), IT concurrently or within 30 days of SRS	167 (23%)	18 (with IT) v. 7 (no IT)	1 year: 65% (with IT) v. 30% (no IT) p<0.0001	Grade ≥3 toxicity NR
Kiess[3]	2015	retrospective	melanoma	46	Ipilimumab (concurrent, n=15; SRS first, n=19; IT first, n=12)	46 (100%)	12.4 (all patients)	1 year: 65% (concurrent) v. 56% (SRS before) v. 40% (IT before) P=0.008	1 year RR: 69% (concurrent) v. 64% (SRS before) v. 92% (IT before) P=0.003
Patel[42]	2015	retrospective	melanoma	54	Ipilimumab (within 4 months of SRS)	20 (37%)	9.1 (with IT) v. 8.0 (no IT) p=0.84	NA	1 year LC: 71.4% (with IT) v. 92.3% (no IT) p=0.40

NR: not reported; IT: immunotherapy; RR: regional recurrence

our study is that ipilimumab alone is no longer the standard of care for previously untreated advanced melanoma. First-line therapy is now either anti-programmed death 1 (PD-1) inhibitor monotherapy (pembrolizumab or nivolumab) or a combination of nivolumab with ipilimumab.[36] This combination of therapies improved overall response rate and PFS as compared with either treatment alone, however, demonstrated significantly increased toxicity. Compared to single agent therapy, the effect of combination therapy on OS has not yet been demonstrated.[37,38] Pembrolizumab alone demonstrated prolonged PFS and OS and had less high-grade toxicity as compared to ipilimumab in patients with advanced melanoma as demonstrated in the KEYNOTE-006 trial.[39] Based on these results, future studies will need to address RT with combination checkpoint inhibitor therapy or pembrolizumab alone.

An additional limitation is the relatively short follow-up possibly limiting the capture of late toxicity. The median follow-up in the arm receiving SRS was 10.5 months which may be long enough to catch some, but not all cases of radionecrosis. A recent report by Colaco et al.[40] evaluating 180 patients with BM who received radiosurgery with either cytotoxic chemotherapy, targeted therapy, or IT noted a significantly increased rate of radionecrosis or treatment-related imaging changes in the IT group (OR 2.40 [95% CI 1.06–5.44]; p = 0.03).[40] The median follow-up was 11.7 months and 31% of patients had melanoma primaries. Of importance, 30% of patients received prior WBRT which increases one's risk for subsequent radionecrosis following radiosurgery. For patients who received IT alone, median time to radionecrosis development was 10.2 months (range, 2.8-22.1 months), which is slightly shorter than the median follow-up in our SRS arm.[40] Therefore, although our study does have relatively short follow-up, it is worthwhile to demonstrate that we have no documented cases of radionecrosis.

In an era where combined modality targeted therapy is becoming more promising and increasingly utilized, it is important to establish the safety profiles of these modalities.[41] Our results demonstrate the safety of combining SRS with either ipilimumab 3 mg/kg or 10 mg/kg.

Future exploration of multi-agent immunotherapy in combination with SRS for melanoma BM is warranted, although currently there are no clinical trials open to accrual evaluating the safety and efficacy of this combination of treatment.

REFERENCES

1. Bafaloukos D, Gogas H. The treatment of brain metastases in melanoma patients. *Cancer Treat Rev.* 2004;30(6):515-520. doi:10.1016/j.ctrv.2004.05.001.
2. Sampson JH, Carter JH, Friedman AH, Seigler HF. Demographics, prognosis, and therapy in 702 patients with brain metastases from malignant melanoma. *J Neurosurg.* 1998;88(1):11-20. doi:10.3171/jns.1998.88.1.0011.
3. Davies MA, Liu P, McIntyre S, Kim KB, Papadopoulos N, Hwu WJ, Hwu P, Bedikian A. Prognostic factors for survival in melanoma patients with brain metastases. *Cancer.* 2011 Apr 15;117(8):1687-96. doi: 10.1002/cncr.25634. PubMed PMID: 20960525.
4. Patchell RA, Tibbs PA, Regine WF, et al. Postoperative radiotherapy in the treatment of single metastases to the brain: a randomized trial. *JAMA.* 1998;4(280(17)):1485-1489. doi:joc80445 [pii].
5. Patchell RA, Tibbs PA, Walsh JW, et al. *A Randomized Trial of Surgery in the Treatment of Single Metastases to the Brain.* Vol 322. 1990. doi:10.1056/NEJM199002223220802.
6. Andrews DW. Current Neurosurgical Management of Brain Metastases. *Semin Oncol.* 2008;35(2):100-107. doi:10.1053/j.seminoncol.2007.12.003.
7. Thomas SS, Dunbar EM. Modern multidisciplinary management of brain metastases. *Curr Oncol Rep.* 2010;12(1):34-40. doi:10.1007/s11912-009-0073-8.
8. Qian JM, Yu JB, Kluger HM, Chiang VL. Timing and type of immune checkpoint therapy affect the early radiographic response of melanoma brain metastases to stereotactic radiosurgery. *Cancer.* 2016 Jun 10. doi: 10.1002/cncr.30138. [Epub ahead of print] *PubMed PMID*: 27285122.
9. Nagorsen D, Scheibenbogen C, Marincola FM, et al. Natural T cell immunity against cancer. *Clin Cancer Res* 2003;9:4296-4303.
10. Clemente CG, Mihm MC, Jr., Bufalino R, et al. Prognostic value of tumor infiltrating lymphocytes in the vertical growth phase of primary cutaneous melanoma. *Cancer* 1996;77:1303-1310.
11. Hakansson A, Gustafsson B, Krysander L, et al. Tumour-infiltrating lymphocytes in metastatic malignant melanoma and response to interferon alpha treatment. *Br J Cancer* 1996;74:670-676.
12. Mihm MC, Jr., Clemente CG, Cascinelli N. Tumor infiltrating lymphocytes in lymph node melanoma metastases: a histopathologic prognostic indicator and an expression of local immune response. *Lab Invest* 1996;74:43-47.
13. Moschos SJ, Edington HD, Land SR, et al. Neoadjuvant treatment of regional stage IIIB melanoma with high-dose interferon alfa-2b induces objective tumor regression in association with modulation of tumor infiltrating host cellular immune responses. *J Clin Oncol* 2006;24:3164-3171.
14. Peggs KS, Quezada SA, Korman AJ, et al. Principles and use of anti-CTLA4 antibody in human cancer immunotherapy. *Curr Opin Immunol* 2006;18:206-213.
15. Robert C, Ghiringhelli F. What is the role of cytotoxic T lymphocyte-associated antigen 4 blockade in patients with metastatic melanoma? *Oncologist* 2009;14:848-861.
16. Kaehler KC, Piel S, Livingstone E, et al. Update on immunologic therapy with anti-CTLA-4 antibodies in melanoma: identification of clinical and biological response patterns, immune-related adverse events, and their management. *Semin Oncol* 2010;37:485-498.
17. Morse MA. Technology evaluation: ipilimumab, Medarex/Bristol-Myers Squibb. *Curr Opin Mol Ther* 2005;7:588-597.
18. Hodi FS, O'Day SJ, McDermott DF, et al. Improved survival with ipilimumab in patients with metastatic melanoma. *N Engl J Med* 2010;363:711-723.
19. Weber JS, O'Day S, Urba W, et al. Phase I/II study of ipilimumab for patients with metastatic melanoma. *J Clin Oncol* 2008;26:5950-5956.
20. Theurich S, Rothschild SI, Hoffmann M, Fabri M, Sommer A, Garcia-Marquez M, Thelen M, Schill C, Merki R, Schmid T, Koeberle D, Zippelius A, Baues C, Mauch C, Tigges C, Kreuter A, Borggrefe J, von Bergwelt-Baildon M, Schlaak M. Local Tumor Treatment in Combination with Systemic Ipilimumab Immunotherapy Prolongs Overall Survival in Patients with Advanced Malignant Melanoma. *Cancer Immunol Res.* 2016 Sep 2;4(9):744-54. doi: 10.1158/2326-6066.CIR-15-0156. PubMed PMID: 27466265.
21. Dewey DL. The radiosensitivity of melanoma cells in culture. *Br J Radiol.* 1971 Oct;44(526):816-7. *PubMed PMID*: 5165659.
22. Barranco SC, Romsdahl MM, Humphrey RM. The radiation response of human malignant melanoma cells grown in vitro. *Cancer Res.* 1971 Jun;31(6):830-3. *PubMed PMID*: 5088486.
23. Bernier J. Immuno-oncology: Allying forces of radio- and immuno-therapy to enhance cancer cell killing. *Crit Rev Oncol Hematol.* 2016 Dec;108:97-108. doi: 10.1016/j.critrevonc.2016.11.001. *Review*. P*ubMed PMID*: 27931845.
24. Popp I, Grosu AL, Niedermann G, Duda DG. Immune modulation by hypofractionated stereotactic radiation therapy: Therapeutic implications. Radiother Oncol. 2016 Aug;120(2):185-94. doi: 10.1016/j.radonc.2016.07.013. *Review. PubMed PMID*: 27495145.
25. Shaw E, Scott C, Souhami L, et al. Single dose radiosurgical treatment of recurrent previously irradiated primary brain tumors and brain metastases: final report of RTOG protocol 90-05. *Int J Radiat Oncol Biol Phys* 2000;47:291-298.
26. Wolchok JD, Neyns B, Linette, G, et al. Ipilimumab monotherapy in patients with pretreated advanced melanoma: A randomised, double-blind, multicentre, phase 2, dose-ranging study *Lancet Oncol*, 11 (2010), pp. 155-164.
27. Eisenhauer EA, Therasse P, Bogaerts J, Schwartz LH, Sargent D, Ford R, Dancey J, Arbuck S, Gwyther S, Mooney M, Rubinstein L, Shankar L, Dodd L, Kaplan R, Lacombe D, Verweij J. New response evaluation criteria in solid tumours: revised RECIST guideline (version 1.1). *Eur J Cancer*. 2009 Jan;45(2):228-47. doi:10.1016/j.ejca.2008.10.026. *PubMed PMID*: 19097774.
28. Wolchok JD, Hoos A, O'Day S, Weber JS, Hamid O, Lebbé C, Maio M, Binder M, Bohnsack O, Nichol G, Humphrey R, Hodi FS. Guidelines for the evaluation of immune therapy activity in solid tumors: immune-related response criteria. *Clin Cancer Res.* 2009 Dec 1;15(23):7412-20. doi: 10.1158/1078-0432.CCR-09-1624. *Epub* 2009 Nov 24. *PubMed PMID*: 19934295.
29. Storer BE. Design and analysis of phase I clinical trials. Biometrics. 1989 Sep;45(3):925-37. *PubMed PMID*: 2790129.
30. Margolin K, Ernstoff MS, Hamid O, Lawrence D, McDermott D, Puzanov I, Wolchok JD, Clark JI, Sznol M, Logan TF, Richards J, Michener T, Balogh A, Heller KN, Hodi FS. Ipilimumab in patients with melanoma and brain metastases: an open-label, phase 2 trial. *Lancet Oncol.* 2012 May;13(5):459-65. doi: 10.1016/S1470-2045(12)70090-6. *Epub* 2012 Mar 27. P*ubMed PMID*: 22456429.
31. Johnson AG, Ruiz J, Hughes R, Page BR, Isom S, Lucas JT, McTyre ER, Houseknecht KW, Ayala-Peacock DN, Bourland DJ, Hinson WH, Laxton AW, Tatter SB, Debinski W, Watabe K, Chan MD. Impact of systemic targeted agents on the clinical outcomes of patients with brain metastases. *Oncotarget*. 2015 Aug 7;6(22):18945-55. PubMed PMID: 26087184; *PubMed Central PMCID*: PMC4662466.
32. Shen C, Lin DD, Redmond KJ, Link K, Kummerlowe M, Douglass J, Lipson EJ, Sharfman W, Bettegowda C, Lim M, Kleinberg LR. Imaging and Clinical Profile Following Concurrent Stereotactic Radiation and Immune Therapy for Melanoma Brain Metastases: Preliminary Results. *Int J Radiat Oncol Biol Phys.* 2016 Oct 1;96(2S):E134. doi: 10.1016/j.ijrobp.2016.06.927. *PubMed PMID*: 27673866.

33. Kiess AP, Wolchok JD, Barker CA, Postow MA, Tabar V, Huse JT, Chan TA, Yamada Y, Beal K. Stereotactic radiosurgery for melanoma brain metastases in patients receiving ipilimumab: safety profile and efficacy of combined treatment. Int J *Radiat Oncol Biol Phys.* 2015 Jun 1;92(2):368-75. doi:10.1016/j.ijrobp.2015.01.004. *Epub* 2015 Mar 5. *PubMed PMID*: 25754629; *PubMed Central PMCID*: PMC4955924.

34. Mole RH. Whole body irradiation; radiobiology or medicine? *Br J Radiol.* 1953 May; 26(305):234-41. *PubMed PMID*: 13042090.

35. Postow MA, Callahan MK, Barker CA, Yamada Y, Yuan J, Kitano S, Mu Z, Rasalan T, Adamow M, Ritter E, Sedrak C, Jungbluth AA, Chua R, Yang AS, Roman RA, Rosner S, Benson B, Allison JP, Lesokhin AM, Gnjatic S, Wolchok JD. Immunologic correlates of the abscopal effect in a patient with melanoma. *N Engl J Med.* 2012 Mar 8;366(10):925-31. doi: 10.1056/NEJMoa1112824. PubMed PMID: 22397654; *PubMed Central PMCID*: PMC3345206.

36. National Comprehensive Cancer Network. Melanoma (Version 1.2017). https://www.nccn.org/professionals/physician_gls/PDF/melanoma.pdf. Accessed February 7, 2017.

37. Larkin J, Chiarion-Sileni V, Gonzalez R, Grob JJ, Cowey CL, Lao CD, Schadendorf D, Dummer R, Smylie M, Rutkowski P, Ferrucci PF, Hill A, Wagstaff J, Carlino MS, Haanen JB, Maio M, Marquez-Rodas I, McArthur GA, Ascierto PA, Long GV, Callahan MK, Postow MA, Grossmann K, Sznol M, Dreno B, Bastholt L, Yang A, Rollin LM, Horak C, Hodi FS, Wolchok JD. Combined Nivolumab and Ipilimumab or Monotherapy in Untreated Melanoma. *N Engl J Med.* 2015 Jul 2;373(1):23-34. doi: 10.1056/NEJMoa1504030. *PubMed PMID*: 26027431.

38. Postow MA, Chesney J, Pavlick AC, Robert C, Grossmann K, McDermott D, Linette GP, Meyer N, Giguere JK, Agarwala SS, Shaheen M, Ernstoff MS, Minor D, Salama AK, Taylor M, Ott PA, Rollin LM, Horak C, Gagnier P, Wolchok JD, Hodi FS. Nivolumab and ipilimumab versus ipilimumab in untreated melanoma. *N Engl J Med.* 2015 May 21;372(21):2006-17. doi: 10.1056/NEJMoa1414428. *PubMed PMID*: 25891304.

39. Robert C, Schachter J, Long GV, Arance A, Grob JJ, Mortier L, Daud A, Carlino MS, McNeil C, Lotem M, Larkin J, Lorigan P, Neyns B, Blank CU, Hamid O, Mateus C, Shapira-Frommer R, Kosh M, Zhou H, Ibrahim N, Ebbinghaus S, Ribas A; KEYNOTE-006 investigators.. Pembrolizumab versus Ipilimumab in Advanced Melanoma. *N Engl J Med.* 2015 Jun 25;372(26):2521-32. doi: 10.1056/NEJMoa1503093. *PubMed PMID*: 25891173.

40. Colaco RJ, Martin P, Kluger HM, Yu JB, Chiang VL. Does immunotherapy increase the rate of radiation necrosis after radiosurgical treatment of brain metastases? *J Neurosurg.* 2016 Jul;125(1):17-23. doi: 10.3171/2015.6.JNS142763. *PubMed PMID*: 26544782.

41. Vatner RE, Cooper BT, Vanpouille-Box C, Demaria S, Formenti SC. Combinations of immunotherapy and radiation in cancer therapy. *Front Oncol.* 2014 Nov 28;4:325. doi: 10.3389/fonc.2014.00325. *eCollection* 2014. *Review*. *PubMed PMID*: 25506582; *PubMed Central PMCID*: PMC4246656.

42. Knisely JP, Yu JB, Flanigan J, Sznol M, Kluger HM, Chiang VL. Radiosurgery for melanoma brain metastases in the ipilimumab era and the possibility of longer survival. *J Neurosurg.* 2012 Aug;117(2):227-33. doi: 10.3171/2012.5.JNS111929. *Epub* 2012 Jun 15. *PubMed PMID*: 22702482.

43. Patel KR, Shoukat S, Oliver DE, Chowdhary M, Rizzo M, Lawson DH, Khosa F, Liu Y, Khan MK. Ipilimumab and Stereotactic Radiosurgery Versus Stereotactic Radiosurgery Alone for Newly Diagnosed Melanoma Brain Metastases. *Am J Clin Oncol.* 2015 May 16. [Epub ahead of print] *PubMed PMID*: 26017484.

Corresponding Author

Wenyin Shi, MD, PhD
Department of Radiation Oncology
Sidney Kimmel Medical College
Thomas Jefferson University
Sidney Kimmel Cancer Center
at Jefferson
111 South 11th Street, Suite G301
Philadelphia, PA 19107

P: 215-955-6702
F: 215-955-0412
E: wenyin.shi@jefferson.edu

Principles of Pituitary Surgery

Christopher J. Farrell, MD[1]; Gurston G. Nyquist, MD[2]; Alexander A. Farag, MD[2]; Marc R. Rosen, MD[2]; James J. Evans, MD[1]

[1] Department of Neurological Surgery, Thomas Jefferson University
[2] Department of Otolaryngology, Thomas Jefferson University

INTRODUCTION

Evolution of Transsphenoidal Surgery

Since the initial description of a transnasal approach for the treatment of pituitary tumors in 1907, transsphenoidal surgery has undergone a continuous evolution marked by close collaboration between neurosurgeons and otolaryngologists. Oskar Hirsch, developed a lateral endonasal approach in 1910 that he initially performed as a five step procedure over a several week period before simplifying the procedure to a single-step submucosal transseptal approach.[1] Contemporaneously, Harvey Cushing began approaching pituitary tumors using a transsphenoidal approach but transitioned to the transcranial route due to his concern that an endonasal approach provided restricted access and poor illumination, compromising adequate decompression of the optic apparatus.[2] Most neurosurgeons followed Cushing's lead and transsphenoidal surgery was not "rediscovered" until Jules Hardy introduced the surgical microscope in the 1960s.[3]

The first completely endoscopic transsphenoidal approach for pituitary tumors was reported in 1992 by Jankowski and further advanced by the collaborative teams of Jho and Carrau in Pittsburgh and Sethi and Pillay in Singapore.[4,5] Over the last 20 years, the endoscopic technique has been adopted by a multitude of surgeons who have favored the dynamic panoramic view afforded by the endoscope, allowing for improved visualization and better resection of tumors extending into the suprasellar area and cavernous sinuses. Additionally, the advent of extended endoscopic endonasal approaches, such as the trans-planum and lateral trans-cavernous, has facilitated resection of large, invasive pituitary tumors that were previously deemed unresectable or requiring transcranial surgery.

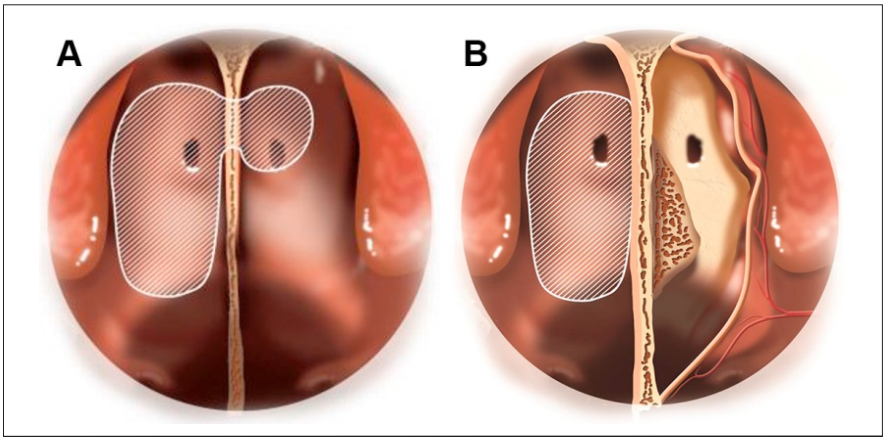

Figure 1. Nasal stage.

A. "1.5" approach to the sphenoid sinus with wide ipsilateral sphenoidotomy and limited contralateral sphenoidotomy with preservation of inferiorly located sphenopalatine arterial supply to the nasoseptal flap. **B.** "Tunnel" approach for patients with septal spurs with ipsilateral wide sphenoidotomy and submucosal elevation of septal mucoperichondrium.

Critics of the endoscopic approach have rightfully focused on the loss of stereoscopic vision as a major limitation with mastery of the procedure demanding a steep learning curve. Prospective studies directly comparing the microscopic and endoscopic approaches for pituitary tumors have not been performed, however, an increasing body of literature has established the safety and non-inferiority of endoscopic endonasal techniques and several studies have demonstrated improvement in the extent of tumor resection. McLaughlin et al. reported that following microsurgical resection of pituitary adenomas, endoscopy revealed residual tumor leading to further resection in 36% of cases.[6] Messerer et al. found their gross total resection rate increased from 50% utilizing the microscope to 76% upon initial conversion to the endoscopic approach.[7] In this review, we describe the principles of pituitary surgery including the key-elements of surgical decision-making and discuss the technical nuances distinguishing the endoscopic from the microscopic approach.

PRINCIPLES OF SURGERY

Indications for Surgery

Pituitary adenomas are most frequently categorized as functional or non-functional depending on their hormonal secretory pattern. Prolactinomas represent the most common functional adenoma and the mainstay of treatment is dopamine-agonist medical therapy, with surgical treatment reserved for patients who fail to respond despite dose-escalation or are intolerant to the medications. Transsphenoidal surgery remains the primary treatment for adenomas secreting ACTH (Cushing's disease) and growth-hormone (acromegaly) with biochemical remission rates significantly correlated with tumor size and invasiveness.[7]

Non-functional pituitary adenomas (NFPA) are extremely common — autopsy and radiographic studies reveal the presence of NFPA in 11-27% of the

population (8,9). While most NFPA are microadenomas (<1cm) and clinically asymptomatic, macroadenomas may present with compressive symptoms including headache, visual impairment, hormonal insufficiency, and cranial nerve palsies due to cavernous sinus extension. Surgery is generally indicated for patients with macroadenomas causing visual compromise or exhibiting growth on serial imaging studies. Approximately 5% of patients with pituitary adenomas present with apoplexy due to intratumoral hemorrhage or infarction.[10]

Preoperative Surgical Planning

The main goal in endoscopic pituitary surgery is to maximize tumor resection while avoiding complications such as visual deterioration, cerebrospinal fluid (CSF) leakage, endocrinopathy, vascular injury, and sinonasal morbidity. Although pituitary adenomas are typically benign lesions, recurrences are common following incomplete surgical removal and thorough preoperative surgical planning is essential to achieve optimal outcomes.

Magnetic resonance imaging (MRI) studies reliably delineate the size and extension of pituitary tumors, with the notable exception of some ACTH-secreting microadenomas that may be radiographically occult. Inspection of the preoperative MRI provides an assessment of the likelihood of gross total resection primarily based on cavernous sinus extension as well as a prediction of the surgical challenges that will be encountered such as intraoperative CSF leakage and a narrow surgical corridor due to reduced distance between the parasellar carotid arteries. Large tumors that extend vertically within the suprasellar area may significantly compromise the diaphragma sellae or even invade the ventricular system resulting in high-flow CSF leaks requiring more extensive repairs such as nasoseptal flap (NSF) placement, lumbar drainage, or use of autologous tissues (e.g., fascia lata or adipose tissue). As discussed in more detail later, preoperative anticipation of the need for a NSF is critical as the flap must either be harvested during the initial nasal stage of the approach or the vascular pedicle to the flap preserved such that a viable flap can be harvested later should it prove necessary. Additionally, detection of the position of the normal compressed pituitary gland on the pre-operative MRI assists with the preservation of hormonal function as intraoperative distinction of the gland from tumor based on color and consistency differences is frequently subtle.

Computed tomography studies provide complementary information helpful in surgical planning. Coronal and sagittal reconstructions reveal bony changes such as erosion of the sellar floor and dorsum and can be used intraoperatively for image guidance, especially in patients with altered sinonasal anatomy related to prior surgery. Similarly, we have found preoperative nasal endoscopy helpful to optimize our surgical plan and avoid complications related to paranasal sinus disease or anatomic variability. Typically, chronic rhinosinusitis does not represent an absolute contraindication to transsphenoidal surgery, however, patients with acute rhinosinusitis, especially those with fungal disease, should be treated appropriately prior to elective surgery.[11] Otolaryngology preoperative evaluation is critical in patients with acromegaly who frequently present challenges for airway management during surgery due to soft tissue hypertrophy and bony abnormalities.[12]

Surgical Approach: Nasal Stage

The endoscopic surgical approach for pituitary tumors can be divided into the nasal, sphenoidal, and sellar stages. Since the inception of our endoscopic skull base program at Thomas Jefferson University in 2005, we have advocated for a team approach between otolaryngology and neurosurgery. The complementary skill of experienced sinus and pituitary surgeons has enabled us to optimize oncologic outcomes and minimize complications, both minor and major. Our approach to pituitary surgery has evolved and we have adopted a tailored approach to these tumors based on their size, invasiveness, and secretory pattern allowing us to minimize sinonasal disruption without compromising tumor resection.

Patients are positioned supine with the head on a gel headrest. Neuronavigation is used routinely to help guide the surgical approach and assess the adequacy of tumor resection with co-registration of the preoperative CT and MR images using facemask fiducials. Although neuronavigation is valuable, over-reliance on this adjunct and a failure to correlate with anatomic landmarks can lead the surgeon off course. The head is slightly elevated to reduce mucosal congestion and venous oozing/bleeding during the approach. We do not routinely prepare the skin of the face or nasal cavity with antiseptic solution, but graft sites such as the lateral thigh for fascia lata or adipose tissue should be prepared in a sterile standard fashion.

The turbinates are gently lateralized with a blunt instrument. Although routine resection of the middle turbinates is favored by some surgeons to increase the nasal working corridor, we have found that turbinate lateralization combined with a limited posterior septectomy provides more than sufficient access to the sella for pituitary tumor resection and minimizes post-operative patient sinonasal morbidity.[13,14] A binarial approach is typically performed allowing for two surgeons to work simultaneously with up to four instruments in the field, including the endoscope. In our experience, a pedicled nasoseptal flap (NSF) is rarely necessary for cranial base repair during standard transsellar pituitary adenoma resection, however, in certain cases the need for a NSF is unanticipated or may become necessary during future surgeries.[15] As such, we advocate at least unilateral preservation of the NSF whenever possible and have described a variety of tailored approaches to the sphenoid sinus that enable NSF preservation applicable to endoscopic pituitary surgery. Our standard approach, termed the "1.5 approach", involves an ipsilateral wide sphenoidotomy ("1") on the working instrument side with a limited contralateral sphenoidotomy ("0.5") on the endoscope side (Figure 1A). The limited sphenoidotomy is performed by extending the natural sphenoid os superiorly with Kerrison rongeurs, thus preserving the more inferiorly located sphenopalatine artery supply to the nasal septal mucoperiosteum and mucoperichondrium. Addition of a limited posterior septectomy (typically 1cm) allows communication of the binarial sphenoid exposures and provides ample working room and maneuverability

(unpublished data). In patients with nasal obstruction due to septal deviation or large spurs, a "tunnel approach" is performed involving a septoplasty and submucosal "tunnel" with a wide contralateral sphenoidotomy (Figure 1B). The approach begins with a standard hemitransfixion incision used for septoplasty and the septal mucoperichondrium is raised and extended posteriorly over the vomer and laterally along the sphenoid rostrum. A septoplasty or spur removal is then performed, with the resultant unilateral "tunnel" analogous to the standard microscopic transeptal approach with preservation of the NSF ipsilaterally. On the contralateral side, a wide sphenoidotomy is performed. If NSF harvest proves necessary, the superior and inferior incisions for the flap can be performed and elevation completed on the "tunnel" side. The NSF harvest and replacement ("raise and return") approach involves a standard harvest of the NSF combined with a wide contralateral sphenoidotomy. We typically reserve this approach for cases in which there is a high likelihood of NSF utilization such as tumors with very significant vertical suprasellar extension or that extend anteriorly over the planum where, depending on tumor consistency, an extended endonasal approach may become necessary for complete tumor resection. This approach is also used for cases with potential for a high-flow CSF leak. If cranial base repair with the NSF proves unnecessary, the flap can be returned to its native position along the septum. These "raised and returned" flaps tend to heal quite well with minimal crusting and post-operative discomfort. We do not advocate routine harvest of the NSF, however, as this technique is associated with increased sinonasal morbidity including the possibility of olfactory dysfunction, septal perforation, and sensory loss due to superior alveolar nerve injury. A variety of authors have described "rescue flap" modifications where the nasoseptal flap is partially raised during the nasal stage such that the vascular pedicle is preserved, although these modifications have been associated in some cases with increased risk of olfactory loss.[16,17]

Surgical Approach: Sphenoid Stage

The anatomy of the sphenoid sinus is highly variable in regard to its bony septa and pneumatization. The configuration of sphenoid sinus pneumatization can significantly affect access to the sella. The pneumatization of the sphenoid sinus is usually completed by age ten and the majority of adults possess the well-pneumatized sellar pattern.[18] The sellar floor lies along the posterior wall of the sphenoid sinus within the midline and the importance of maintaining a midline orientation cannot be overstated. In addition to the sellar prominence, anatomic landmarks along the posterior sphenoid wall include the medial and lateral opticocarotid recesses, parasellar carotid prominences, and clival recess. Frequently, the entirety of these landmarks may not be plainly apparent and careful attention to the preoperative imaging combined with judicious use of neuronavigation will prevent inadvertent complications. The intra-sphenoidal septa should be taken down with use of the high-speed drill or Thru-cutting instruments, avoiding any fracturing or rotational maneuvers as these septa often have posterior attachments along the carotid prominences. Additionally, anticipating the presence of Onodi air cells will prevent injury to the optic nerves. Endoscopic transsphenoidal pituitary approaches can be safely performed in children and adults with the conchal and pre-sellar variant patterns, but prolonged drilling will be required along with an increased reliance on neuronavigation.

The sella is typically expanded in the presence of macroadenomas and the bony floor may be thinned or absent. Conversely, microadenomas do not cause expansion or thinning of the sellar floor, often requiring bone removal with a diamond burr to access the dura. The sphenoid mucosa should be stripped from the sellar floor bluntly or with gentle bipolar cautery prior to drilling the sella. Monopolar cautery may lead to optic nerve or carotid injury and its use is highly contraindicated along the posterior sphenoid wall. If a NSF will be placed for repair, further mucosal stripping should be performed to prevent delayed mucocele development by trapping mucosa under the flap. Bony removal of the sellar floor is usually performed with rotatable Kerrison rongeurs after a pilot bony opening has been created with the drill or Cottle elevator. As opposed to the microscopic approach where all but the central portion of the intrasellar tumor is removed based on "feel", bony removal for the endoscopic approach needs to be more extensive to maximize the visualization benefits of the endoscope and allow for tumor dissection. In the endoscopic approach, the anterior wall of the sella should be removed to the medial edges of the cavernous sinuses bilaterally and extended superiorly to the intracavernous sinus in the region of the tuberculum sella (Figure 2A). The amount of bony removal of the sellar floor is variable, however, for tumors with significant suprasellar extension additional removal of the floor allows for introduction of more vertically angled instruments helpful in removing tumor that fails to descend into the sella following debulking. For tumors that clearly invade the cavernous sinuses, further lateral bony removal across the anterior face of the parasellar carotid arteries can be performed.

Surgical Approach: Sellar Stage

The exposed dura of the sella is then opened in a cruciate fashion with a retractable knife and angled scissors. Horizontal cuts should be made in a lateral-to-medial direction to avoid carotid injury while the vertical incision should be made in a superior-to-inferior direction to avoid inadvertent entry into the anterior arachnoid cistern with resultant CSF leakage (Figure 2A). The principles of tumor removal differ for micro- and macro-adenomas. Historically, pituitary adenomas have been resected in a piecemeal fashion using a variety of blunt ring curette-type instruments. Oldfield et al., however, demonstrated the advantages of dissection of the histologic pseudocapsule surrounding pituitary adenomas, allowing microadenomas to ideally be resected in an en-bloc extracapsular fashion (Figure 2B).[19] When feasible, en bloc resection reduces the likelihood of tumor remnants and increases biochemical remission for functional adenomas.[20] Rarely, in patients with Cushing's disease, a pituitary microadenoma may not be visible on MR imaging but the diagnosis confirmed by adrenocorticotropic hormone (ACTH)-dependent elevation of cortisol levels and

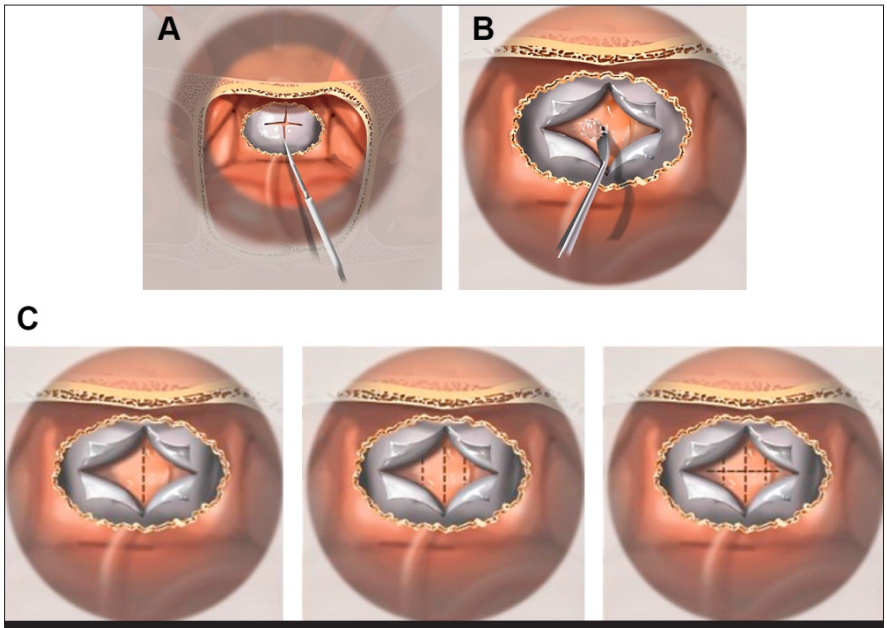

Figure 2. Microadenoma removal.

A. Bony removal of sellar floor to medial extent of cavernous sinuses bilateral and cruciate dural opening performed with retractable blade. **B.** En bloc resection of pituitary microadenoma with extracapsular dissection. **C.** Pituitary gland exploration for occult microadenoma with staged vertical and horizontal gland incisions.

high-dose dexamethasone suppression. In these cases, ACTH levels are measured from the inferior petrosal sinuses using invasive catheters to determine the likely side of the adenoma within the sella. The pituitary gland is then explored systematically using a series of horizontal and vertical incisions to identify the adenoma beginning on the presumptive side (Figure 2C).

En bloc resection of macroadenomas is rarely possible and we advocate a strategy of systematic internal debulking followed by extracapsular dissection along the cavernous sinus walls and diaphragm. As shown in Figure 3, the inferior aspect of the tumor is first debulked with ring curettes in the midline before extending posteriorly to the dorsum sella and laterally toward the medial cavernous sinus walls. Pituitary adenomas are frequently soft tumors and overzealous interior debulking can lead to premature diaphragma sellae herniation with subsequent trapping of tumor within the folds of the collapsed arachnoid. Manipulation of the diaphragm in order to complete tumor removal from these folds often leads to compromise and intraoperative CSF leakage. To avoid this, the lateral superior recesses should be debulked prior to continued midline debulking. Once the tumor has been adequately debulked, the interface between the dura and the tumor pseudocapsule is defined with angled curettes and developed in an extracapsular fashion toward the medial cavernous sinus wall. For tumors without true cavernous sinus invasion, this pseudocapsule can be dissected circumferentially and then brought down away from the diaphragm. The transition zone between the normal gland and the tumor must be anticipated and carefully developed to avoid injury to the gland and resultant pituitary insufficiency.

Infrequently, pituitary macroadenomas may be extremely fibrous and resection of these tumors can be considerably more dangerous due to the need for sharp debulking, placing the carotid arteries and optic apparatus at increased risk for injury. We have found use of ultrasonic aspirators and side-cutting rotatable microdebriders (NICO Myriad System, NICO corp.) extremely helpful in performing tumor debulking with location of the carotid arteries repetitively confirmed with neuronavigation and the micro-Doppler. In rare cases where adequate decompression cannot be safely performed through a standard transsphenoidal transsellar opening, we convert to an extended endoscopic approach (EEA) with drilling of the tuberculum sella and planum. The additional bony removal and more anterior dural opening enables tumor to be dissected from the optic nerves and chiasm under direct visualization but requires more extensive skull base repair.

The most frequent areas of tumor residual following transsphenoidal resection of pituitary macroadenomas are the cavernous sinuses and suprasellar area.[21] Once tumor resection is felt to be completed, the sellar cavity is directly inspected with 30-70° endoscopes, with careful attention to these areas as well as for detection of tumor remnants adherent to the normal pituitary gland.

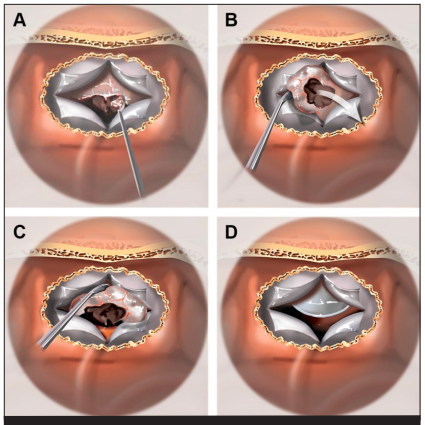

Figure 3. Macroadenoma removal.

A. Initial debulking with blunt ring curettes is performed within the midline inferior extent of the pituitary macroadenoma. **B.** After interior debulking, extracapsular dissection of the lateral aspect of tumor is performed with separation of the tumor pseudocapsule from the medial wall of the cavernous sinus. **C.** Superior extracapsular dissection of the tumor away from the diaphragma sellae. **D.** Symmetric descent of the diaphragm after complete macroadenoma removal.

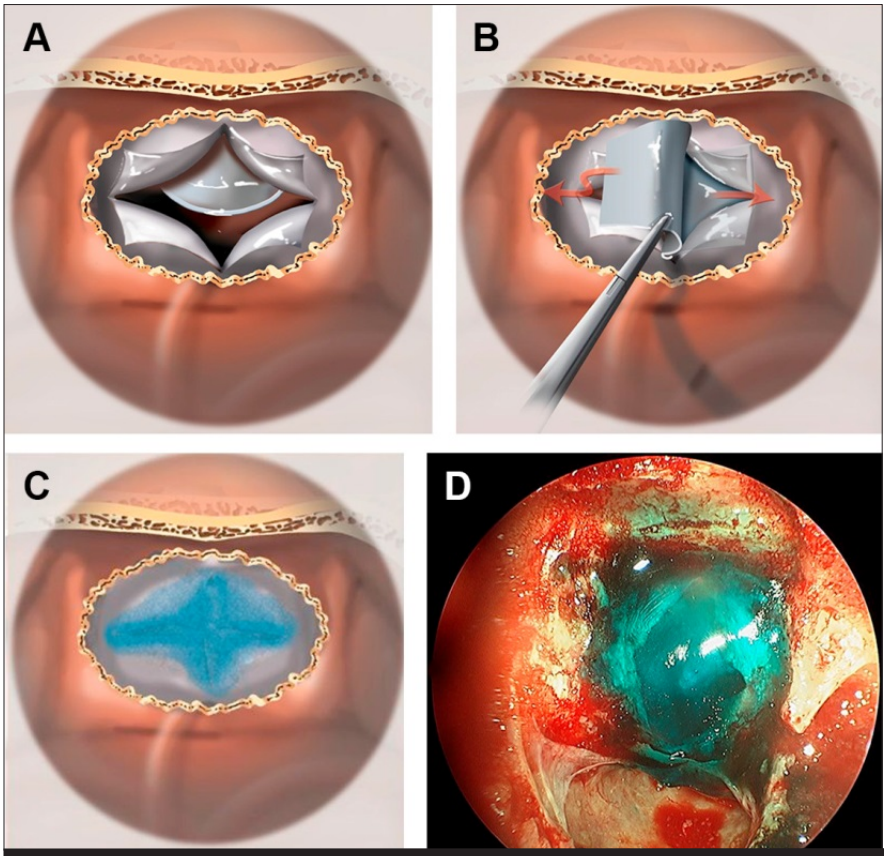

Figure 4. Dural reconstruction.

A. Intrasellar cavity after tumor resection with incompetent diaphragma sellae and low-flow CSF leakage. **B.** Placement of "inlay" synthetic dural substitute beneath leaves of dura. **C.** Supplementation of dural graft with tissue sealant. **D.** Intraoperative view after dural reconstruction with watertight closure.

Symmetric descent of the diaphragm into the sella is usually indicative of optic chiasm decompression and failure of the diaphragm to descend or asymmetric descent should prompt further search for residual tumor. After final confirmation of complete tumor resection, meticulous hemostasis is achieved with the use of hemostatic matrix agents and gentle packing with cottonoids. In our experience, the most common reason for postoperative hemorrhage has been incomplete tumor resection and absolute hemostasis is necessary when residual tumor is expected.

A graded approach to dural reconstuction is performed and in the absence of any intraoperative CSF leakage as confirmed by Valsalva maneuver, the dura is simply covered with a layer of absorbable hemostatic cellulose to promote epithelialization. Small dural defects resulting in low-flow CSF leakage are repaired with a synthetic dural substitute inlay graft placed under the leaflets of the dural opening and supplemented with a thin layer of dural sealant (Figure 4). For larger diaphragmatic defects, the arachnoid is directly repaired with an onlay dural substitute covering the site of leakage followed by placement of an inlay dural graft and sealant. For EEA and high-flow leaks related to entry into the ventricular system, a NSF is used to buttress the synthetic dural graft repair or a fascia lata "button" graft repair as previously described.[25] Lumbar drain placement and nasal packing are rarely necessary for CSF leak avoidance.

Cavernous Sinus Invasion

The cavernous sinuses are paired thin-walled venous channels located lateral to the sella. The internal carotid artery (ICA) and its branches course within the center of the channel with the oculomotor, trochlear, abducens, and trigeminal cranial nerves located more laterally. Pituitary adenomas commonly invade the medial wall of the cavernous sinus within the carotid siphon with the extent of invasion predicting the likelihood of gross total tumor resection. Although the endoscopic approach provides improved visualization of tumor within the cavernous sinus, complete resection remains challenging.[23] In the majority of patients, the presence of residual benign adenoma within the cavernous sinuses can be managed expectantly or with radiation therapy (e.g., stereotactic radiosurgery or stereotactic radiotherapy) with control rates for non-functional tumors typically around 90%.[24] Tumor control rates following radiosurgery are significantly reduced, however, for larger volume tumors demonstrating the importance of maximal surgical debulking prior to radiation treatment. Biochemical remission rates for functional adenomas are significantly lower than tumor control rates with remission achieved in only approximately half of patients with Cushing's disease and acromegaly.[25] As such, more aggressive resection of functional tumors invading the cavernous sinus is often appropriate with the goal of either achieving complete resection or reduction of the residual tumor volume for subsequent radiosurgery.

Surgical approaches to the cavernous sinus include the medial and lateral approaches. The medial approach (Figure 5A) is a continuation of the standard transsphenoidal approach but involves following the adenoma through the cavernous sinus medial wall breach. To increase access to the cavernous sinus, the sellar bony opening is extended laterally across the anterior face of the carotid artery. Intrasellar tumor resection is completed before entry into the cavernous sinus. The cavernous sinus should be approached through the contralateral nare using angled ring curettes and suctions to optimize the angle of attack with visualization performed using a 30-70° endoscope.

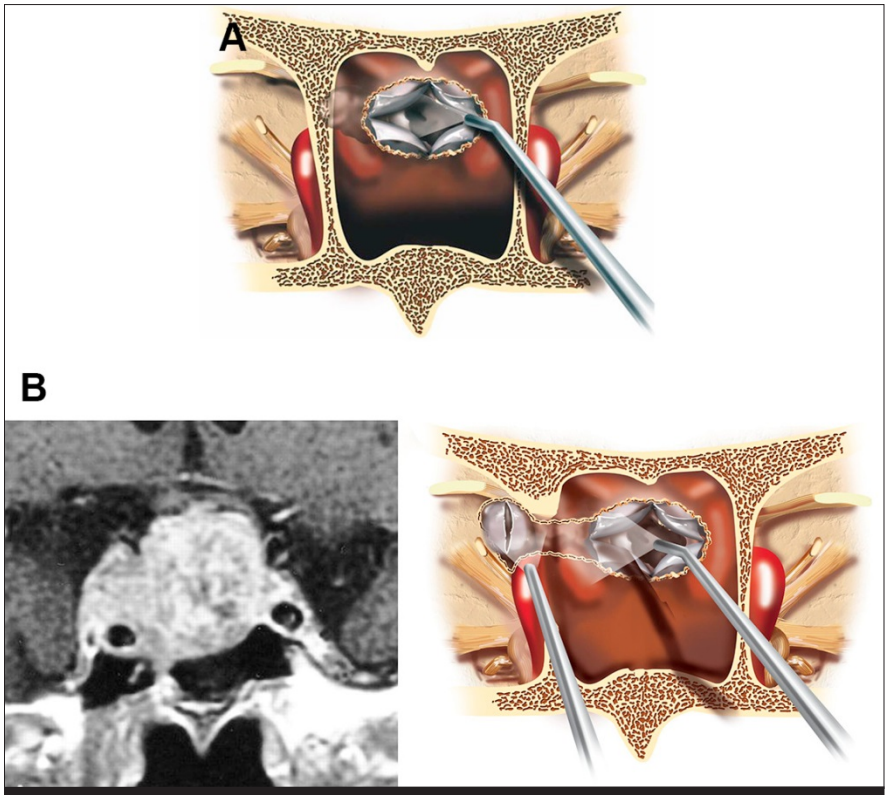

Figure 5. Cavernous sinus approaches.

A. Medial cavernous sinus approach with widened bony opening over carotid prominence and tumor debulking through the medial cavernous sinus wall with angled endoscopes and curettes. **B.** Lateral cavernous sinus approach with removal of pterygoid process after ipsilateral ethmoidectomies. After maximal debulking of the tumor within the sella and medial aspect of the cavernous sinus, the carotid artery is localized with the micro-Doppler and the lateral cavernous sinus wall opened sharply for further macroadenoma removal.

Further opening of the medial cavernous wall may be required to allow for instrument entry and is done using sharp dissection after the exact position of the carotid artery has been confirmed with Doppler ultrasonography. Vigorous venous bleeding is expected following removal of tumor from the cavernous sinus and is usually easily controlled with hemostatic matrix agents.

A lateral cavernous sinus approach may be considered in patients harboring functional adenomas or who have failed prior radiation with the bulk of their cavernous sinus tumor volume lateral to the carotid artery, although the risk of cranial nerve and ICA injury are significantly increased with this approach (Figure 5B). Fortunately, the majority of cranial nerve palsies are transient, resolving within several weeks or months, and use of electrophysiologic monitoring of the oculomotor, trochlear, and abducens nerves may further reduce the likelihood of permanent injury. To access the region lateral to the carotid artery, a wide lateral sphenoid sinus exposure is necessary often with a transpterygoid extension. During the nasal stage, a complete unilateral anterior and posterior ethmoidectomy is performed after removal of the middle turbinate. The vidian canal is identified in the lateral floor of the sphenoid sinus and the superomedial aspect of the pterygoid process is removed to expose the lateral aspect of the cavernous sinus. Careful evaluation of the preoperative CT images helps determine the access to the lateral cavernous sinus and in some patients with large, well-pneumatized sphenoid sinuses, access may be achieved through the lateral sphenoid sinus recess without extensive pterygoid drilling. After carotid artery localization with the micro-Doppler, the dura is opened sharply and tumor resected. A multi-layered closure with NSF coverage is then performed.

The most feared and potentially devastating morbidity with the cavernous sinus approaches is ICA rupture with the likelihood of injury increased with fibrous tumors and prior irradiation. Management of carotid artery injury will be more extensively discussed in other chapters of this edition but typically requires intraoperative control using direct compression followed by vessel sacrifice in the interventional angiography suite.[26]

CONCLUSION

Endoscopy represents the most recent evolution of transsphenoidal surgery. Although the endoscopic approach has not been proven to be superior to the classical microscopic approach for resection of pituitary adenomas, the benefits of endoscopy become most apparent during removal of large, invasive tumors where the panoramic visualization afforded by the endoscope allows for more complete resections to be performed. As neurosurgeons continue to take on the challenge of endoscopy and surmount their learning curve, endoscopic transsphenoidal surgery for pituitary adenomas will certainly become the standard.

REFERENCES

1. Lanzino G, Laws ER. Pioneers in the development of transsphenoidal surgery: Theodor Kocher, Oskar Hirsch, and Norman Dott. *J Neurosurg.* 2001 Dec;95(6):1097–103.
2. Liu JK, Cohen-Gadol AA, Laws ER, Cole CD, Kan P, Couldwell WT. Harvey Cushing and Oskar Hirsch: early forefathers of modern transsphenoidal surgery. *J Neurosurg.* 2005 Dec;103(6):1096–104.

3. Patel SK, Husain Q, Eloy JA, Couldwell WT, Liu JK. Norman Dott, Gerard Guiot, and Jules Hardy: key players in the resurrection and preservation of transsphenoidal surgery. *Neurosurg Focus*. 2012 Aug;33(2):E6.
4. Jankowski R, Auque J, Simon C, Marchal JC, Hepner H, Wayoff M. Endoscopic pituitary tumor surgery. *The Laryngoscope*. 1992 Feb;102(2):198–202.
5. Jho HD, Carrau RL. Endoscopic endonasal transsphenoidal surgery: experience with 50 patients. *J Neurosurg.* 1997 Jul;87(1):44–51.
6. McLaughlin N, Eisenberg AA, Cohan P, Chaloner CB, Kelly DF. Value of endoscopy for maximizing tumor removal in endonasal transsphenoidal pituitary adenoma surgery. *J Neurosurg.* 2013 Mar;118(3):613–20.
7. Messerer M, De Battista JC, Raverot G, Kassis S, Dubourg J, Lapras V, et al. Evidence of improved surgical outcome following endoscopy for nonfunctioning pituitary adenoma removal. *Neurosurg Focus*. 2011 Apr;30(4):E11.
8. Naidich MJ, Russell EJ. Current approaches to imaging of the sellar region and pituitary. *Endocrinol Metab Clin North Am.* 1999 Mar;28(1):45–79, vi.
9. Molitch ME, Russell EJ. The pituitary "incidentaloma." *Ann Intern Med.* 1990 Jun 15;112(12):925–31.
10. Nawar RN, AbdelMannan D, Selman WR, Arafah BM. Pituitary tumor apoplexy: a review. *J Intensive Care Med.* 2008 Apr;23(2):75–90.
11. Nyquist GG, Friedel ME, Singhal S, Beahm DD, Farrell CJ, Evans JJ, et al. Surgical management of rhinosinusitis in endoscopic-endonasal skull-base surgery. *Int Forum Allergy Rhinol.* 2015 Apr;5(4):339–43.
12. Friedel ME, Johnston DR, Singhal S, Al Khalili K, Farrell CJ, Evans JJ, et al. Airway management and perioperative concerns in acromegaly patients undergoing endoscopic transsphenoidal surgery for pituitary tumors. *Otolaryngol–Head Neck Surg Off J Am Acad Otolaryngol-Head Neck Surg.* 2013 Dec;149(6):840–4.
13. Schmitt H, Buchfelder M, Radespiel-Tröger M, Fahlbusch R. Difficult intubation in acromegalic patients: incidence and predictability. *Anesthesiology*. 2000 Jul;93(1):110–4.
14. Cavallo LM, Messina A, Cappabianca P, Esposito F, de Divitiis E, Gardner P, et al. Endoscopic endonasal surgery of the midline skull base: anatomical study and clinical considerations. *Neurosurg Focus.* 2005 Jul 15;19(1):E2.
15. Nyquist GG, Anand VK, Brown S, Singh A, Tabaee A, Schwartz TH. Middle turbinate preservation in endoscopic transsphenoidal surgery of the anterior skull base. *Skull Base Off J North Am Skull Base Soc Al.* 2010 Sep;20(5):343–7.
16. Hadad G, Bassagasteguy L, Carrau RL, Mataza JC, Kassam A, Snyderman CH, et al. A novel reconstructive technique after endoscopic expanded endonasal approaches: vascular pedicle nasoseptal flap. *The Laryngoscope*. 2006 Oct;116(10):1882–6.
17. Griffiths CF, Cutler AR, Duong HT, Bardo G, Karimi K, Barkhoudarian G, et al. Avoidance of postoperative epistaxis and anosmia in endonasal endoscopic skull base surgery: a technical note. *Acta Neurochir* (Wien). 2014 Jul;156(7):1393–401.
18. Otto BA, Bowe SN, Carrau RL, Prevedello DM, Ditzel Filho LF, de Lara D. Transsphenoidal approach with nasoseptal flap pedicle transposition: modified rescue flap technique. *The Laryngoscope*. 2013 Dec;123(12):2976–9.
19. Hong SD, Nam D-H, Park J, Kim HY, Chung S-K, Dhong H-J. Olfactory outcomes after endoscopic pituitary surgery with nasoseptal "rescue" flaps: electrocautery versus cold knife. *Am J Rhinol Allergy*. 2014 Dec;28(6):517–9.
20. Hamid O, El Fiky L, Hassan O, Kotb A, El Fiky S. Anatomic Variations of the Sphenoid Sinus and Their Impact on Trans-sphenoid Pituitary Surgery. *Skull Base Off J North Am Skull Base Soc Al.* 2008 Jan;18(1):9–15.
21. Reittner P, Doerfler O, Goritschnig T, Tillich M, Koele W, Stammberger H, et al. Magnetic resonance imaging patterns of the development of the sphenoid sinus: a review of 800 patients. *Rhinology*. 2001 Sep;39(3):121–4.
22. Luginbuhl AJ, Campbell PG, Evans J, Rosen M. Endoscopic repair of high-flow cranial base defects using a bilayer button. The Laryngoscope. 2010 May;120(5):876–80.
23. Oldfield EH, Vortmeyer AO. Development of a histological pseudocapsule and its use as a surgical capsule in the excision of pituitary tumors. *J Neurosurg.* 2006 Jan;104(1):7–19.
24. Monteith SJ, Starke RM, Jane JA, Oldfield EH. Use of the histological pseudocapsule in surgery for Cushing disease: rapid postoperative cortisol decline predicting complete tumor resection. J Neurosurg. 2012 Apr;116(4):721–7.
25. Hofstetter CP, Nanaszko MJ, Mubita LL, Tsiouris J, Anand VK, Schwartz TH. Volumetric classification of pituitary macroadenomas predicts outcome and morbidity following endoscopic endonasal transsphenoidal surgery. *Pituitary*. 2012 Sep;15(3):450–63.
26. Woodworth GF, Patel KS, Shin B, Burkhardt J-K, Tsiouris AJ, McCoul ED, et al. Surgical outcomes using a medial-to-lateral endonasal endoscopic approach to pituitary adenomas invading the cavernous sinus *J Neurosurg.* 2014 May;120(5):1086–94.
27. Ceylan S, Koc K, Anik I. Endoscopic endonasal transsphenoidal approach for pituitary adenomas invading the cavernous sinus. *J Neurosurg.* 2010 Jan;112(1):99–107.
28. Ding D, Starke RM, Sheehan JP. Treatment paradigms for pituitary adenomas: defining the roles of radiosurgery and radiation therapy. *J Neurooncol.* 2014 May;117(3):445–57.
29. Dallapiazza RF, Jane JA. Outcomes of Endoscopic Transsphenoidal Pituitary Surgery. *Endocrinol Metab Clin North Am.* 2015 Mar;44(1):105–15.
30. Shakir HJ, Garson AD, Sorkin GC, Mokin M, Eller JL, Dumont TM, et al. Combined use of covered stent and flow diversion to seal iatrogenic carotid injury with vessel preservation during transsphenoidal endoscopic resection of clival tumor. *Surg Neurol Int.* 2014;5:81.
31. Koitschev A, Simon C, Löwenheim H, Naegele T, Ernemann U. Management and outcome after internal carotid artery laceration during surgery of the paranasal sinuses. *Acta Otolaryngol* (Stockh). 2006 Jul;126(7):730–8.

Key Points

1. *Understand the principles of pituitary surgery including the key-elements of surgical planning and decision-making*
2. *Identify the technical nuances distinguishing the endoscopic from the microscopic transsphenoidal approach*
3. *Understand the strategies utilized during the nasal, sphenoidal, and sellar stages of surgery that maximize tumor resection while minimizing complications and preserving sinonasal anatomy/function*

Corresponding Author

Christopher J. Farrell, MD
Department of Neurological Surgery
Sidney Kimmel Medical College
Thomas Jefferson University
909 Walnut St, 2nd Floor
Philadelphia, PA 19107

E: christopher.farrell@jefferson.edu

Advanced Magnetic Resonance Imaging in Glioblastoma: A Review

Gaurav Shukla, MD[1,2]; G.S. Alexander, BS[1]; Spyridon Bakas, PhD[2,3]; Rahul Nikam, MD[4]; Kiran Talekar, MD[4]; Joshua Palmer, MD[5]; Wenyin Shi, MD[1]

[1]Department of Radiation Oncology, Thomas Jefferson University, Sidney Kimmel Cancer Center at Jefferson, Philadelphia, PA
[2]Center for Biomedical Image Computing and Analytics, University of Pennsylvania, Philadelphia, PA
[3]Department of Radiology, University of Pennsylvania, Philadelphia, PA
[4]Department of Radiology, Thomas Jefferson University, Philadelphia, PA
[5]Department of Radiation Oncology, The Ohio State University Wexner Medical Center, Columbus, OH

INTRODUCTION

In 2017, it is estimated that 26,070 patients will be diagnosed with a malignant primary brain tumor in the United States, with more than half having the diagnosis of glioblastoma (GBM).[1] Magnetic resonance imaging (MRI) is a widely utilized examination in the diagnosis and post-treatment management of patients with glioblastoma; standard modalities available from any clinical MRI scanner, including T1, T2, T2-FLAIR, and T1-contrast-enhanced (T1CE) sequences, provide critical clinical information. In the last decade, advanced imaging modalities are increasingly utilized to further characterize glioblastomas. These include multi-parametric MRI sequences, such as dynamic contrast enhancement (DCE), dynamic susceptibility contrast (DSC), diffusion tensor imaging (DTI), functional imaging, and spectroscopy (MRS), to further characterize glioblastomas, and significant efforts are ongoing to implement these advanced imaging modalities into improved clinical workflows and personalized therapy approaches. A contemporary review of standard and advanced MR imaging in clinical neuro-oncologic practice is presented.

Initial diagnosis and surgical management

Most patients with glioblastoma undergo computed tomography of the brain upon initial presentation. Once a mass is identified and hemorrhage is excluded, a contrast-enhanced MRI is typically ordered, with standard T1, T2, FLAIR, and contrast-enhanced T1 (T1CE) sequences.[2,3] Many institutions will also capture gradient echo and diffusion sequences. Maximal safe debulking surgery is recommended as the initial standard of care. Neurosurgeons will often utilize high-resolution MRI (0.5 – 1.2mm slice thickness) for surgical planning and intraoperative guidance, as well as to make the determination of how aggressively to resect based on risk of toxicity to nearby eloquent regions.[4] Standard imaging also can identify other important characteristics of the mass in situ, including the amount of necrosis, compression of the surrounding normal tissue, and midline deviation.

A recent meta-analysis of over 40,000 glioblastoma patients demonstrated that gross-total resection was associated with improved survival as compared to subtotal resection.[5] Historically, the determination of gross-total resection was made in the operating room by the neurosurgeon. However, in the modern era, the practice of obtaining a post-operative contrast-enhanced MRI within 24-48 hours of surgery has become routine after publication of a study showing that radiological determination of the extent of resection via MRI had prognostic significance.[6] Several series have attempted to quantify a threshold value for the extent of resection as a guide for neurosurgeons, utilizing the amount or enhancing tumor present in the preoperative and post-operative T1CE images. These series report thresholds ranging from 70% to 100%[7-9], with the caveats that they were obtained retrospectively. To date, no formal threshold is recommended other than "maximal safe resection" as mentioned previously.

Standard preoperative images can be analyzed for macroscopic shape and location features that are associated with improved survival,[10-13] providing potential biomarkers that may be utilized in stratifying patients in clinical trials.

Advanced MR imaging sequences have utility in the preoperative domain as well. Functional imaging (fMRI) has been particularly useful in preoperative surgical planning in cases where tumors or their resection may disrupt eloquent areas. Many patients who were once felt to be unresectable due to uncertain risk of neurologic compromise are now candidates for more aggressive resection after functional mapping.[14] Diffusion tensor imaging (DTI) generates rich white matter tractography images which may guide neurosurgical planning[15] and can help distinguish between post-operative vascular damage and residual enhancing tumor.[16] Dynamic contrast-enhanced (DCE) sequences in the preoperative setting measure pharmacokinetic parameters of contrast uptake, which may be associated with early disease progression and survival.[17] Dynamic susceptibility contrast (DSC) MR imaging may be helpful in preoperative diagnosis[18] of malignant lesions. Imaging features extracted from standard and advanced preoperative MR sequences can predict survival, molecular subtype, and mutational status in glioblastoma,[19,20] potentially enhancing the set of imaging biomarkers available to clinicians.

Post-operative imaging and radiation planning

After maximal safe resection, which is evaluated on immediate post-operative MRI, the standard of care for patients with glioblastoma is chemoradiation with concurrent temozolomide, after the results of a large randomized Phase III trial.[21] Typically, chemoradiation begins 3-6 weeks after surgery to allow

DOI: https://doi.org/10.29046/JHNJ.013.1


Figure 1

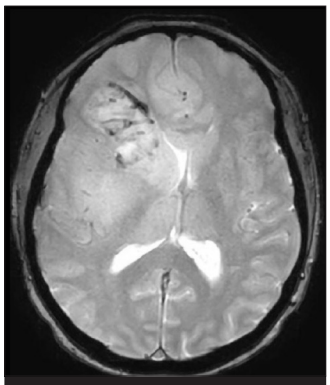
Figure 2

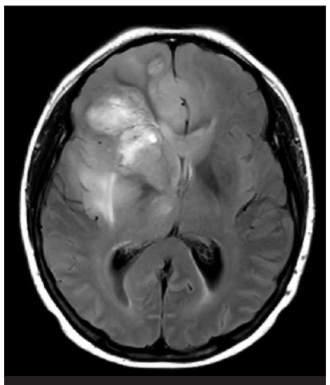
Figure 3

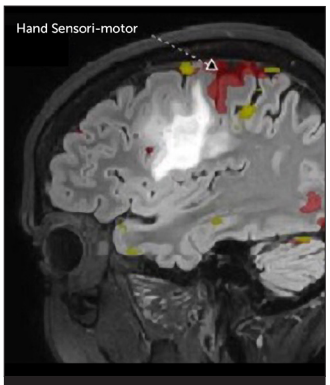

Figure 4

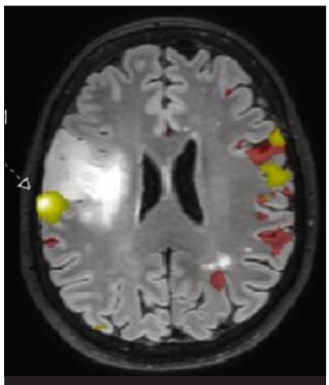
Figure 5

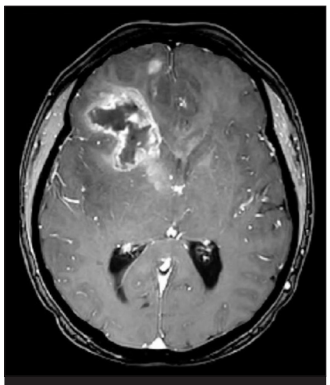
Figure 6

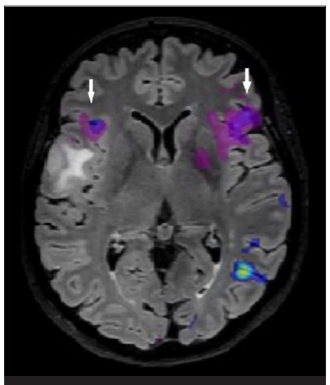
Figure 7

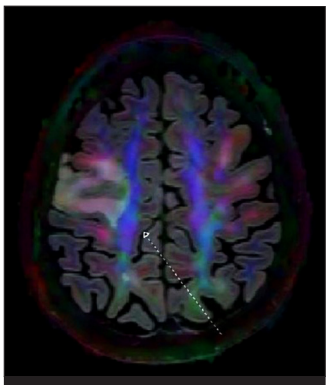
Figure 8

Figure 1. Axial CT image at the level of basal ganglia demonstrates a large heterogeneous mass in the right frontal lobe with mass effect on the right lateral ventricle and leftward shift of midline. Ct, computed tomography.

Figure 2. Axial FLAIR weighted image at the level of basal ganglia demonstrates heterogeneous mass centered in the right frontal lobe and basal ganglia with surrounding infiltrating signal abnormality 'FLAIR envelope' which extends medially across the corpus callosum posteriorly in the insular region. The 'FLAIR envelope' is typically a manifestation of combination of tumor infiltration and edema. There is associated mass effect on the right ventricle and leftward midline shift. FLAIR, fluid-attenuated inversion recovery.

Figure 3. Axial gradient echo (GRE) image depicts multiple foci of hypointense signal 'susceptibility artifacts' within the right frontal mass compatible with intra-tumoral blood products.

Figure 4. Post gadolinium based contrast administration T1 weighted axial image (T1CE). There is heterogeneous irregular peripheral enhancement associated with the right frontal lobe mass with central non-enhancing area, consistent with necrosis. Of note are additional patchy areas of enhancement in the right anterior frontal lobe and right basal ganglia region. These additional areas of enhancement lie within the previously described region of 'FLAIR envelope'. FLAIR, fluid-attenuated inversion recovery; T1CE, T1 contrast-enhanced.

Figure 5. BOLD fMRI for localization of hand sensorimotor cortex in a patient with right frontal glial neoplasm. BOLD fMRI data is superimposed on sagittal FLAIR weighted image for anatomic localization. In the right hemisphere, the hand sensorimotor cortex (arrow) is located along the posterosuperior aspect of the frontal mass and is separated by less than one gyrus distance. fMRI, functional magnetic resonance imaging; FLAIR, fluid-attenuated inversion recovery.

Figure 6. BOLD fMRI for localization of tongue sensorimotor cortex. BOLD fMRI data is superimposed on axial FLAIR weighted image for anatomic localization. In the right hemisphere, the area of activation (arrow), tongue sensorimotor cortex is in immediate proximity of the posterior margin of the right frontal mass. FLAIR envelope seems to extend into this region of activation. fMRI, functional magnetic resonance imaging; FLAIR, fluid-attenuated inversion recovery.

Figure 7. BOLD fMRI for localization of Broca's area in a patient with right frontal glial neoplasm. There is bilateral Broca's area activation on sentence completion and verb generation tasks (arrows), with the right hemispheric area of activation located at the anteroinferior aspect of tumor within one gyrus distance. fMRI, functional magnetic resonance imaging.

Figure 8. Color fractional anisotropy map superimposed on axial FLAIR weighted image. There is loss of fractional anisotropy in the expected region of right corticospinal tract (arrow, blue colored fibers). This tract is located at the posteromedial margin of the FLAIR envelope. Loss of fractional anisotropy may be related edema, infiltration by tumor or displacement. FLAIR, fluid-attenuated inversion recovery.

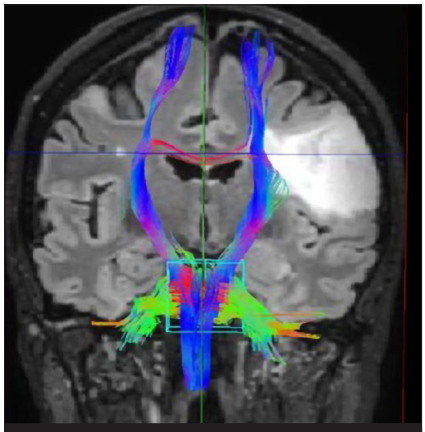

Figure 9.

Tractography image demonstrates the intimate relationship of right frontal mass with the corticospinal tract (blue colored fibers).

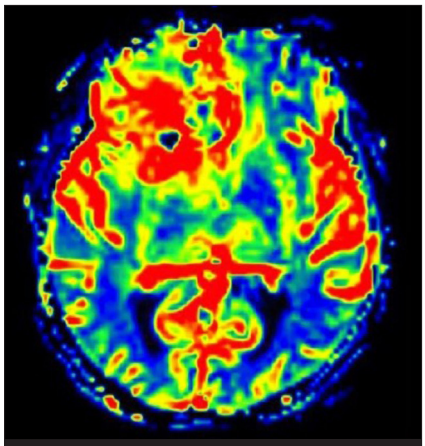

Figure 10.

Dynamic susceptibility contrast (DSC) perfusion weighted image. There is increase in rCBV (relative cerebral blood volume) in the region of right frontal mass (Figures 1-4), a finding favoring high grade neoplasm.

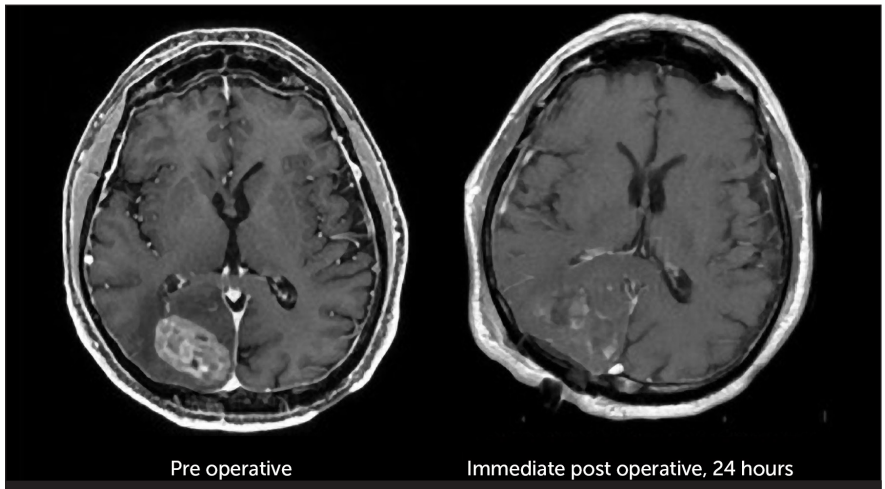

Figure 11.

Pre- and immediate post-operative (at 24 hours) axial t1CE weighted images. On post-operative image, there is minimal residual enhancement particularly along the medial aspects of the surgical site, concerning for minimal residual tumor. Majority of the hyperintense signal in the right parieto-occipital region is related to blood post-operative blood products. T1CE, T1-weighted contrast-enhanced.

for adequate post-operative recovery. Radiotherapy planning includes registration (aka "fusion") of the post-operative MRI (T1CE and FLAIR sequences) with the planning simulation CT, which allows for delineation of the FLAIR abnormality and residual enhancement in treatment planning. Guidelines for these delineations exist, but substantial variation is observed among practitioners from different cooperative groups (e.g., RTOG[22] vs. EORTC[23]), and even among practitioners from one country,[24] but all utilize post-operative MR imaging to define the at risk target volumes and organs at risk.

It is common to identify shifting of brain parenchyma on planning CT in the weeks after craniotomy as the normal brain tissue expands to fill the space taken out by the tumor. One study demonstrated a 4mm shift in the position of the treatment isocenter between CT and MRI-based target delineation,[25] even with only a few days between studies. The magnitude of the shift can be several centimeters, resulting in inaccurate registration between post-operative MRI and simulation CT. Many institutions have begun the practice of obtaining repeat MRI at the time of simulation to better characterize the soft tissues for target delineation.

Advanced imaging at this time point may play a role in radiation planning. A Polish study demonstrated the discordance between gross tumor volume (GTVs) delineated from MRI as compared to 18F-fluoroethylthyrosine-PET (FET-PET), a functional imaging modality; FET-PET was better associated with the site of eventual failure, suggesting that traditional target volumes may not be adequate.[26] ADC maps generated from diffusion imaging can identify areas of restricted diffusion that may predict for areas of eventual recurrence with high concordance;[27,28] along with fractional anisotropy measurements from diffusion images, ADC values may be associated with poor response to treatment and worse survival among high grade glioma patients.[29] Diffusion and perfusion parameters, when combined with standard MR sequences, may allow radiation oncologists to better characterize the highest-risk regions to include in high-dose target volumes, utilizing macroscopically visible features[30] as well as radiomic features.[31] Voxel-based MR spectroscopy (MRS) and whole-brain spectroscopic MRI (sMRI) may identify regions of tumor infiltration and areas at high risk of recurrence;[32] regions with metabolic abnormalities on sMRI are correlated with intraoperative tissue samples showing increased immunohistochemical staining for neoplastic cells.[33]

Response Assessment

As demonstrated at any multidisciplinary tumor board, imaging is of utmost importance in the interpretation of the response to treatment in glioblastoma. The first widely-adopted set of guidelines for standardizing the assessment of treatment response that utilized MR imaging was the Macdonald criteria,[34] which used clinical parameters in conjunction with imaging measurements to classify responses into four broad categories (complete response, partial response, stable disease, and progressive disease).

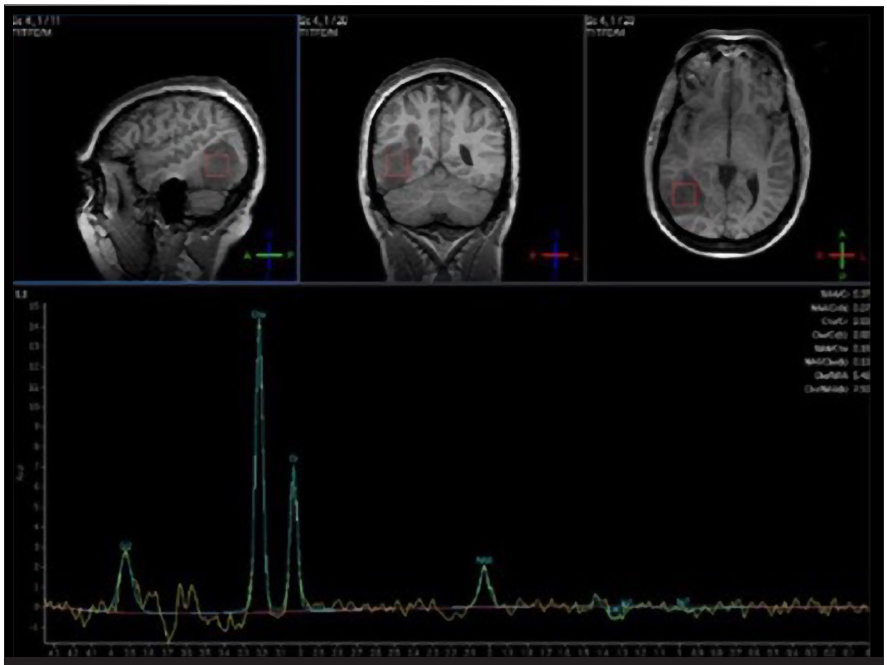

Figure 12.

Single voxel MR spectroscopy at long TE (288 ms) acquired through the right temporoparietal region mass with imaging appearance compatible with glial neoplasm. There is markedly elevated choline (resonates at 3.2 ppm) with markedly decreased NAA (resonates at 2 ppm), a finding consistent with high grade glial neoplasm. MR, magnetic resonance.

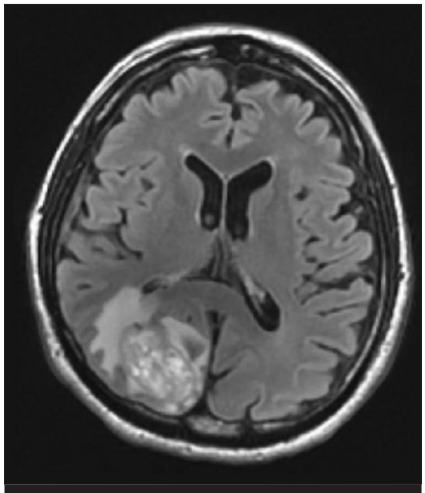

Figure 13.

Axial FLAIR and post contrast T1 weighted images demonstrate a large heterogeneously enhancing mass in the right parieto-occipital region with surrounding FLAIR hyperintense signal, compatible with high grade glial neoplasm. FLAIL, fluid-attenuated inversion recovery.

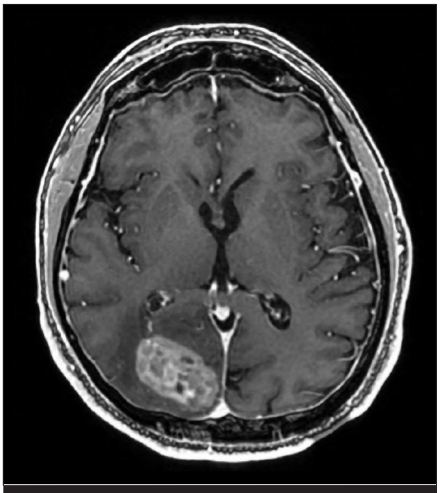

Figure 14.

Immediate post-operative (at 24 hours) axial post contrast T1 weighted image. There is minimal residual peripheral enhancement particularly along the medial aspects of the surgical site concerning for small amount of residual tumor.

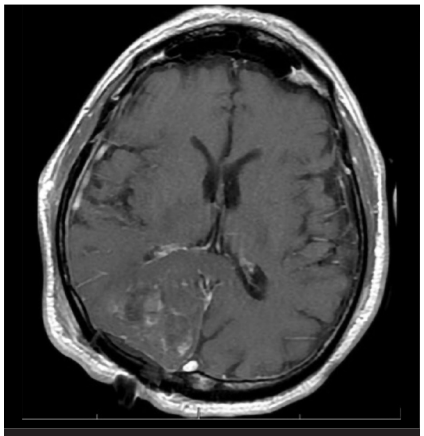

Figure 15.

Immediate post-operative (at 24 hours) axial post contrast T1 weighted image. There is minimal residual peripheral enhancement particularly along the medial aspects of the surgical site concerning for small amount of residual tumor.

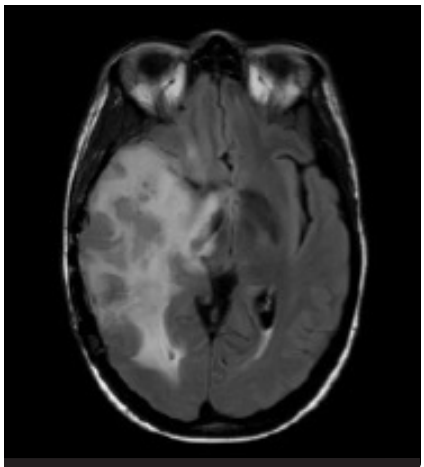

Figure 16.

Follow up of a case of glioblastoma on therapy. Axial FLAIR weighted image demonstrates a large area of infiltrating hyperintense signal abnormality in right temporo-occipital region, with associated mass effect and leftwards shift of midline. FLAIR, fluid-attenuated inversion recovery.

Challenges and limitations of the Macdonald criteria became apparent as imaging modalities revealed more details about gliomas and their response to treatment. The importance of non-contrast-enhancing regions of abnormality has become better understood; for example, changes in the volume of

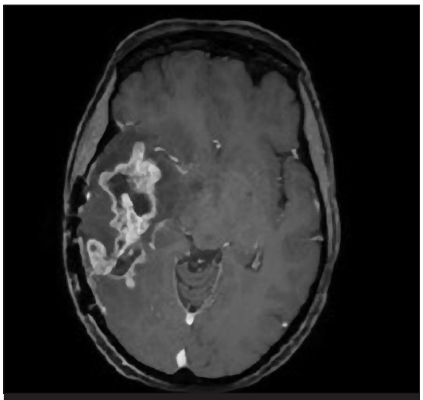

Figure 17.

Axial T1CE image depicts an area of heterogeneous enhancement in right temporal lobe within the region of FLAIR signal abnormality. FLAIR, fluid-attenuated inversion recovery. T1CE, T1-weighted contrast-enhanced.

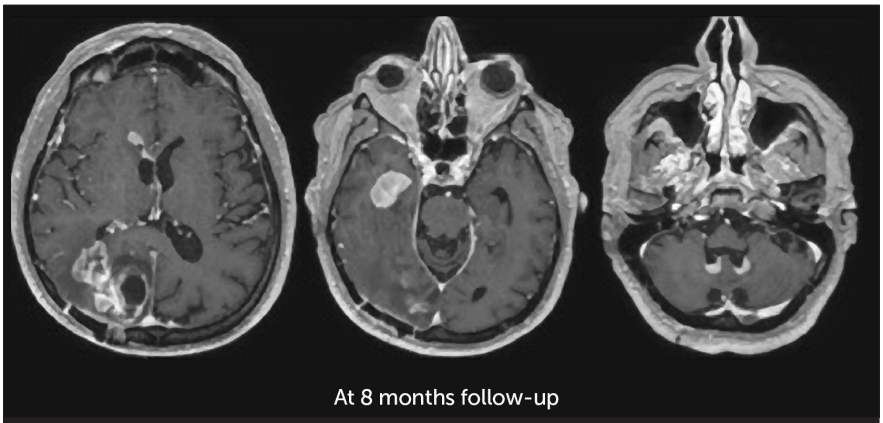

Figure 18.

Axial post-contrast T1 (T1CE) images at 8 months. There is a large heterogeneously enhancing mass in the right parieto-occipital region at the operative site. There is interval development of multiple enhancing nodules along the ependymal surface of ventricles, particularly along the right frontal and temporal horn, and roof of fourth ventricles. These findings are compatible with tumor progression. T1CE, T1-weighted contrast-enhanced.

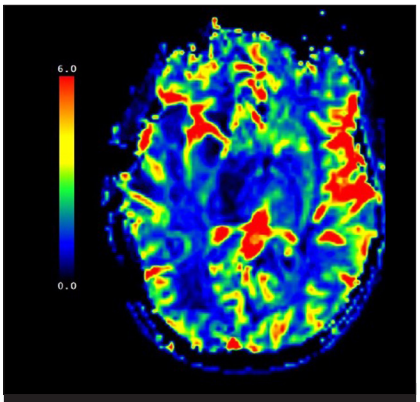

Figure 19.

On dynamic susceptibility contrast (DSC) perfusion weighted imaging, the area of signal abnormality predominantly demonstrates low relative cerebral blood volumes. The overall findings were consistent with pseudoprogression.

hyperintensity on post-treatment FLAIR imaging, relative to baseline, are correlated with improved survival.[35] Furthermore, some glioblastomas demonstrate imaging changes consistent with progression under the Macdonald criteria, but upon repeat surgical intervention, viable tumor cannot be identified in the resection specimen, suggesting that the adjuvant treatment may actually be having a positive effect that eludes detection on conventional imaging. This finding, termed "pseudoprogression," is most commonly observed in patients whose tumors harbored a methylated MGMT promoter region,[36] and makes accurate assessment of response difficult, especially in the setting of clinical trials attempting to answer the question of efficacy of novel treatment regimens. Some medications, including anti-angiogenic drugs and immunologic agents, elicit unique radiographic changes which may mask accurate response assessment as well.

These limitations, among others, led to the development of a new set of guidelines developed by the Response Assessment in Neuro-Oncology (RANO) working group,[37] which incorporates more information from MR imaging, including FLAIR sequence changes, into the objective assessment. The RANO criteria have been incorporated into clinical trials and daily clinical practice, allowing better apples-to-apples comparisons.[38]

Clinical trials in the last decade demonstrated the benefit of bevacizumab, an anti-angiogenic monoclonal antibody, in recurrent glioblastoma.[39] The radiographic appearance of malignant gliomas changes dramatically after treatment with bevacizumab as a result of changes in vessel permeability and contrast dynamics.[40] Initial studies showed the difficulty in distinguishing these radiographic changes from true tumor effect; the temporal dynamics were also unclear.[41] These issues led to the development of the immunotherapy response assessment in neuro-oncology (iRANO) criteria,[42] which attempted to provide standardized guidelines for the determination of tumor progression in the setting of immune-related therapy.

MRI imaging features have the potential to predict treatment response to specific modalities of treatment. Relative cerebral blood volume and dynamics parameters (K¬trans and Ve), measured by perfusion-weighted MR imaging and other features may predict treatment response to standard chemoradiation and VEGF inhibitors,[43-45] prior to initiation of therapy. Radiomic features derived from these images have been shown to have predictive value as well.[46]

CONCLUSIONS

The volume of medical imaging data continues to grow at an exponential rate. As MR imaging becomes more cost-effective and the adoption of advanced MR modalities becomes more widespread, it will become more critical than ever to incorporate advanced imaging and the power of large datasets into the management of glioblastoma. We anticipate that these changes will include not only the utilization of new MR sequences but also novel image analysis techniques, including radiomic analysis, to better drive treatment decision-making, with the goal of improving clinical outcomes in glioblastoma.

REFERENCES

1. Ostrom, Q.T., et al., American Brain Tumor Association Adolescent and Young Adult Primary Brain and Central Nervous System Tumors Diagnosed in the United States in 2008-2012. *Neuro Oncol*, 2016. 18 Suppl 1: p. i1-i50.
2. Cha, S., Update on brain tumor imaging: from anatomy to physiology. *AJNR Am J Neuroradiol*, 2006. 27(3): p. 475-87.
3. Young, G.S., Advanced MRI of adult brain tumors. Neurol Clin, 2007. 25(4): p. 947-73, viii.
4. Price, S.J. and J.H. Gillard, Imaging biomarkers of brain tumour margin and tumour invasion. *Br J Radiol*, 2011. 84 Spec No 2: p. S159-67.
5. Brown, T.J., et al., Association of the Extent of Resection With Survival in Glioblastoma: A Systematic Review and Meta-analysis. *JAMA Oncol*, 2016. 2(11): p. 1460-1469.
6. Albert, F.K., et al., Early postoperative magnetic resonance imaging after resection of malignant glioma: objective evaluation of residual tumor and its influence on regrowth and prognosis. *Neurosurgery*, 1994. 34(1): p. 45-60; discussion 60-1.
7. Lacroix, M., et al., A multivariate analysis of 416 patients with glioblastoma multiforme: prognosis, extent of resection, and survival. *J Neurosurg*, 2001. 95(2): p. 190-8.
8. Stummer, W., et al., Extent of resection and survival in glioblastoma multiforme: identification of and adjustment for bias. *Neurosurgery*, 2008. 62(3): p. 564-76; discussion 564-76.
9. Sanai, N. and M.S. Berger, Operative techniques for gliomas and the value of extent of resection. *Neurotherapeutics*, 2009. 6(3): p. 478-86.
10. Wangaryattawanich, P., et al., Multicenter imaging outcomes study of The Cancer Genome Atlas glioblastoma patient cohort: imaging predictors of overall and progression-free survival. *Neuro Oncol*, 2015. 17(11): p. 1525-37.
11. Archive, T.C.I. VASARI Research Project. 3/25/2015 5/3/2017]; Available from: https://wiki.cancerimagingarchive.net/display/Public/VASARI+Research+Project.
12. Perez-Beteta, J., et al., Glioblastoma: does the pre-treatment geometry matter? A postcontrast T1 MRI-based study. *Eur Radiol*, 2017. 27(3): p. 1096-1104.
13. Czarnek, N., et al., Algorithmic three-dimensional analysis of tumor shape in MRI improves prognosis of survival in glioblastoma: a multi-institutional study. *J Neurooncol*, 2017. 132(1): p. 55-62.
14. Sanai, N., Z. Mirzadeh, and M.S. Berger, Functional outcome after language mapping for glioma resection. *N Engl J Med*, 2008. 358(1): p. 18-27.
15. Abdullah, K.G., et al., Use of diffusion tensor imaging in glioma resection. *Neurosurg Focus*, 2013. 34(4): p. E1.
16. Lee, S.K., Diffusion tensor and perfusion imaging of brain tumors in high-field MR imaging. *Neuroimaging Clin N Am*, 2012. 22(2): p. 123-34, ix.
17. Kim, R., et al., Prognosis prediction of non-enhancing T2 high signal intensity lesions in glioblastoma patients after standard treatment: application of dynamic contrast-enhanced MR imaging. *Eur Radiol*, 2017. 27(3): p. 1176-1185.
18. Chakravorty, A., T. Steel, and J. Chaganti, Accuracy of percentage of signal intensity recovery and relative cerebral blood volume derived from dynamic susceptibility-weighted, contrast-enhanced MRI in the preoperative diagnosis of cerebral tumours. *Neuroradiol J*, 2015. 28(6): p. 574-83.
19. Bakas, S., et al., In vivo detection of EGFRvIII in glioblastoma via perfusion magnetic resonance imaging signature consistent with deep peritumoral infiltration: the φ index. *Clinical Cancer Research*, 2017, epub ahead of print.
20. Macyszyn, L., et al., Imaging patterns predict patient survival and molecular subtype in glioblastoma via machine learning techniques. *Neuro Oncol*, 2016. 18(3): p. 417-425.
21. Stupp, R., et al., Effects of radiotherapy with concomitant and adjuvant temozolomide versus radiotherapy alone on survival in glioblastoma in a randomised phase III study: 5-year analysis of the EORTC-NCIC trial. *Lancet Oncol*, 2009. 10(5): p. 459-66.
22. Gilbert, M.R., et al., Dose-dense temozolomide for newly diagnosed glioblastoma: a randomized phase III clinical trial. *J Clin Oncol*, 2013. 31(32): p. 4085-91.
23. Stupp, R., et al., Radiotherapy plus concomitant and adjuvant temozolomide for glioblastoma. *N Engl J Med*, 2005. 352(10): p. 987-96.
24. Wee, C.W., et al., Evaluation of variability in target volume delineation for newly diagnosed glioblastoma: a multi-institutional study from the K*orean Radiation Oncology Group*. Radiat Oncol, 2015. 10: p. 137.
25. Bagri, P.K., et al., Addition of magnetic resonance imaging to computed tomography-based three-dimensional conformal radiotherapy planning for postoperative treatment of astrocytomas: Changes in tumor volume and isocenter shift. *South Asian J Cancer*, 2015. 4(1): p. 18-20.
26. Harat, M., B. Malkowski, and R. Makarewicz, Pre-irradiation tumour volumes defined by MRI and dual time-point FET-PET for the prediction of glioblastoma multiforme recurrence: A prospective study. *Radiother Oncol*, 2016. 120(2): p. 241-7.
27. Elson, A., et al., Evaluation of pre-radiotherapy apparent diffusion coefficient (ADC): patterns of recurrence and survival outcomes analysis in patients treated for glioblastoma multiforme. *J Neurooncol*, 2015. 123(1): p. 179-88.
28. Jeong, D., et al., Mean apparent diffusion coefficient values in defining radiotherapy planning target volumes in glioblastoma. *Quant Imaging Med Surg*, 2015. 5(6): p. 835-45.
29. Qu, J., et al., Residual low ADC and high FA at the resection margin correlate with poor chemoradiation response and overall survival in high-grade glioma patients. *Eur J Radiol*, 2016. 85(3): p. 657-64.
30. Guo, L., et al., Diffusion and perfusion weighted magnetic resonance imaging for tumor volume definition in radiotherapy of brain tumors. *Radiat Oncol*, 2016. 11(1): p. 123.
31. Akbari, H., et al., Imaging Surrogates of Infiltration Obtained Via Multiparametric Imaging Pattern Analysis Predict Subsequent Location of Recurrence of Glioblastoma. *Neurosurgery*, 2016. 78(4): p. 572-80.
32. Deviers, A., et al., Evaluation of the lactate-to-N-acetyl-aspartate ratio defined with magnetic resonance spectroscopic imaging before radiation therapy as a new predictive marker of the site of relapse in patients with glioblastoma multiforme. Int *J Radiat Oncol Biol Phys*, 2014. 90(2): p. 385-93.
33. Cordova, J.S., et al., Whole-brain spectroscopic MRI biomarkers identify infiltrating margins in glioblastoma patients. *Neuro Oncol*, 2016. 18(8): p. 1180-9.
34. Macdonald, D.R., et al., Response criteria for phase II studies of supratentorial malignant glioma. *J Clin Oncol*, 1990. 8(7): p. 1277-80.
35. Grossman, R., et al., Dynamics of FLAIR Volume Changes in Glioblastoma and Prediction of Survival. Ann Surg Oncol, 2017. 24(3): p. 794-800.
36. Brandes, A.A., et al., MGMT promoter methylation status can predict the incidence and outcome of pseudoprogression after concomitant radiochemotherapy in newly diagnosed glioblastoma patients. *J Clin Oncol*, 2008. 26(13): p. 2192-7.
37. Wen, P.Y., et al., Updated response assessment criteria for high-grade gliomas: response assessment in neuro-oncology working group. *J Clin Oncol*, 2010. 28(11): p. 1963-72.
38. Chinot, O.L., et al., Response assessment criteria for glioblastoma: practical adaptation and implementation in clinical trials of antiangiogenic therapy. *Curr Neurol Neurosci Rep*, 2013. 13(5): p. 347.
39. Kreisl, T.N., et al., Phase II trial of single-agent bevacizumab followed by bevacizumab plus irinotecan at tumor progression in recurrent glioblastoma. *J Clin Oncol*, 2009. 27(5): p. 740-5.
40. Pope, W.B., et al., MRI in patients with high-grade gliomas treated with bevacizumab and chemotherapy. *Neurology*, 2006. 66(8): p. 1258-60.
41. Ananthnarayan, S., et al., Time course of imaging changes of GBM during extended bevacizumab treatment. *J Neurooncol*, 2008. 88(3): p. 339-47.
42. Okada, H., et al., Immunotherapy response assessment in neuro-oncology: a report of the RANO working group. *Lancet Oncol*, 2015. 16(15): p. e534-42.
43. Bennett, I.E., et al., Early perfusion MRI predicts survival outcome in patients with recurrent glioblastoma treated with bevacizumab and carboplatin. *J Neurooncol*, 2017. 131(2): p. 321-329.
44. O'Neill, A.F., et al., Demonstration of DCE-MRI as an early pharmacodynamic biomarker of response to VEGF Trap in glioblastoma. *J Neuro Oncol*, 2016. 130(3): p. 495-503.
45. Khalifa, J., et al., Identification of a candidate biomarker from perfusion MRI to anticipate glioblastoma progression after chemoradiation. *Eur Radiol*, 2016. 26(11): p. 4194-4203.
46. Kickingereder, P., et al., Large-scale Radiomic Profiling of Recurrent Glioblastoma Identifies an Imaging Predictor for Stratifying Anti-Angiogenic Treatment Response. *Clin Cancer Res,* 2016. 22(23): p. 5765-5771.

Stereotactic Radiosurgery Practice Patterns for Brain Metastases in the United States: A National Survey

Erik Scott Blomain, BA[1]; Hyun Kim, MD[1]; Shivank Garg, MD[1]; Deepak Bhamidipati, BS[1]; Jenny Guo, BS[1]; Ingrid Kalchman, BS[1]; John McAna, PhD[2] and Wenyin Shi, MD, PhD[1]

[1] Department of Radiation Oncology, Thomas Jefferson University, Sidney Kimmel Cancer Center at Jefferson, Philadelphia, PA

[2] Jefferson College of Population Health, Thomas Jefferson University, Philadelphia, PA

Running Title

Brain metastases SRS use practice

Conflict of Interest Notification

No actual or potential conflicts of interest.

Acknowledgements

E.S.B. received an F30 Ruth Kirschstein MD-PhD Fellowship Award (CA180500).

ABSTRACT

Background: Stereotactic radiosurgery (SRS) has emerged as an important modality for the treatment of intracranial metastases. There are currently few established guidelines delineating indications for SRS use and fewer still regarding plan evaluation in the treatment of multiple brain metastases.

Methods: An 18 question electronic survey was distributed to radiation oncologists at National Cancer Institute (NCI) designated cancer centers in the US (60). Centers without radiation oncologists were excluded. Physicians who indicated that they do not prescribe SRS were excluded from the remaining survey questions. Sign test and Chi-square test were used to determine if responses differed significantly from random distribution.

Results: 116 of the 697 radiation oncologists surveyed completed the questionnaire, representing 51 institutions. 62% reported treating patients with brain metastases using SRS. Radiation oncologists prescribing SRS most commonly treat CNS (66.2%) and lung (49.3%) malignancies. SRS was used more frequently for <10 brain metastases (73.7%; p<.0001) and whole brain radiation therapy (WBRT) for >10 brain metastases (82.5%; p<.0001). The maximum number of lesions physicians were willing to treat with SRS without WBRT was 1-4 (40.4%) and 5-10 (42.4%) (p<.0001 compared to 11-15, 16-20 and no limit). The most important criteria for choosing SRS or WBRT were number of lesions (p<.0001) and performance status (p=.016). The most common margin for SRS was 0 mm (49.1%; p=.0021). The most common dose constraints other than critical structure was conformity index (84.2%) and brain V12 (61.4%). The LINAC was the most common treatment modality (54.4%) and mono-isocenter technique for multiple brain metastases was commonly used (43.9%; p=.23). Most departments do not have a policy for brain metastases treatment (64.9%; p=.024).

Conclusions: This is one of the first national surveys assessing the use of SRS for brain metastases in clinical practice. These data highlight some clinical considerations for physicians treating brain metastases with SRS.

Summary: This is among the first national surveys to assess the use of SRS for brain metastases in clinical practice. Specifically, radiation oncologist reported increasingly using SRS instead of WBRT for treating <10 metastases, with the LINAC being the most common modality. Further, treatment parameters considered the most important included 0 mm margins, conformity index, brain V12, and mono-isocenter technique for multiple brain metastases. These results may provide context regarding the use of SRS for brain metastases in clinical practice.

INTRODUCTION

Brain metastases are a significant cause of morbidity and mortality among oncologic patients, affecting 20-40% of this population.[1] Several therapeutic strategies for intracranial metastases exist, including stereotactic radiosurgery (SRS), whole brain radiotherapy (WBRT), surgical resection and supportive care with steroids, though systemic therapy remains an option for patients with selected cancers.[2] WBRT was historically the treatment modality of choice for brain metastases with or without surgical resection.[3,4] Technological improvements in Gamma Knife and LINAC-based SRS coupled with data indicating decreased cognitive toxicity with SRS5, have led to increased utilization of SRS6. Although evidence-based clinical practice guidelines exist for the use of SRS for brain metastases,[7-12] there are comparatively fewer reports that study specific aspects of SRS plan evaluation or if current use reflects the recommendations of professional societies. In that context, the current study represents one of the few national surveys which specifically investigates these issues to clarify the role of SRS for intracranial metastases in clinical practice.

MATERIALS AND METHODS

Study Design

An 18 question, non-incentivized electronic survey was distributed to radiation oncologists at National Cancer Institute

designated cancer centers in the United States (60). Centers without radiation oncologists were excluded. The total number of physicians contacted was 697. Physicians who reported not prescribing SRS were not invited to complete remaining survey questions. Per institutional policy, this study was IRB-exempt.

Statistical Analysis

Depending on type of question, 95% confidence interval (estimate of proportion), sign test (difference from expected mean) or Chi-square test (difference from expected distribution) were used to determine if responses differed significantly from random distribution. All data analyses were completed using Stata software and a P value<0.05 was considered to be statistically significant.

RESULTS

Response and Demographic Data

All survey results are reproduced in Table 1. Of 697 physicians surveyed, 118 (16.9%) responded, with 28.7% reporting that they do not treat brain metastases with SRS. Respondents represented 51 different institutions across 28 states with varying years of practice experience.

Indications and Use in Practice

Respondents primarily treated CNS (66.2%, 95% CI [54-77%]); lung was numerically the second most commonly treated disease site (49.3%). SRS (73.7%) was used more frequently than WBRT (10.5%) for <10 brain metastases (p<.0001) while WBRT (82.5%) was used more frequently than SRS (5.3%) for >=10 brain metastases (p<.0001). The maximum number of lesions physicians were willing to treat with SRS without WBRT in the treatment session was 1-4 (40.4%) and 5-10 (42.4%) (p<.0001; compared to 11-15, 16-20 and no limit). Most physicians reported they would not treat more than 10 lesions over multiple sessions with SRS (43.9%; p=.0003) but 19.3% reported there was no limit to the number they would treat. Physicians indicated that their practice had changed in the past 5 years by more frequently using SRS without WBRT (84.2%) and SRS without other treatments (i.e. surgery or WBRT; 82.5%). Criteria used to determine SRS versus WBRT use were number of lesions (p<.0001), histology (p=.0014), performance status (p=.016) and location (p<.0001) as determined by sign-test. Leptomeningeal disease was statistically significant versus all other choices as the predominant contraindication to prescribing SRS without WBRT (93%; CI [83-98%]).

Treatment Modality and Planning

LINAC (54.4%) was more commonly used than the CyberKnife (14.0%) or Gamma Knife (31.6%) for SRS treatment (p=.0009). The mono-isocenter technique for multiple brain metastases was commonly used (43.9%; p=.23). The most common margin for SRS was 0 mm (49.1%; p=.0021), with 38.6% and 12.3% prescribing a 1 mm and 2 mm margin, respectively. The most common dose constraints other than critical structure were conformity index (84.2%) and V12 (61.4%). Diameter, volume and histology of lesion were all ranked as significant in determining the SRS prescription dose (sign-test, p<.0001, p=.001 and p<.0001, respectively). Notably, most departments do not have a policy in place for treating brain metastases with SRS (64.9%; p=.024).

DISCUSSION

Despite increasing use of SRS to treat brain metastases, little exists in terms of guidance for physicians using this modality. Moreover, our data indicate that most departments do not have policies governing SRS use. Importantly, no clear guidelines exist regarding the maximum number of metastases for which SRS is recommended, despite a historically-used cutoff of 4 in clinical trials.[5,13,14] In this study, 42.4% of respondents reported using SRS for patients with 5-10 metastases and 17.5% of respondents offering it for more than 10 lesions without WBRT. Thus, a significant number of respondents are using SRS for more than the standard 4 lesions. In total, 73.7% of respondents reported using SRS more often for <10 metastasis, and 82.5% used WBRT more often for >10 lesions. These physicians may be influenced by a shifting paradigm towards SRS alone for a greater than 5 or greater than 10 lesions.[15-17] Indeed, the majority of respondents reported increasing their use of SRS over the last five years. While the survey did not evaluate the role insurers play in physicians' decision making, private insurance typically recognizes the role of SRS in treating multiple brain metastases with no clear maximum identified.[18] Additionally, citing a growing body of literature regarding safety and efficacy, current National Comprehensive Cancer Network (NCCN) recommendations for SRS alone do not specify a maximum number of lesions.[19]

Knisely et al first examined the use of SRS in clinical practice several years ago; physicians at two conferences hosted by national stereotactic radiosurgery societies were asked to fill a questionnaire, with a majority of respondents considering it "reasonable" to treat greater than 5 metastases with SRS alone.[20] More recently, Sandler et al evaluated practicing physicians' "cutoff" for treating brain metastases with SRS alone versus WBRT, among other scenarios.[21] Importantly, they found CNS-specialists to be comfortable treating a mean of 8.1 lesions compared to 5.6 and 5.1 lesions for low-volume CNS specialists and non-CNS specialists respectively.[21] While our survey did not stratify SRS use according to specialization, our results reflect a similar trend among physicians at a national level for treating greater than five lesions with SRS alone.

Notably, recent American Society for Therapeutic Radiology and Oncology (ASTRO) Choosing Wisely guidelines recommend against using adjuvant WBRT with SRS, and instead recommend SRS monotherapy for brain metastases.[12,22] However, no guidance is provided regarding the SRS plan evaluation. The present study identifies several parameters in current SRS use for brain metastasis in practice, including the use of 0 mm margins, conformity index, brain V12, and the mono-isocenter technique for multiple brain metastases. While our survey did not specifically assess the values used for each parameter, retrospective data indicate that V12 greater than 10.9 cm3 is associated with a 51% 1 year risk of radionecrosis.[23] Likewise, other treatment parameters appear to play an important role in the development of a safe and effective treatment plan.

The overall response rate was low for this study, introducing the potential for

response bias. Despite this potential limitation, emerging research suggests that low response rates are not inherently associated with inaccurate results or nonresponder bias.[24,25] Moreover, the wide geographic spread and distribution of practice experience among respondents suggests that the current sample was representative of the academic field at large. As this survey was distributed to physicians practicing at NCI-designated cancer centers however, the responses may not be reflective of the patterns of SRS use in private practice. Another potential limitation of the survey was that it did not account for patient volume per institution, which may be a surrogate for expertise in SRS and could influence aggressiveness in treating multiple brain metastases. Furthermore, individual practitioners were not asked about their patient volumes, which may be a surrogate for clinical versus research time in an academic setting and therefore influence management preferences. Future studies will be needed to continue to address these issues and refine clinical practice.

CONCLUSIONS

To our knowledge, this is among the first national assessments of the use of SRS for brain metastases in clinical practice in the U.S. The data indicate that radiation oncologists are increasingly using SRS for the treatment of intracranial lesions, even in situations which were historically treated with WBRT. Treatment parameters considered most by respondents include 0 mm margins, conformity index, brain V12, and a mono-isocenter technique for multiple brain metastases. These data may reveal areas that require guidance and instruction from cooperative group committees.

REFERENCES

1. Mehta MP, Tsao MN, Whelan TJ, et al. The American Society for Therapeutic Radiology and Oncology (ASTRO) evidence-based review of the role of radiosurgery for brain metastases. *International Journal of Radiation Oncology, Biology, Physics* 2005;63(1):37-46. doi: 10.1016/j.ijrobp.2005.05.023
2. Shonka N, Venur VA, Ahluwalia MS. Targeted Treatment of Brain Metastases. *Current Neurology and Neuroscience Reports* 2017;17(4):37. doi: 10.1007/s11910-017-0741-2
3. Patchell RA, Tibbs PA, Regine WF, et al. Postoperative radiotherapy in the treatment of single metastases to the brain: a randomized trial. *Jama* 1998;280(17):1485-9.
4. Patchell RA, Tibbs PA, Walsh JW, et al. A randomized trial of surgery in the treatment of single metastases to the brain. *The New England Journal of Medicine* 1990;322(8):494-500. doi: 10.1056/NEJM199002223220802
5. Chang EL, Wefel JS, Hess KR, et al. Neurocognition in patients with brain metastases treated with radiosurgery or radiosurgery plus whole-brain irradiation: a randomised controlled trial. *Lancet Oncol* 2009;10(11):1037-44. doi: 10.1016/S1470-2045(09)70263-3
6. Lippitz B, Lindquist C, Paddick I, et al. Stereotactic radiosurgery in the treatment of brain metastases: the current evidence. *Cancer Treatment Reviews* 2014;40(1):48-59. doi: 10.1016/j.ctrv.2013.05.002
7. Tsao MN, Rades D, Wirth A, et al. Radiotherapeutic and surgical management for newly diagnosed brain metastasis(es): An *American Society for Radiation Oncology* evidence-based guideline. *Practical Radiation Oncology* 2012;2(3):210-25. doi: 10.1016/j.prro.2011.12.004
8. Gaspar LE, Mehta MP, Patchell RA, et al. The role of whole brain radiation therapy in the management of newly diagnosed brain metastases: a systematic review and evidence-based clinical practice guideline. *Journal of Neuro-Oncology* 2010;96(1):17-32. doi: 10.1007/s11060-009-0060-9
9. Kalkanis SN, Kondziolka D, Gaspar LE, et al. The role of surgical resection in the management of newly diagnosed brain metastases: a systematic review and evidence-based clinical practice guideline. Journal of neuro-oncology 2010;96(1):33-43. doi: 10.1007/s11060-009-0061-8
10. Mehta MP, Paleologos NA, Mikkelsen T, et al. The role of chemotherapy in the management of newly diagnosed brain metastases: a systematic review and evidence-based clinical practice guideline. *Journal of Neuro-Oncology* 2010;96(1):71-83. doi: 10.1007/s11060-009-0062-7
11. Linskey ME, Andrews DW, Asher AL, et al. The role of stereotactic radiosurgery in the management of patients with newly diagnosed brain metastases: a systematic review and evidence-based clinical practice guideline. *Journal of Neuro-Oncology* 2010;96(1):45-68. doi: 10.1007/s11060-009-0073-4
12. ASTRO. ChoosingWisely. ASTRO releases second list of five radiation oncology treatments to question, as part of national Choosing Wisely campaign. *Choosing Wisely* 2014
13. Aoyama H, Shirato H, Tago M, et al. Stereotactic radiosurgery plus whole-brain radiation therapy vs stereotactic radiosurgery alone for treatment of brain metastases: a randomized controlled trial. *Jama* 2006;295(21):2483-91. doi: 10.1001/*Jama*.295.21.2483
14. Kocher M, Soffietti R, Abacioglu U, et al. Adjuvant whole-brain radiotherapy versus observation after radiosurgery or surgical resection of one to three cerebral metastases: results of the EORTC 22952-26001 study. *Journal of Clinical Oncology: Official Journal of the American Society of Clinical Oncology* 2011;29(2):134-41. doi: 10.1200/JCO.2010.30.1655
15. Yamamoto M, Serizawa T, Shuto T, et al. Stereotactic radiosurgery for patients with multiple brain metastases (JLGK0901): a multi-institutional prospective observational study. *Lancet Oncol* 2014;15(4):387-95. doi: 10.1016/S1470-2045(14)70061-0
16. Rava P, Leonard K, Sioshansi S, et al. Survival among patients with 10 or more brain metastases treated with stereotactic radiosurgery. *Journal of Neurosurgery* 2013;119(2):457-62. doi: 10.3171/2013.4.JNS121751
17. Yamamoto M, Kawabe T, Sato Y, et al. Stereotactic radiosurgery for patients with multiple brain metastases: a case-matched study comparing treatment results for patients with 2-9 versus 10 or more tumors. *Journal of Neurosurgery* 2014;121 Suppl:16-25. doi: 10.3171/2014.8.GKS141421
18. Shield BCB. Stereotactic Radiosurgery (SRS) and Stereotactic Body Radiation Therapy (SBRT)

POLICY NUMBER A60110 2016

19. Nabors LB, Portnow J, Ammirati M, et al. Central nervous system cancers, version 2. 2014. Featured updates to the NCCN Guidelines. *Journal of the National Comprehensive Cancer Network*: JNCCN 2014;12(11):1517-23.
20. Knisely JP, Yamamoto M, Gross CP, et al. Radiosurgery alone for 5 or more brain metastases: expert opinion survey. *Journal of Neurosurgery* 2010;113 Suppl:84-9. doi: 10.3171/2010.8.GKS10999
21. Sandler KA, Shaverdian N, Cook RR, et al. Treatment trends for patients with brain metastases: Does practice reflect the data? *Cancer* 2017;123(12):2274-82. doi: 10.1002/cncr.30607
22. Soliman H, Das S, Larson DA, et al. Stereotactic radiosurgery (SRS) in the modern management of patients with brain metastases. *Oncotarget* 2016;7(11):12318-30. doi: 10.18632/oncotarget.7131

23. Minniti G, Clarke E, Lanzetta G, et al. Stereotactic radiosurgery for brain metastases: analysis of outcome and risk of brain radionecrosis. *Radiat Oncol* 2011;6:48. doi: 10.1186/1748-717X-6-48

24. Keeter S KC, Dimock M, Best J, Craighill P. . Gauging the impact of growing nonresponse on estimates from a national RDD telephone survey. *Public Opin Q* 2006;70:759-79.

25. Holbrook A KJ, Pfent A. T In: Lepkowki JM, Tucker C, Brick JM,, al. e. The causes and consequences of response rates in surveys by the news media and government contractor survey research firms. *Advances in Telephone Survey Methodology John Wiley & Sons* 2008:499-500.

Corresponding Author

Wenyin Shi, MD, PhD
Department of Radiation Oncology
Sidney Kimmel Medical College
Thomas Jefferson University
Sidney Kimmel Cancer Center
at Jefferson
111 South 11th Street
Philadelphia, PA 19107

P: 215-955-6700
F: 215-503-0013
E: wenyin.shi@jefferson.edu

Dr. David Andrews is honored as the first Anthony Alfred Chiurco Professor

The Jefferson family had a double celebration on July 19, 2017, to thank Dr. and Mrs. Anthony Chiurco for establishing the Anthony Alfred Chiurco, MD Professor in the Department of Neurological Surgery, and to recognize the neurosurgical talents of Dr. David Andrews, who was installed as the first Anthony Alfred Chiurco Professor.

The celebration served as a reminder of how Jefferson improves lives every day through philanthropic partnerships that establish initiatives such as the Vickie and Jack Farber Institute for Neuroscience. The investiture was also a great opportunity to acknowledge Dr. Chiurco's Class of 1967, which is celebrating its 50-year reunion this year.

ABOUT DAVID W. ANDREWS, MD

As a neurosurgeon practicing neuro-oncologic neurosurgery over a 28-year period, Dr. Andrews has vast experience in the diagnosis, management and treatment of brain tumors. He established the Brain Tumor Division in the Department of Neurological Surgery at Thomas Jefferson University in 1995, and as division chief has built a world-class group including four neurosurgeons and two neuro-oncologists currently performing more than 1,200 major cases a year. While training as a resident at New York-Presbyterian/Weill Cornell Medicine he also completed a one-year fellowship at Memorial Sloan-Kettering Cancer Center.

As a junior attending surgeon, he was awarded a K11 Physician Scientist Award and studied the molecular pathogenesis of malignant gliomas under Dr. Carlo Croce. Currently he is the sponsor investigator and chief architect of a novel FDA-approved phase 1b immunotherapy trial for patients with newly diagnosed glioblastoma, which is achieving remarkable results in the highest vaccine cohort.

This has led to the formation of a company to accelerate this research, and his team has raised $14.8M in an initial round to achieve this. He is recognized as a pioneer in radiosurgery and established the first radiosurgery program in the Delaware Valley in 1991. He designed a low-dose fractionated radiotherapy technique that restored vision in patients with optic nerve sheath meningiomas. His landmark paper summarizing the results of a phase III randomized trial demonstrating the benefit of radiosurgery in treating brain metastases was published in The Lancet in 2004. He has lectured throughout the world and has published more than 120 peer-reviewed and invited papers.

ABOUT ANTHONY A. CHIURCO, MD

Dr. Anthony A. Chiurco is recognized as one of the best diagnostic and clinical neurosurgeons in the country. For more than 30 years he served as chief of Neurosurgery at the University Medical Center of Princeton and also served as chairman of the Department of Surgery at Capital Health System (Fuld and Mercer campuses).

Since 2002, Dr. Chiurco has been annually named among America's top surgeons by the Consumers Research Council of America. He was attending neurosurgeon to the New Jersey State Police, a spine surgeon for the U.S. Olympic rowing team, and is a past president of the New Jersey Neurosurgical Society.

He has performed more than 6,000 major intracranial and spinal operations, with particular attention to brain tumors, cerebral aneurysms, spinal stenosis and herniated cervical and lumbar discs.

Dr. Chiurco is a 1967 graduate of the Sidney Kimmel Medical College.

https://jdc.jefferson.edu/jhnj/vol13/iss1/7
DOI: https://doi.org/10.29046/JHNJ.013.1

Selected Recent Neuro-Oncology Publications

- Shi W, Blomain ES, Siglin J, Palmer JJ, Dan T, Wang Y, Werner-Wasik M, Glass J, Kim L, Bar Ad V, Bhamidipati D, Evans JJ, Judy K, Farrell CJ, Andrews DW. Salvage fractionated stereotactic re-irradiation (FSRT) for patients with recurrent high grade gliomas progressed after bevacizumab treatment. *J Neuro-Oncology.* 2017.

- Williams NL, Wuthrick EJ, Kim H, Palmer JD, Garg S, Eldredge-Hindy H, Daskalakis C, Feeney KJ, Mastrangelo MJ, Kim LJ, Sato T, Kendra KL, Olencki T, Liebner DA, Farrell CJ, Evans JJ, Judy KD, Andrews DW, Dicker AP, Werner-Wasik M, Shi W. Phase 1 Study of Ipilimumab Combined With Whole Brain Radiation Therapy or Radiosurgery for Melanoma Patients With Brain Metastases. *International Journal of Radiation Oncology Biology Physics.* 2017.

- Park HR, Kshettry VR, Farrell CJ, Lee JM, Kim YH, Won TB, Han DH, Do H, Nyguist G, Rosen M, Kim DG, Evans JJ, Paek SH. Clinical Outcome After Extended Endoscopic Endonasal Resection of Craniopharyngiomas: Two-Institution Experience. *World Neurosurgery.* 2017.

- Do H, Kshettry VR, Siu A, Belinsky I, Farrell CJ, Nyquist G, Rosen M, Evans JJ. Extent of Resection, Visual, and Endocrinologic Outcomes for Endoscopic Endonasal Surgery for Recurrent Pituitary Adenomas. *World Neurosurgery.* 2017.

- Belinsky I, Murchison AP, Evans JJ, Andrews DW, Farrell CJ, Casey JP, Curtis MT, Nowak Choi KA, Werner-Wasik M, Bilyk JR. Spheno-Orbital Meningiomas: An Analysis Based on World Health Organization Classification and Ki-67 Proliferative Index. *Ophthalmic Plastic and Reconstructive Surgery.* 2017.

- Li J, Shi W, Andrews D, Werner-Wasik M, Lu B, Yu Y, Dicker A, Liu H. Comparison of Online 6 Degree-of-Freedom Image Registration of Varian TrueBeam Cone-Beam CT and BrainLab ExacTrac X-Ray for Intracranial Radiosurgery. Technology in Cancer Research and Treatment. 2017.

- Alyemni D, Miller AF, Couto P, Athas D, Roberts AL, Rufail M, Andrews DW, Strayer DS, Kenyon LC. Histopathologic identification of Trypanosoma cruzi (Chagas') encephalitis in an AIDS patient. *Human Pathology: Case Reports.* 2017.

- Hernández-Estrada RA, Kshettry VR, Vogel AN, Curtis MT, Evans JJ. Cholesterol granulomas presenting as sellar masses: a similar, but clinically distinct entity from craniopharyngioma and Rathke's cleft cyst. *Pituitary.* 2017.

- Gill KS, Hsu D, Tassone P, Pluta J, Nyquist G, Krein H, Bilyk J, Murchison AP, Iloreta A, Evans JJ, Heffelfinger RN, Curry JM. Postoperative cerebrospinal fluid leak after microvascular reconstruction of craniofacial defects with orbital exenteration. *Laryngoscope.* 2017.

Support Groups

Brain Aneurysm and AVM Support Group at Jefferson

The Brain Aneurysm and AVM (arteriovenous malformation) Support Group provides support for individuals, family members and friends who have been affected by cerebral aneurysms, subarachnoid hemorrhage and AVMs. The purpose of the group is to gain and share knowledge and understanding of these vascular anomalies and the consequences of these disease processes. The group provides mutual support to its members by creating an atmosphere that engenders active listening and sincere and thoughtful speech within a caring environment.

When	Third Wednesday of every month (September through June)
Time	6:30-8:30 p.m.
Place	900 Walnut Street, 3rd Floor, Conference Room Philadelphia, PA 19107
Moderator/ Secretary	Jill Galvao
Parking	Complimentary parking is provided in the parking garage located in the JHN Building (Jefferson Hospital for Neuroscience) on 9th Street (between Locust & Walnut)
Information	For additional information please call: 215-503-1714

The Brain Tumor Support Group at Jefferson

The Delaware Valley Brain Tumor Support Group at Jefferson provides an opportunity for patients and their families to gain support in obtaining their optimum level of well-being while coping with, and adjusting to the diagnosis of brain tumor. Members are encouraged to share their support strategies so members can confront the challenges that this disease process has imposed on their lives. The strength gained from group can be a source of comfort and hope for whatever lies ahead.

When	Second Thursday of every month
Time	7-8:30 p.m.
Place	Jefferson Hospital for Neuroscience, 3rd Floor conference room 900 Walnut Street Philadelphia, PA 19107
Facilitator	Joseph McBride, BSN, RN and Katelyn Salvatore, BSN, RN. 215-955-4429 or katlyn.salvatore@jefferson.edu
Parking	Complimentary parking is available at the Jefferson Hospital for Neuroscience parking lot.
	Light refreshments and snacks will be served.

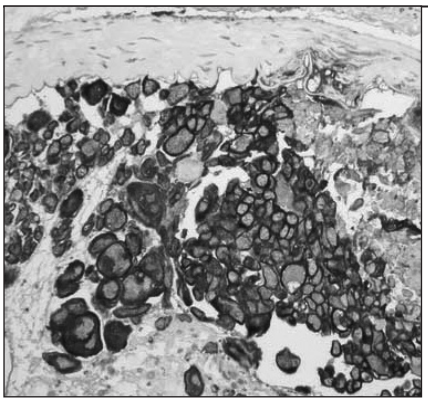

Neurosurgical Emergency Hotline

Jefferson Hospital for Neuroscience

Aneurysms • AVMs • Intracranial Bleeds

7 day • 24 hour coverage

1-866-200-4854

UPCOMING JEFFERSON NEUROSURGERY CME PROGRAMS

As a part of the Vickie and Jack Farber Institute for Neuroscience at Jefferson, the Department of Neurological Surgery is one of the busiest academic neurosurgical programs in the country, offering state-of-the-art treatment to patients with neurological diseases affecting the brain and spine, such as brain tumors, spinal disease, vascular brain diseases, epilepsy, pain, Parkinson's disease and many other neurological disorders (**Jefferson.edu/Neurosurgery**).

As part of a larger educational initiative from the Jefferson Department of Neurological Surgery, the Sidney Kimmel Medical College Office of Continuing Medical Education is offering the following continuing professional educational opportunities for 2018:

- **7th Annual Neurocritical Care Symposium**
  January 26-27, 2018
  Jefferson Alumni Hall, Center City Campus of Thomas Jefferson University

- **17th Annual Cerebrovascular Update**
  March 15-16, 2018
  Hyatt at the Bellevue, Philadelphia

- **Fundamental Critical Care Support Course**
  April 12-13, 2018
  Dorrance H. Hamilton Building, Center City Campus of Thomas Jefferson University

- **4th Annual Philadelphia Spine Summit**
  May 11, 2018
  Jefferson Alumni Hall, Center City Campus of Thomas Jefferson University

- **8th Annual Brain Tumor Symposium**
  October 2018
  Philadelphia, PA

- **30th Annual Pan Philadelphia Neurosurgery Conference**
  December 2018
  Philadelphia, PA

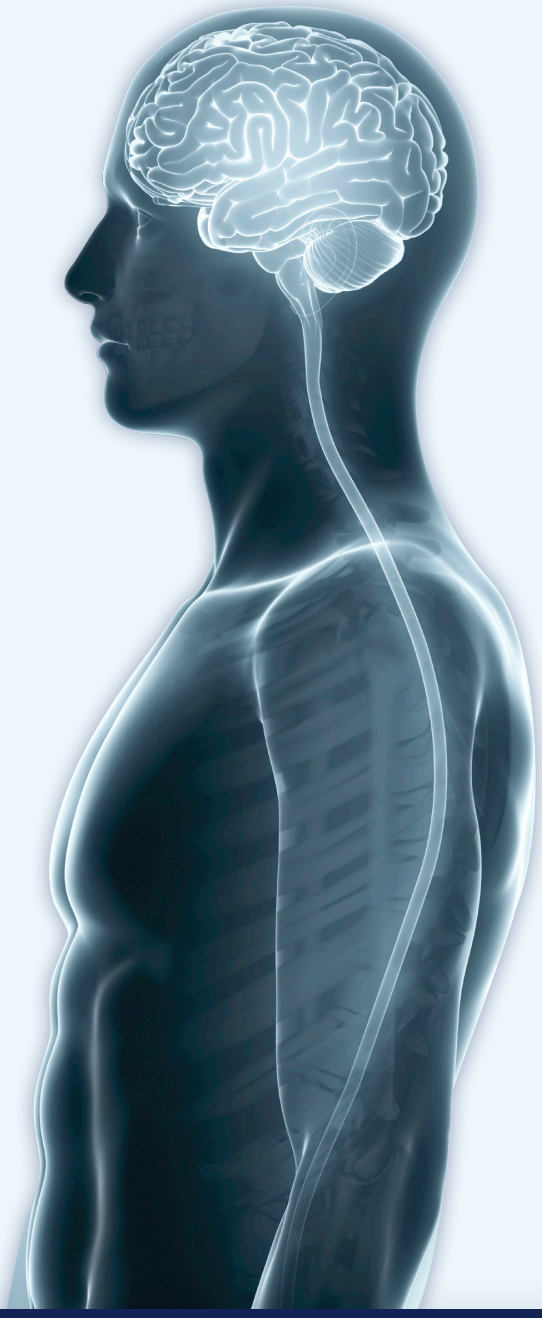

For additional information regarding these and other Jefferson CME programs, please visit our website at CME.Jefferson.edu or call the Office of CME at 888-JEFF-CME (888-533-3263).

Sidney Kimmel Medical College at Thomas Jefferson University is accredited by the ACCME to provide continuing medical education for physicians.

Many of the activities above offer additional CE accreditations.

Vickie and Jack Farber Institute for Neuroscience
Jefferson Health®

Follow us on Twitter at @JeffCME for updates and new information

https://jdc.jefferson.edu/jhnj/vol13/iss1/7
DOI: https://doi.org/10.29046/JHNJ.013.1